Electronic Supplementary Information (ESI)

NADH-mediated primordial synthesis of amino acids

Noemí Nogal, Javier Luis-Barrera, Sonia Vela-Gallego, Fernando Aguilar-Galindo, Andrés de la Escosura

Table of Contents

1. Methods

General experimental conditions. Reagents and authentic samples (standards) were obtained from commercial sources and used without further purification. β-nicotinamide adenine dinucleotide reduced disodium salt was purchased from TCI. Glyoxylic acid monohydrate (**1c**), glycine (**2c**), glutamic acid (**2b**), lactic acid 85 % solution, glycolic acid and deuterium oxide (D_2O) were purchased from Sigma Aldrich. β-nicotinamide adenine dinucleotide monosodium salt dihydrate was purchased from Alfa Aesar. Sodium pyruvate (**1a**), L-alanine (**2a**) and L-aspartic acid (**2d**) were purchased from TCI chemicals. α-ketoglutaric acid disodium salt dihydrate (**1b**) was purchased from BLDpharm. 2-oxobutanedioic acid (**1d**) was purchased from Fluorochem. All the synthetic procedures were performed with a Schlenk line and Schlenk glassware under inert nitrogen atmosphere.

NMR spectroscopy. NMR spectra were recorded with a Bruker Advance III-HD Nanobay with two channel 300 MHz spectrometer using H_2O:D_2O (9:1) solutions at 298 K. The ^{1}H-NMR water signal was suppressed using noseygppr1d pulse, acquiring 128 scans for each sample with a relaxation delay of 2 seconds. To prepare samples for analysis, 450 µL of the reaction mixture were taken and mixed with 50 µL of a solution of TMSP-d_4 3 mM in D_2O, reaching the ratio H_2O:D_2O (9:1). All chemical shifts are referenced to the standard TMSP-d_4: 0.00 (s, 9H) ppm.

UV-Visible absorption spectroscopy. The absorption spectra of freshly prepared solutions were acquired with a JASCO V-660 spectrophotometer at room temperature (Integration = 0.02 s, interval = 1 nm). The samples were subjected to a 1:100 dilution before measuring.

MALDI-TOF mass spectrometry. MS spectra were recorded on a Bruker ULTRAFLEX III spectrometer. MALDI-TOF mass spectra were obtained in the negative linear mode, and were collected in a mass range of 200–1600 *m*/*z*. A mixture of 2,3,4-trihydroxyacetophenone (2,3,4-THAP) or 2,4,6-trihydroxyacetophenone (2,4,6-THAP) with ammonium citrate was used as matrix.

GC-MS spectrometry. GC analyses were performed on a 7820A gas chromatographer coupled to an Agilent Technologies 5977A mass selective detector equipped with an achiral capillary column HP-5 (30 m, 0.25 mm inner diameter, 25µm thickness), which operated at 1,372V using He as the carrier gas, supplied at a constant flow rate of 1.0 mL min^{-1}. The analysis was carried out on a 1 µL injection volume (split 20:1). The injection port temperature was 250 °C, and the column oven temperature program was: 100 °C for 2 min, then increased to 275 °C with a 20 °C min^{-1} ramp, followed by a 5-min hold (total running time 15.75 min).

The protocol to derivatize samples was based on the literature:[1]

1. In an eppendorf, 50 mg of KOH were added to 700 µL of sample, and the mixture was centrifuged for 3 min at 6000 rpm.
2. To 600 µL of supernatant, 300 µL of ethanol, 40 µL of pyridine and 40 µL of ethyl chloroformate were added, and the mixture was vortexed for 30 s.
3. Another 40 µL of ethyl chloroformate were added, and the mixture was vortexed for 30 s.
4. 200 µL of chloroform were added, and the mixture was vortexed for 10 s.
5. 600 µL of sat. $NaHCO_3$ solution were added, and the mixture was vortexed for 10 s.
6. The organic phase was separated and 400 µL of ethyl acetate were added.
7. The organic phase was dried with anhydrous Na_2SO_4, filtered and added to the analysis vial.

pH measurements. pH was determined with a Mettler Toledo SevenCompact pH meter equipped with a InLab Routine Pro sensor.

2. Experimental procedures

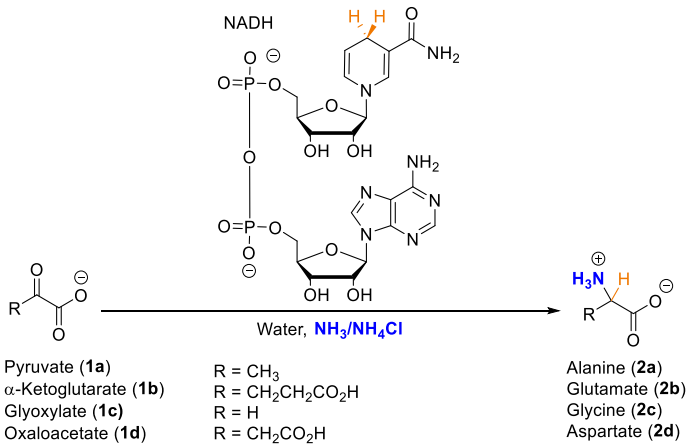

Scheme S1. Synthesis of amino acids from α-ketoacids in presence of NADH.

Preparation of the ammonia/ammonium solution. ***NH_3/NH_4Cl 200 mM:*** Solutions of ammonia (NH_3, 200 mM) and ammonium chloride (NH_4Cl, 200 mM) were prepared and mixed in the tabulated volumes (Table S1), and the pH was then adjusted with more NH_3 solution (200 mM) or NH_4Cl solution (200 mM) until reaching the desired value.

pH value	**Volume NH_3 200 mM** (mL)	**Volume NH_4Cl 200 mM** (mL)	**Ratio $V(NH_3):V(NH_4Cl)$**
7	0.2	50	1:250
8	1	35	1:35
9	20	45	1:2.25
10	90	30	3:1

Table S1. Approximate ratios of NH_3 and NH_4Cl to reach the required pH.

Same procedure and similar ratios were used to prepare NH_3/NH_4Cl solution with other concentrations (600 mM or 1 M), employing ammonia (NH_3) and ammonium chloride (NH_4Cl) stock solutions with the desired concentration. In the main text, these mixtures are named "ammonia solution", independently of the NH_3:NH_4Cl ratio.

Reactions: Two different stock solutions of the α-ketoacid (**1**, 60 mM) and NADH (60 mM)* were prepared in NH_3/NH_4Cl solution of the desired pH and concentration. For each solution, once the compound had been dissolved, the pH was measured again and, if needed, adjusted with aqueous HCl (1 M) or NaOH (1 M).** For each tested conditions, three Schlenk flasks charged with a magnetic stirring bar were purged through three vacuum-nitrogen cycles and left under a nitrogen atmosphere. The stock solutions of **1** and NADH were added separately to two of them, and 3 freeze-pump-thaw cycles were carried out to eliminate oxygen. With a needle purged 3 times with nitrogen, 3 mL of each solution (**1** and NADH) were transferred to the third flask, reaching a concentration of each component of 30 mM. The reaction was stirred at 300 rpm and rt over periods of maximum 168 h. For the controls, containing either **1** or NADH, the same procedure was applied.

* For reactions with 3 equiv. of NADH, the cofactor initial concentration must be 180 mM.

** In some cases, considerable amounts of NaOH (1M) had to be added to the ketoacid solution, reaching appreciable changes in the ketoacid concentrations. See final concentrations for each case.

3. Calibration

3.1 Calibration lines

All the stock solutions and dilutions for the calibration lines are made using aqueous NH_3/NH_4Cl mixture (200 mM, pH = 8) as solvent, since it is one of the most common solvents used in this work; to simplify, it will be named "*ammonia solution A*" in this section. Only the stock solution of TMSP-d_4 is made with pure D_2O as solvent. The concentrations shown in tables are related to the samples before mixing the analyte solution with TMSP-d_4 solution in D_2O.

Preparation of stock solution: The desired amount of the commercial analyte is firstly dissolved in half the required volume of *ammonia solution A*. The pH was measured and, if needed, adjusted with aqueous HCl (1 M) or NaOH (1 M) to reach pH = 8. It was transferred to a volumetric flask and more *ammonia solution A* was added to complete the desired final volume.

Preparation of dilutions and NMR tubes: Solutions of 2 mL of the analyte were made diluting the stock solution of the analyte with *ammonia solution A*. To prepare the samples for measurements in NMR, 450 µL of the solution were taken and mixed with 50 µL of a solution of TMSP-d_4 3 mM in D_2O, reaching the ratio H_2O:D_2O (9:1).

The integral value of the TMSP-d_4 is arbitrarily set to 9.00 in all the cases. The integral value of the analyte is taken after this adjustment. Correlation line was obtained from the least-squares fitting (intercept = 0).

In each case, a theoretical line is made supposing the hypothetical scenario in which the analyte protons and the TMPS-d_4 protons give exactly the same area in ^{1}H-NMR in order to see the deviation of the real experimental calibration line. Since the integral of TMSP-d_4 is set to 9.00, the theoretical integral of alanine has been calculated as follows:

$$\text{Theoretical analyte signal integral} = \frac{\text{Analyte mmol x Analyte signal number of protons}}{\text{TMSP mmol}}$$

Alanine (**2a**)

(25 µL of NaOH 1M had to be added to reach pH=8)

Table S2. Integrals for alanine (**2a**) as a function of concentration.

Stock solution	**Weighted mass** (mg)	**Mmol** (g/mol)	**V** (mL)	**Conc.** (mM)	**V** (mL) aliquot	**n** (mmol) in aliquot	**Integrated signal** (ppm)
Alanine	53.5	89.09	20	30.03	0.450	See each case	3.80 (q, *J* = 7.2 Hz, 1H)
TMSP-d_4	10.3	172.27	10	2.98	0.050	0.000149	0.00 (s, 9H) ppm

Dilution	**Concentration** (mM)	**n** (mmol) in aliquot	**Measured integral of analyte**	**Theoretical integral of analyte**
02:98	0.60	0.00027	2.04	1.81
05:95	1.50	0.00068	4.75	4.52
10:90	3.00	0.00135	9.88	9.04
20:80	6.01	0.00270	19.66	18.08
40:60	12.01	0.00540	39.48	36.16
60:40	18.02	0.00811	57.34	54.24
80:40	24.02	0.01081	77.06	72.32
100:0	30.03	0.01351	98.39	90.39

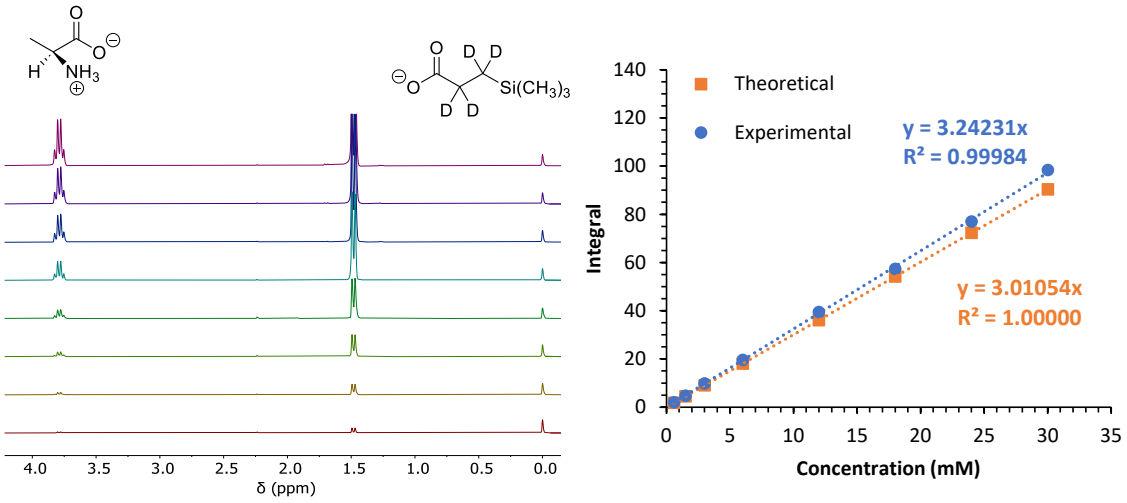

Figure S1. Left) ^{1}H-NMR spectra of alanine (**2a**) solutions, from more to less concentrated. Right) Theoretical and experimental calibration line.

Glutamic acid (**2b**)

(580 μL of NaOH 1M had to be added to reach pH=8. Sonication bath was used to dissolve the amino acid)

Table S3. Integrals for glutamic acid (**2b**) as a function of concentration.

Stock solution	**Weighted mass** (mg)	**Mmol** (g/mol)	**V** (mL)	**Conc.** (mM)	**V** (mL) aliquot	**n** (mmol) in aliquot	**Integrated signal** (ppm)
Glutamic acid	89.0	147.13	20	30.25	0.450	See each case	3.77 (dd, *J* = 7.1, 4.8 Hz, 1H)
TMSP-d_4	10.3	172.27	10	2.98	0.050	0.000149	0.00 (s, 9H) ppm

Dilution	**Concentration** (mM)	**n** (mmol) in aliquot	**Experimental integral of analyte**	**Theoretical integral of analyte**
05:95	1.51	0.00068	5.91	4.55
10:90	3.02	0.00136	11.45	9.11
20:80	6.05	0.00272	22.85	18.21
40:60	12.10	0.00544	45.01	36.42
60:40	18.15	0.00817	68.40	54.63
80:40	24.20	0.01089	91.40	72.84
100:0	30.25	0.01361	115.30	91.05

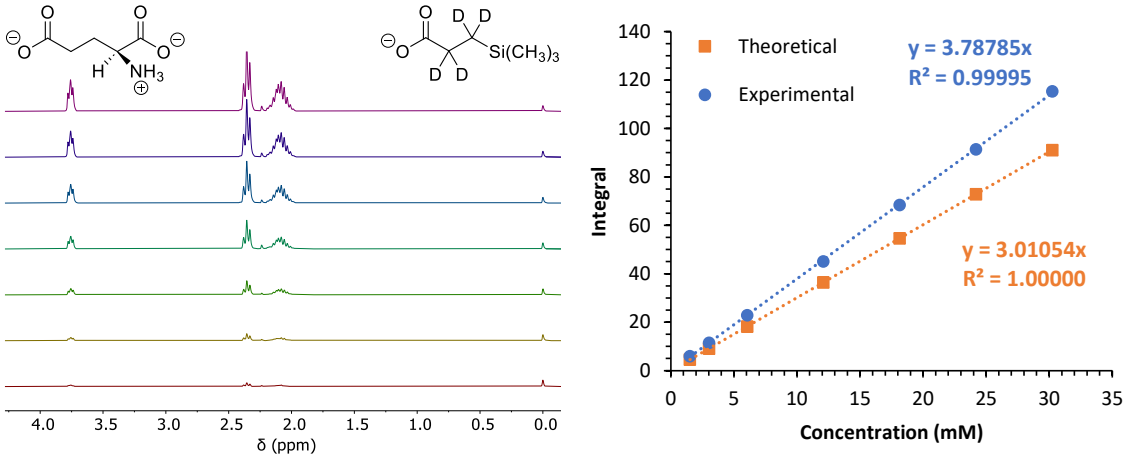

Figure S2. Left) ^{1}H-NMR spectra of glutamic acid (**2b**) solutions, from more to less concentrated. Right) Theoretical and experimental calibration line.

Glycine (**2c**)

(4 µL of NaOH 1M had to be added to reach pH=8)

Table S4. Integrals for glycine (**2c**) as a function of concentration.

Stock solution	**Weighted mass** (mg)	**Mmol** (g/mol)	**V** (mL)	**Conc.** (mM)	**V** (mL) aliquot	**n** (mmol) in aliquot	**Integrated signal** (ppm)
Glycine	18.0	75.07	20	11.99	0.450	See each case	3.58 (s, 2H)
TMSP-d_4	10.3	172.27	10	2.98	0.050	0.000149	0.00 (s, 9H) ppm

Dilution	**Concentration** (mM)	**n** (mmol) in aliquot	**Experimental integral of analyte**	**Theoretical integral of analyte**
05:95	0.60	0.00027	3.86	3.61
10:90	1.20	0.00054	8.19	7.22
20:80	2.40	0.00108	16.10	14.44
40:60	4.80	0.00216	31.81	28.87
60:40	7.19	0.00324	46.66	43.31
80:40	9.59	0.00432	61.10	57.75
100:0	11.99	0.00539	78.34	72.19

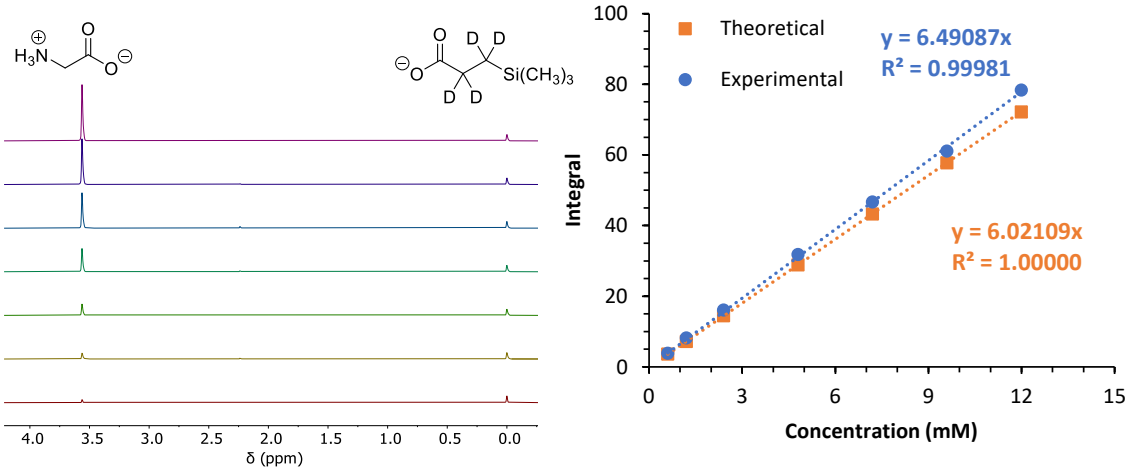

Figure S3. Left) ^{1}H-NMR spectra of glycine (**2c**) solutions, from more to less concentrated. Right) Theoretical and experimental calibration line.

NADH

(11 µL of HCl 1M had to be added to reach pH=8)

Table S5. Integrals for **NADH** as a function of concentration.

Stock solution	**Weighted mass** (mg)	**Mmol** (g/mol)	**V** (mL)	**Conc.** (mM)	**V** (mL) aliquot	**n** (mmol) in aliquot	**Integrated signal** (ppm)
NADH	212.8	709.41	10	30.00	0.450	See each case	8.47 (s, 1H)
TMSP-d_4	10.3	172.27	10	2.98	0.050	0.000149	0.00 (s, 9H) ppm

Dilution	**Concentration** (mM)	**n** (mmol) in aliquot	**Experimental integral of analyte**	**Theoretical integral of analyte**
05:95	1.50	0.00067	5.99	4.52
10:90	3.00	0.00135	12.42	9.03
20:80	6.00	0.00270	23.75	18.06
40:60	12.00	0.00540	47.26	36.12
60:40	18.00	0.00810	70.76	54.18
80:40	24.00	0.01080	98.67	72.25
100:0	30.00	0.01350	120.64	90.31

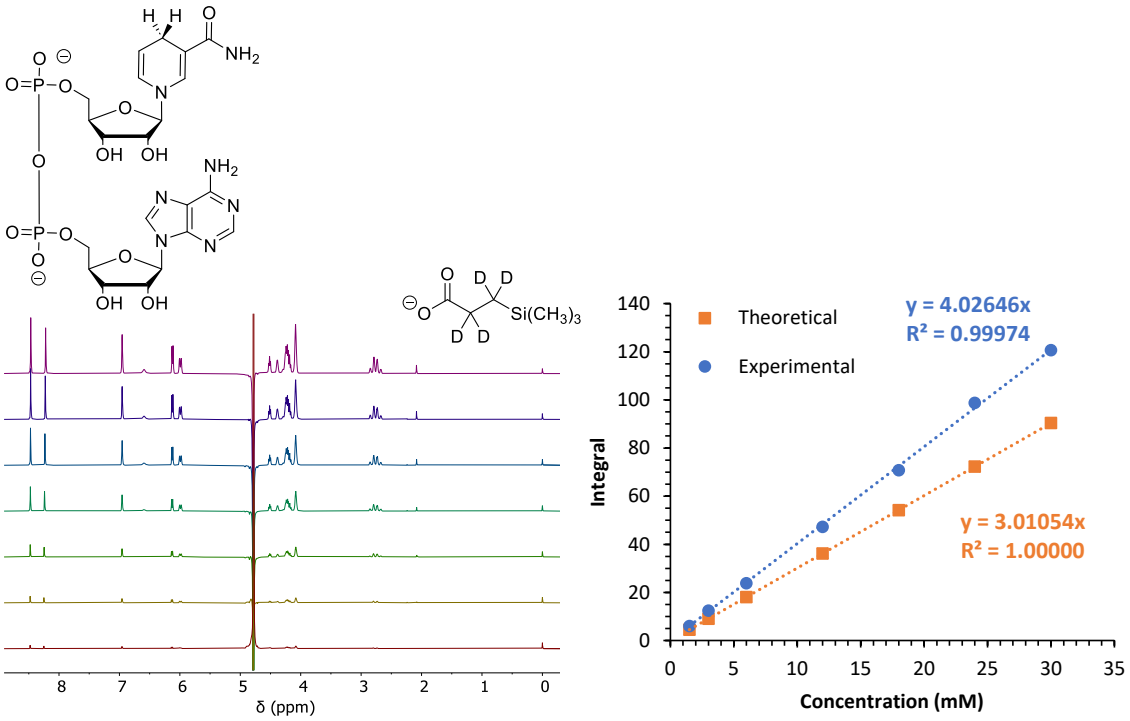

Figure S4. Left) ^{1}H-NMR spectra of **NADH** solutions, from more to less concentrated. Right) Theoretical and experimental calibration line.

NAD$^+$

(1 µL of HCl 1M had to be added to reach pH=8)

Table S6. Integrals for **NAD$^+$** as a function of concentration.

Stock solution	**Weighted mass** (mg)	**Mmol** (g/mol)	**V** (mL)	**Conc.** (mM)	**V** (mL) aliquot	**n** (mmol) in aliquot	**Integrated signal** (ppm)
NAD$^+$	216.3	721.44	10	29.98	0.450	See each case	9.34 (s, 1H)
TMSP-d_4	10.3	172.27	10	2.98	0.050	0.000149	0.00 (s, 9H) ppm

Dilution	**Concentration** (mM)	**n** (mmol) in aliquot	**Experimental integral of analyte**	**Theoretical integral of analyte**
05:95	1.50	0.00067	6.11	4.51
10:90	3.00	0.00135	12.47	9.03
20:80	6.00	0.00270	24.42	18.05
40:60	11.99	0.00540	48.72	36.10
60:40	17.99	0.00810	72.69	54.16
80:40	23.99	0.01079	97.97	72.21
100:0	29.98	0.01349	118.98	90.26

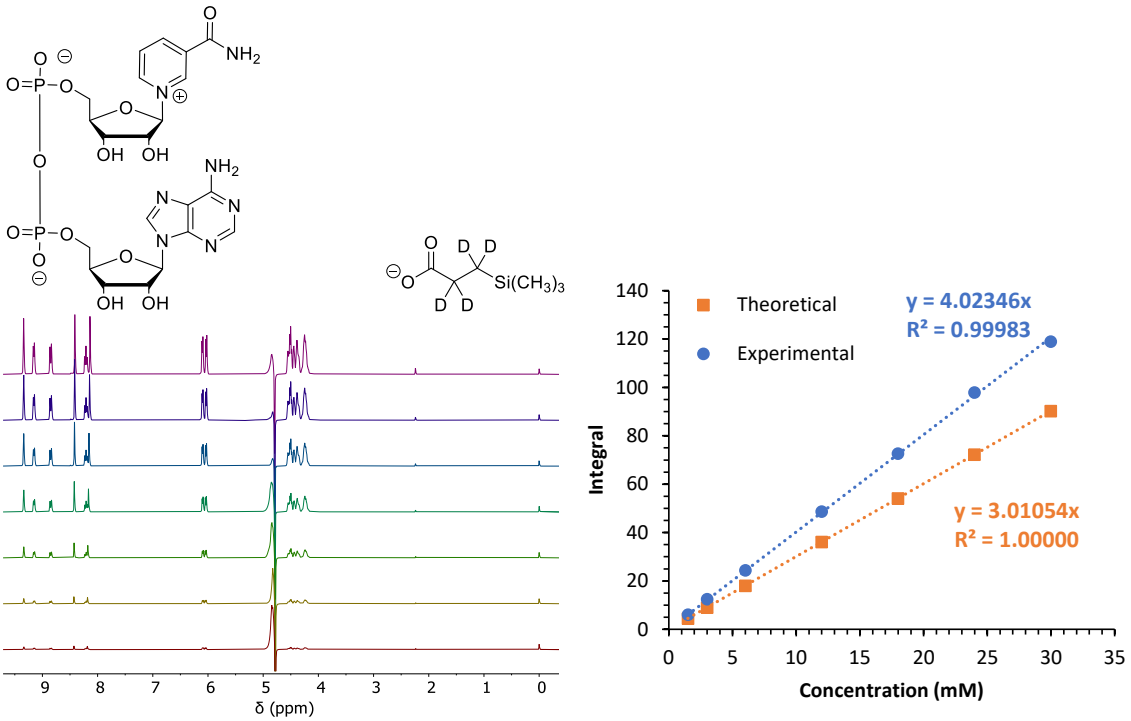

Figure S5. Left) ^{1}H-NMR spectra of **NAD$^+$** solutions, from more to less concentrated. Right) Theoretical and experimental calibration line.

3.2 Quantification and preparation of samples

Amino acids

Alanine (**2a**) and glycine (**2c**) present measured calibration lines which are similar (although not the same) to the theoretical line. In contrast, glutamate (**2b**) calibration line has a considerably greater slope. This fact indicates that the protons of the different amino acids and TMPS-d_4 exhibit distinct integral values in the conditions of ^{1}H-NMR acquisition, likely due to differences in their relaxation times. Therefore, these calibration lines will be used for the quantification of amino acids formation.

Cofactors

In the reaction mixtures, the signals which are more distinguishable from each cofactor and that have been used for integration are:

NADH: 8.47 (s, 1H) ppm. **ADPR:** 8.49 (s, 1H) ppm. **NAD$^+$:** 9.34 (s, 1H) ppm. Referenced to the standard TMSP: 0.00 (s, 9H) ppm.

NADH and NAD$^+$, whose integrated signals have a heteroaromatic nature, have a similar slope in their calibration lines, although substantially different to the theoretical slope. ADPR is expected to present a similar behaviour. Unfortunately, signals of NADH and ADPR partially overlap. For this reason and the lack of a calibration line for ADPR, the measurements of these cofactors were carried out in a simplified manner:

To calculate the conversion of NADH into ADPR and NAD$^+$ (and the percentage of remaining NADH), the aforementioned signals of the three compounds are integrated and the sum of the three integrals are normalized to 100, obtaining the molar percentage of each component.

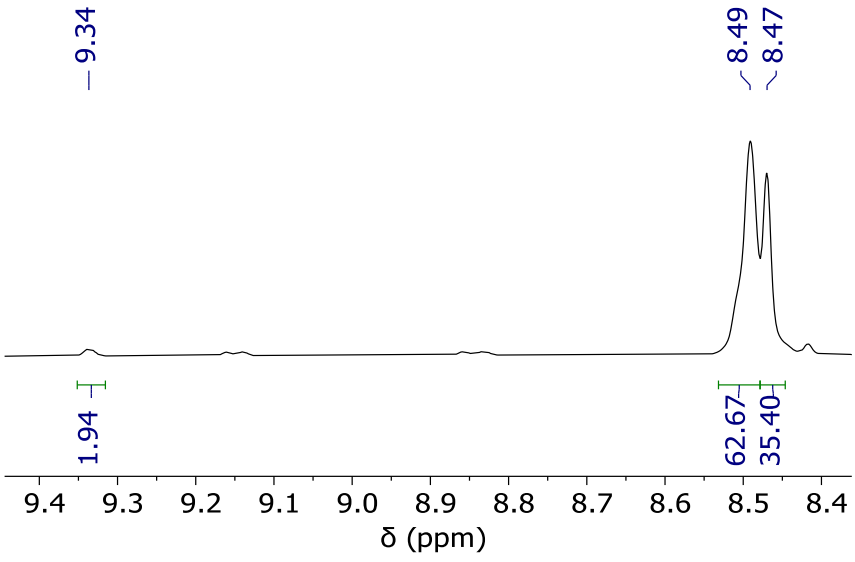

Figure S6. Example of integration. Mixture of the three co-factor derivatives, showing a composition with 1.9 % of NAD$^+$, 62.8 % of ADPR and 35.4% of NADH.

Albeit this measurement is not so accurate as the quantification of amino acids, it must be understood as a semi-quantitative method to follow the tendency of NADH in these reactions. Comparison of the NADH/ADPR/NAD$^+$ ratio (using this approximation) in the studied reactions

(Tables S7-15) can draw correct conclusions about the behaviour that NADH shows with different amino acids, different control experiments, etc.

Preparation of samples

To prepare samples for analysis, an aliquot of 450 µL of the reaction mixture was taken and mixed with 50 µL of a solution of TMSP-d_4 3 mM in D_2O, reaching the ratio H_2O:D_2O (9:1) and the mixture was transferred to an NMR tube. The reaction aliquots tubes were always frozen until analysis.

The integral of TMSP-d_4 is set to 9.00 and then the integral of the amino acid is taken. The corresponding calibration line is applied to obtain the amino acid concentration (Section 5, "^{1}H-NMR spectra" present some examples of quantification for each amino acid). Independently, the signals of NADH, NAD^+ and ADPR are integrated and their sum is normalized to 100 to obtained the molar ratio.

In some reactions in which three equivalents of NADH were added, the base line resulted slightly distorted, and so a baseline correction had to be applied.

4. Tables of results

NOTE: For every amino acid formation at the optimal conditions, *i.e.*, three equivalents of NADH (90 mM) in aqueous NH_3/NH_4Cl solution (1 M) at pH 8, yields were calculated as an average from three independent experiments, therefore presenting the standard deviations in Figure 2B.

The time past from the reaction start to the recording of the first NMR spectrum (ca. 1 h) is an estimation (could vary slightly from experiment to experiment), and so conversion % values at 1 h bear a higher degree of error.

4.1 Results of reactions from ketoacids to amino acids

Table S7. Data of conversion determined by ^{1}H-NMR in the reaction of pyruvate (**1a**, 30 mM) with NADH (30 mM) to produce alanine (**2a**), in aqueous NH_3/NH_4Cl solution (200 mM) as a function of pH and reaction time.

pH	**Time** (h)	**Alanine** (**2a**) (^{1}H-NMR Yield %)	**NADH** (remaining %)	**ADPR** (conversion %)	**NAD$^+$** (conversion %)
10	1	**0.0**	94.0	6.0	Traces
	24	**0.0**	94.0	6.0	Traces
	48	**0.0**	93.8	6.2	Traces
	72	**0.0**	90.1	9.9	Traces
	168	**0.0**	90.4	9.6	Traces
9	1	**0.0**	94.7	3.9	1.4
	24	**0.0**	91.6	6.7	1.7
	48	**1.8**	91.3	6.4	2.3
	72	**2.9**	89.7	8.0	2.3
	168	**6.7**	85.8	11.5	2.7
8	1	**3.7**	89.8	7.6	2.5
	24	**6.8**	87.0	10.7	2.3
	48	**9.9**	81.7	16.0	2.2
	72	**11.1**	76.4	19.4	4.2
	168	**9.3**	65.9	30.2	3.8
7	1	**1.2**	90.7	7.7	1.6
	24	**5.7**	81.1	17.6	1.3
	48	**9.8**	77.0	21.1	1.9
	72	**11.2**	71.9	25.1	3.0
	168	**8.8**	67.2	28.5	4.3

Table S8. Data of conversion determined by ^{1}H-NMR in the reactions of pyruvate (**1a**, 30 mM), with NADH (30 mM or 90 mM, see each case) to give alanine (**2a**), in aqueous NH_3/NH_4Cl solution at pH 8 and at different reaction times.

[NH_3/NH_4Cl] (mM) 1a : NADH [a]	**Time** (h)	**Alanine** (**2a**) (^{1}H-NMR Yield %)	**NADH** (remaining %)	**ADPR** (conversion %)	**NAD^+** (conversion %)
200 mM 1:1	1	**3.7**	89.8	7.6	2.5
	24	**6.8**	87.0	10.7	2.3
	48	**9.9**	81.7	16.0	2.2
	72	**11.1**	76.4	19.4	4.2
	168	**9.3**	65.9	30.2	3.8
600 mM 1:1	1	**0.0**	94.3	4.8	0.9
	24	**9.8**	90.4	7.8	1.7
	48	**10.1**	84.8	12.6	2.6
	72	**12.0**	82.3	14.5	3.2
	168	**15.6**	71.5	23.6	4.9
1000 mM 1:1	1	**0.0**	93.5	5.0	1.5
	24	**10.4**	88.2	9.6	2.2
	48	**11.2**	84.4	12.4	3.2
	168	**20.9**	64.9	28.8	6.3

[NH_3/NH_4Cl] (mM) 1a : NADH [a]	**Time** (h)	**Alanine** (**2a**) (^{1}H-NMR Yield %)
200 mM 1:3	1	**3.9**
	24	**8.8**
	48	**13.1**
	72	**13.9**
	168	**19.1**
600 mM 1:3	1	**0.0**
	24	**14.4**
	48	**14.9**
	72	**17.1**
	168	**26.7**
1000 mM 1:3	1	**0.0** ($\sigma = 0.0$)
	24	**16.4** ($\sigma = 0.8$)
	48	**23.0** ($\sigma = 4.1$)
	72	**29.7** ($\sigma = 1.4$)
	168	**35.5** ($\sigma = 5.5$)

[a] Ratio pyruvate (**1a**): NADH.

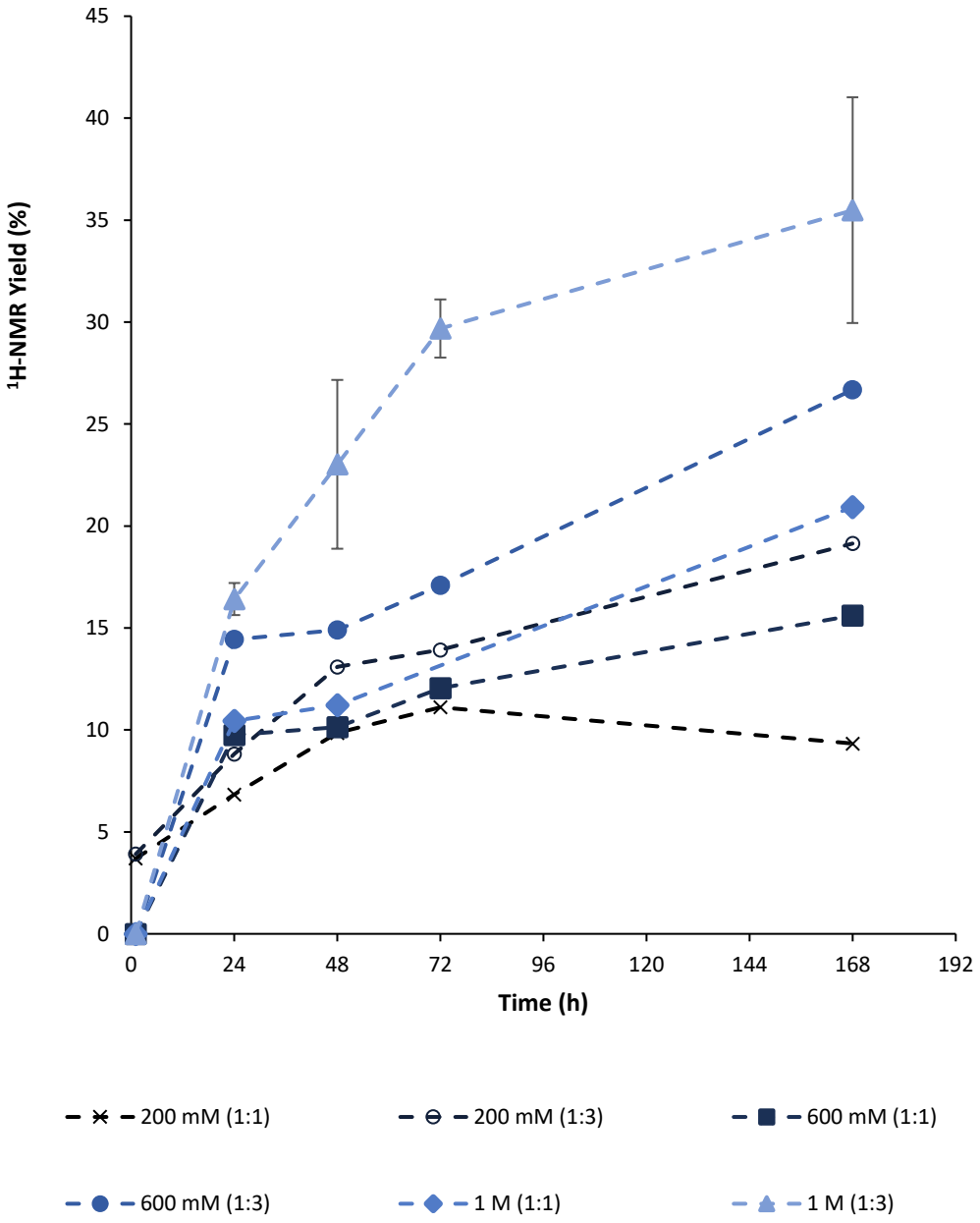

Figure S7. Plots of ^{1}H-NMR yield (%) relative to TMSP-d_4 at different times of reaction of pyruvate (**1a**, 30 mM) and NADH (30 or 90 mM) to yield alanine (**2a**) in different concentrations of the NH_3/NH_4Cl solution at pH 8. In each case, the NH_3/NH_4Cl concentration and the pyruvate (**1a**) : NADH ratio (in parenthesis) is indicated.

Table S9. Data of conversion determined by ^{1}H-NMR in the reactions of α-ketoglutarate (**1b**, 30 mM), with NADH (30 mM or 90 mM, see each case) to give glutamate (**2b**), in aqueous NH_3/NH_4Cl solution at pH 8 and at different reaction times.

[NH_3/NH_4Cl] (mM) 1b : NADH [a]	**Time** (h)	**Glutamate** (**2b**) (^{1}H-NMR Yield %)	**NADH** (remaining %)	**ADPR** (conversion %)	**NAD^+** (conversion %)
200 mM 1:1	1	**0.0**	93.4	5.2	1.4
	24	**3.5**	90.5	8.1	1.5
	48	**4.8**	85.6	12.8	1.7
	72	**7.9**	81.0	16.6	2.4
	168	**10.8**	53.0	43.7	3.4
600 mM 1:1	1	**0.0**	95.4	3.6	1.0
	24	**0.0**	93.0	6.1	0.9
	48	**3.8**	90.8	8.5	0.7
	72	**4.8**	87.3	11.0	1.7
	168	**24.3**	71.5	25.0	3.4
1000 mM 1:1	1	**0.0**	95.8	3.5	0.7
	48	**6.1**	84.8	12.8	2.4
	72	**9.0**	81.4	15.9	2.8
	168	**13.3**	67.6	28.1	4.3

[NH_3/NH_4Cl] (mM) 1b : NADH	**Time** (h)	**Glutamate** (**2b**) (^{1}H-NMR Yield %)
200 mM 1:3	1	**0.0**
	24	**Traces**
	48	**5.9**
	72	**6.6**
	168	**15.1**
600 mM 1:3	1	**0.0**
	24	**9.3**
	48	**12.8**
	72	**14.6**
	168	**18.1**
1000 mM 1:3	1	**0.0** ($\sigma = 0.0$)
	24	**7.5** ($\sigma = 1.8$)
	48	**11.9** ($\sigma = 2.0$)
	72	**18.5** ($\sigma = 1.3$)
	168	**32.6** ($\sigma = 5.2$)

[a] Ratio α-ketoglutarate (**1b**) : NADH.

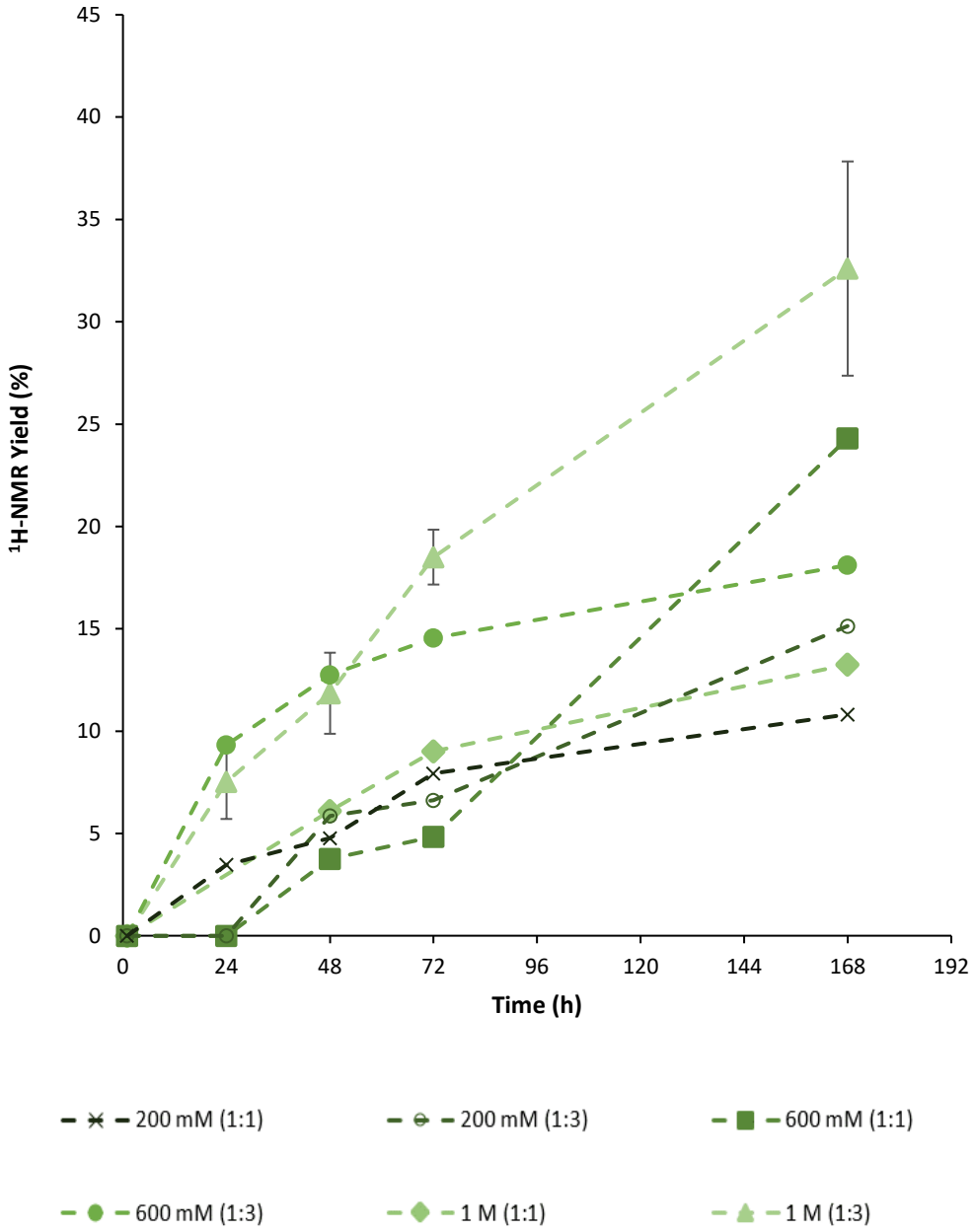

Figure S8. Plots of ^{1}H-NMR yield (%) relative to TMSP-d_4 at different times of reaction of α-ketoglutarate (**1b**, 30 mM) and NADH (30 or 90 mM) to yield glutamate (**2b**) in different concentrations of the NH_3/NH_4Cl solution. In each case, the NH_3/NH_4Cl concentration and the α-ketoglutarate (**1b**) : NADH ratio (in parenthesis) is indicated.

Table S10. Data of conversion determined by ^{1}H-NMR in the reactions of glyoxylate (**1c**, 27 mM to 30 mM), with NADH (30 mM or 90 mM, see each case) to give glycine (**2c**), in aqueous NH_3/NH_4Cl solution at pH 8 and at different reaction times.

[NH_3/NH_4Cl] (mM) 1c : NADH [a]	**Time** (h)	**Glycine** (**2c**) (^{1}H-NMR Yield %)	**NADH** (remaining %)	**ADPR** (conversion %)	**NAD^+** (conversion %)
200 mM 1:1	1	**0.0**	63.1	34.8	2.1
	24	**1.6**	27.1	70.1	2.8
	48	**2.0**	24.2	73.1	2.7
	72	**1.9**	24.0	71.8	4.3
	168	**1.8**	18.4	76.2	5.4
600 mM 1:1	1	**1.7**	89.0	9.9	1.1
	24	**3.6**	37.5	59.7	2.8
	72	**3.4**	27.6	68.7	3.7
	168	**2.6**	20.1	74.7	5.2
1000 mM 1:1	1	**0.7**	85.3	13.3	1.4
	24	**2.8**	42.9	54.7	2.4
	48	**3.2**	38.0	58.8	3.2
	72	**3.3**	29.4	67.0	3.6
	168	**5.0**	26.9	66.8	6.3

[NH_3/NH_4Cl] (mM) 1c : NADH [a]	**Time** (h)	**Glycine** (**2c**) (^{1}H-NMR Yield %)
200 mM 1:3	1	**0.7**
	24	**0.7**
	48	**1.2**
	72	**2.3**
	168	**1.0**
600 mM 1:3	1	**1.6**
	24	**2.9**
	72	**3.8**
	168	**4.2**
1000 mM 1:3	1	**2.2** ($\sigma = 0.7$)
	24	**4.2** ($\sigma = 0.7$)
	48	**4.4** ($\sigma = 1.3$)
	72	**5.1** ($\sigma = 0.6$)
	168	**4.8** ($\sigma = 0.8$)

[a] Ratio glycine (**1c**) : NADH.

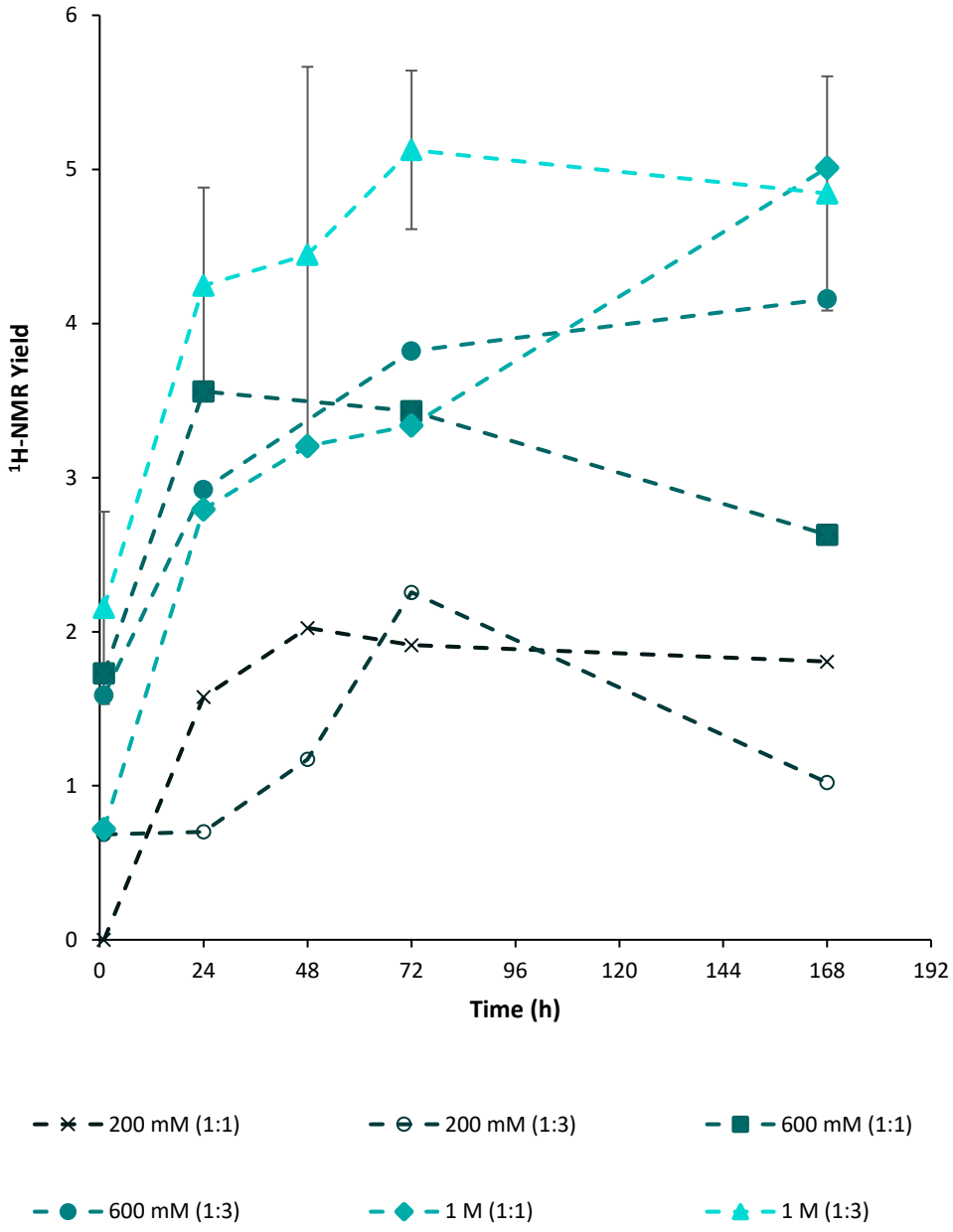

Figure S9. Plots of ^{1}H-NMR yield (%) relative to TMSP-d_4 at different times of reaction of α-ketoglutarate (**1c**, 30 mM) and NADH (30 or 90 mM) to yield glycine (**2c**) in different concentrations of the NH_3/NH_4Cl solution. In each case, the NH_3/NH_4Cl concentration and the glyoxylate (**1c**) : NADH ratio (in parenthesis) is indicated. The reactions at the worst conditions, i.e., with 200 mM of NH_3/NH_4Cl, have ^{1}H-NMR yields between 0% and 2%. These values are within the estimated error of quantitative NMR, and so the erratic behaviour of the corresponding curves is not conclusive.

Table S11. Data of conversion determined by ^{1}H-NMR in the reactions of oxaloacetate (**1d,** 25.6 mM), with NADH (30 mM) to give alanine (**2a**) (due to the decarboxylation of oxaloacetate into pyruvate), in aqueous NH_3/NH_4Cl solution (200 mM) at pH 8 and at different reaction times.

Ketoacid	**Time** (h)	**Alanine** (**2a**) (^{1}H-NMR Yield %)	**NADH** (remaining %)	**ADPR** (conversion %)	**NAD$^+$** (conversion %)
Oxaloacetate (1d)	1	**0.0**	94.0	3.1	2.9
	24	**Traces**	90.8	7.2	2.0
	48	**Traces**	87.6	9.5	2.9
	72	**5.0**	83.4	13.4	3.2
	168	**14.0**	75.9	20.1	4.0

Table S12. pH measurements after selected aforesaid reactions of the ketoacids (**1**, 25.6 mM to 30 mM) with NADH (30 or 90 mM, see each case) in aqueous NH_3/NH_4Cl solution at initial pH 8. These measurements show very small variations of pH in 168h. Although this NH_3/NH_4Cl mixture if far from the NH_4^+ pKa (9.25) and cannot be considered as an efficient buffer, in these conditions the pH is relatively maintained throughout the reaction progression.

Ketoacid	**Conditions**	**Amino acid** (**2**) (^{1}H-NMR Yield %) at 168 h	pH after 168 h of reaction
Pyruvate (1a)	NH_3/NH_4Cl (200 mM) 1equiv. NADH	9% (**2a**)	8.10
α-Ketoglutarate (1b)	NH_3/NH_4Cl (200 mM) 1equiv. NADH	11% (**2b**)	7.98
Glyoxylate (1c)	NH_3/NH_4Cl (200 mM) 1equiv. NADH	2% (**2c**)	7.88
Oxaloacetate (1d)	NH_3/NH_4Cl (200 mM) 1equiv. NADH	14% (**2a**)	8.15
Pyruvate (1a)	NH_3/NH_4Cl (1 M) 3 equiv. NADH	43%* (**2a**)	7.86

*One of the three independent reactions that were carried out in the same conditions.

4.2 Results of control reactions

Table S13. Data of conversion determined by ^{1}H-NMR of a pure sample of NADH (30 mM) in aqueous NH_3/NH_4Cl solution (200 mM) at pH 8 and at different reaction times. This data shows the appearance of ADPR and NAD^+ due to hydrolysis (and other redox side reactions) in the ammonia / ammonium aqueous solution, collected for comparison with the appearance of ADPR and NAD^+ in other reactions.

Ketoacid	**Time** (h)	**Amino acid** (**2**) (^{1}H-NMR Yield %)	**NADH** (remaining %)	**ADPR** (conversion %)	**NAD^+** (conversion %)
-	1	-	95.6	3.9	0.5
	24	-	91.2	6.4	2.4
	48	-	87.1	8.4	4.5
	72	-	85.4	10.0	4.6
	168	-	77.5	17.9	4.6

Table S14. Data of conversion determined by ^{1}H-NMR of a sample of NADH (30 mM), a mixture of pyruvate (**1a**, 30 mM) and NADH (30 mM) and a mixture of glyoxylate (**1c**, 28.3 mM) and NADH (30 mM), all of them in aqueous Na_2HPO_4/ NaH_2PO_4 solution (200 mM) at pH 8 and at different reaction times. Although it can be concluded that in phosphate solution there is more appearance of ADPR due to hydrolysis, it can also be derived that the presence of pyruvate (**1a**) and glyoxylate (**1c**) provokes more degradation to ADPR, even in the absence of ammonia. Remarkably, glyoxylate (**1c**) is the additive which generates the highest amount of ADPR by far.

Ketoacid	**Time** (h)	**Amino acid** (**2**) (^{1}H-NMR Yield %)	**NADH** (remaining %)	**ADPR** (conversion %)	**NAD^+** (conversion %)
-	1	-	93.4	4.5	2.0
	24	-	79.5	16.2	4.3
	48	-	70.0	25.4	4.6
	72	-	68.5	26.6	4.9
	168	-	59.7	32.9	7.4
Pyruvate (1a)	1	**0.0**	92.1	5.9	2.0
	24	**0.0**	72.5	24.8	2.7
	48	**0.0**	71.1	25.8	3.0
	72	**0.0**	58.8	38.1	3.1
	168	**0.0**	30.1	64.5	5.4
Glyoxylate (1c)	1	**0.0**	73.9	24.0	2.1
	24	**0.0**	22.7	74.1	3.2
	48	**0.0**	14.6	82.7	2.7
	72	**0.0**	9.4	88.7	1.9
	168	**0.0**	0.0	98.5	1.5

Table S15. Data of conversion determined by ^{1}H-NMR of a sample of NADH (30 mM), and a mixture of glyoxylate (**1c**, 30 mM) and NADH (30 mM), all of them in aqueous Na_2CO_3/ $NaHCO_3$ solution (200 mM) at pH 9 and at different reaction times.

Ketoacid	**Time** (h)	**Amino acid** (**2**) (^{1}H-NMR Yield %)	**NADH** (remaining %)	**ADPR** (conversion %)	**NAD^{+}** (conversion %)
-	1	-	91.84	6.50	1.66
	72	-	93.44	4.82	1.74
Glyoxylate (1c)	1	**0.0**	65.29	33.94	0.77
	72	**0.0**	34.27	63.91	1.82

5. ^{1}H-NMR spectra

NOTE: In all cases, to prepare samples for analysis, 450 µL of the reaction mixture were taken and mixed with 50 µL of a solution of TMSP-d_4 3 mM in D_2O, reaching the ratio H_2O:D_2O (9:1). The concentrations of NH_3/NH_4Cl and the concentration of compounds that appear at the bottom of the figures and in the tables are related to the sample before adding the TMSP-d_4 solution in D_2O. Signals referenced to TMSP-d_4 (0.00 ppm).

5.1 Spectra of cofactors NADH and NAD$^+$

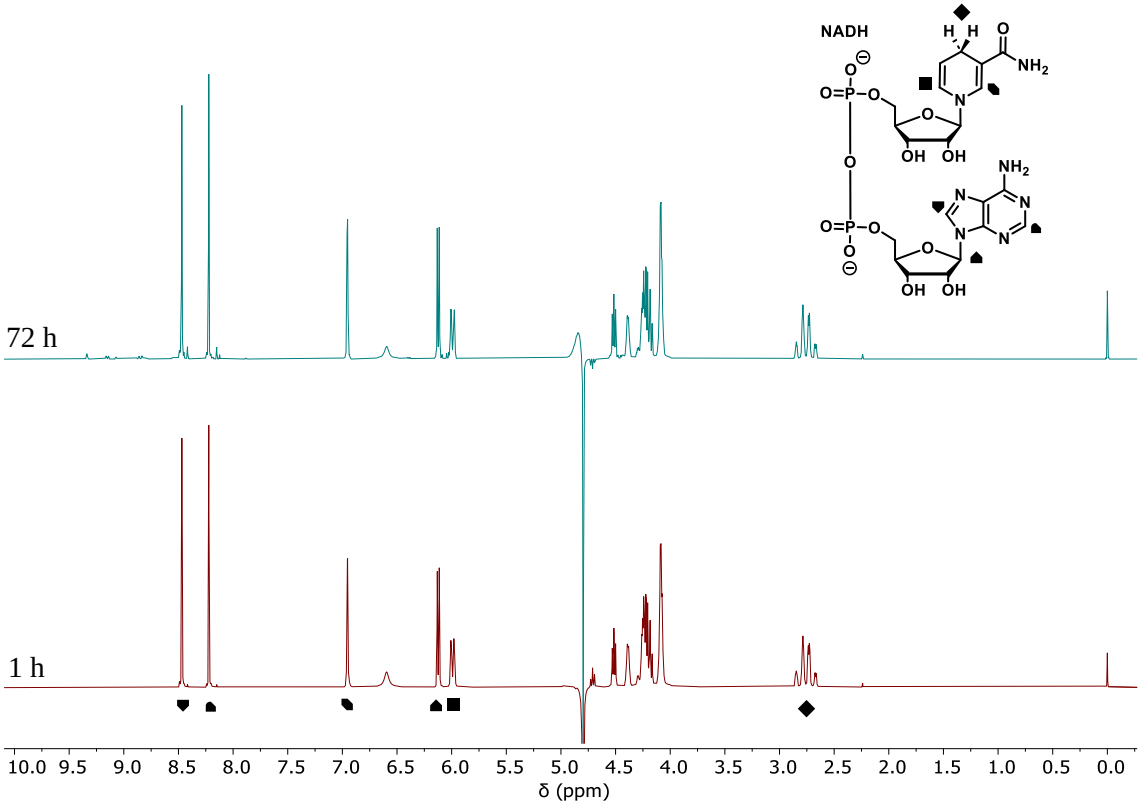

Figure S10. ^{1}H-NMR (300 MHz, H_2O:D_2O 9:1, noesygppr1d) spectra of NADH (30 mM) in aqueous NH_3/NH_4Cl solution (200 mM) at pH 8, after 1 h and 72 h, showing that NADH is quite stable in the reaction medium and experiences low levels of hydrolysis.

In these conditions, the signals of NADH are the following:

^{1}H NMR (300 MHz, H_2O:D_2O 9:1, noesygppr1d) δ 8.47 (s, 1H), 8.22 (s, 1H), 6.95 (d, *J* = 1.6 Hz, 1H), 6.12 (d, *J* = 5.4 Hz, 1H), 5.99 (dq, *J* = 8.2, 1.7 Hz, 1H), 4.71 (t, *J* = 5.3 Hz, 1H), 4.54 – 4.48 (m, 1H), 4.42 – 4.35 (m, 1H), 4.31 – 4.15 (m, 4H), 4.12 – 4.05 (m, 3H), 2.82 (dt, *J* = 18.1, 2.7 Hz, 1H), 2.70 (ddd, *J* = 18.2, 3.8, 1.5 Hz, 1H) (ribose signals and other signals are in the water suppression zone, presenting less integral than they should). Data match those previously reported.[2]

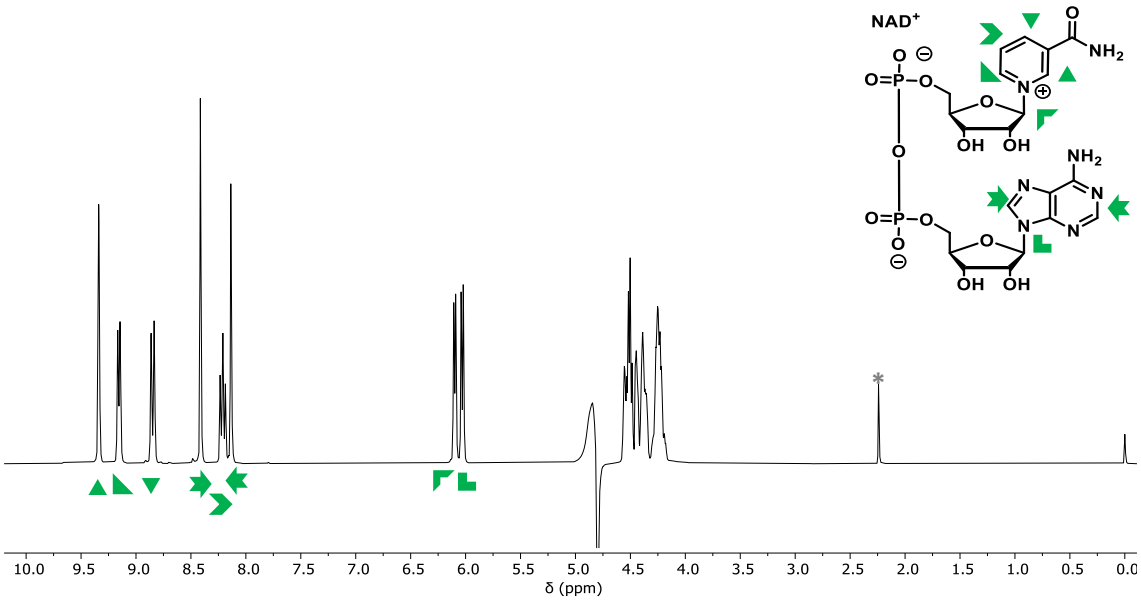

Figure S11. ^{1}H-NMR (300 MHz, H_2O:D_2O 9:1, noesygppr1d) spectrum of NAD^+ (30 mM) in aqueous NH_3/NH_4Cl solution (200 mM) at pH 8.

(* residual peak of acetone due to washing the NMR tube)

In these conditions, the signals of NAD^+ are the following:

^{1}H NMR (300 MHz, H_2O:D_2O 9:1, noesygppr1d) δ 9.34 (s, 1H), 9.16 (d, *J* = 6.2 Hz, 1H), 8.85 (d, *J* = 8.1 Hz, 1H), 8.41 (s, 1H), 8.21 (t, *J* = 7.1 Hz, 1H), 8.14 (s, 1H), 6.10 (d, *J* = 5.2 Hz, 1H), 6.03 (d, *J* = 5.9 Hz, 1H), 4.58 – 4.47 (m, 2H), 4.47 – 4.33 (m, 3H), 4.31 – 4.16 (m, 3H) (ribose signals are in the water suppression zone, presenting less integral than they should). Data match those previously reported.[2]

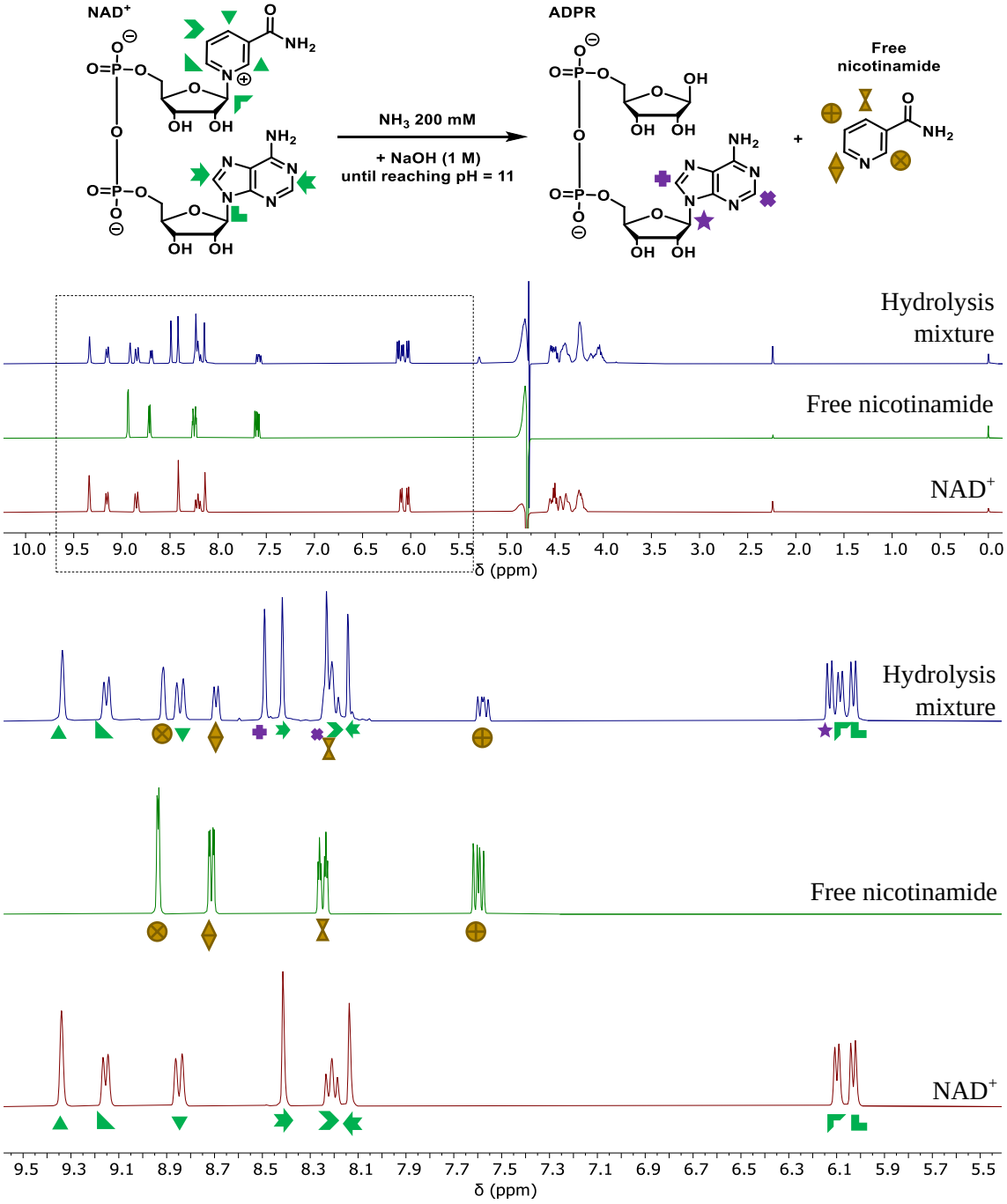

Figure S12. ^{1}H-NMR (300 MHz, H_2O:D_2O 9:1, noesygppr1d) spectrum of NAD^+ (30 mM) in aqueous NH_3 solution (200 mM) at pH 11 after 2 h, showing a partial hydrolysis into ADPR and free nicotinamide. The spectrum is compared with those of pure NAD^+ (30 mM, pH 8) and free nicotinamide (30 mM, pH 11) in NH_3/NH_4Cl 200 mM. Although this experiment was carried out in extreme conditions (pH 11), it is evidence that ADPR can be formed from hydrolysis of NAD^+.

In these conditions, the signals of the nicotinamide are the following ones:

^{1}H NMR (300 MHz, H_2O:D_2O 9:1, noesygppr1d) δ 8.93 (dd, *J* = 2.3, 0.9 Hz, 1H), 8.71 (dd, *J* = 5.0, 1.6 Hz, 1H), 8.25 (ddd, *J* = 8.0, 2.3, 1.6 Hz, 1H), 7.60 (ddd, *J* = 8.0, 5.0, 0.9 Hz, 1H).

In these conditions, the recognisable signals of ADPR which do not overlap with others are:

^{1}H NMR (300 MHz, H_2O:D_2O 9:1, noesygppr1d) δ 8.49 (s, 1H), 8.23 (s, 1H), 6.13 (d, *J* = 5.8 Hz, 1H). Data match those previously reported.[3]

5.2 Spectra related to the conversion of pyruvate (1a) into alanine (2a)

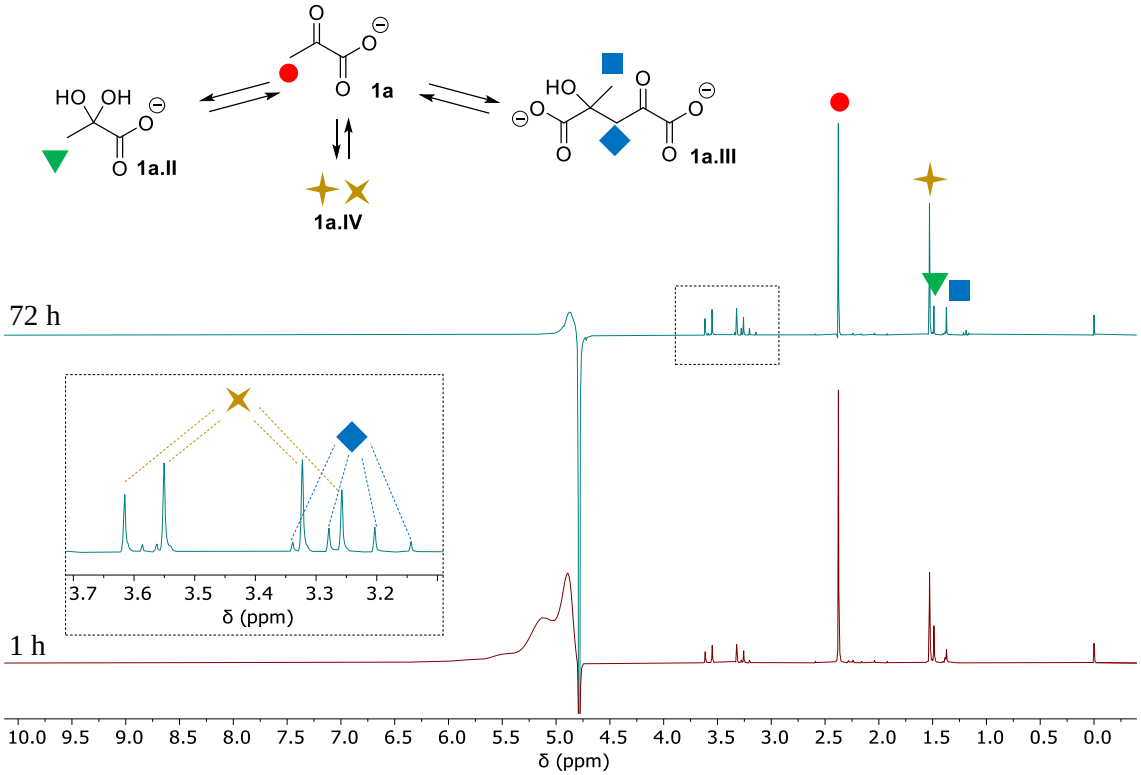

Figure S13. ^{1}H-NMR (300 MHz, H_2O:D_2O 9:1, noesygppr1d) spectra of pyruvate (**1a**, 30 mM) in aqueous NH_3/NH_4Cl solution (200 mM) at pH 8, after 1 h and 72 h, showing the stability of this substrate in the reaction medium when it is in absence of NADH.

Several forms are identified in the equilibrium. ^{1}H NMR (300 MHz, H_2O:D_2O, noesygppr1d):

Pyruvate (**1a**): δ 2.38 (s, 3H) ppm. According to R. J. Mayer *et al.*, pyruvate is in equilibrium with the corresponding imine and the signal is an average of these compounds.[4]

Pyruvate hydrate (**1a.II**): δ 1.49 (s, 3H) ppm. Data match those previously reported.[5, 6]

Parapyruvate (**1a.III**): δ 3.31 (d, *J* = 18.0 Hz, 1H), 3.17 (d, J = 17.9 Hz, 1H), 1.37 (s, 3H) ppm. Data match those previously reported.[6]

Byproduct (**1a.IV**): δ 3.58 (d, J = 19.5 Hz, 1H), 3.29 (d, J = 19.5 Hz, 1H), 1.53 (s, 3H). Since these spectroscopic signals have a similar pattern that those from the parapyruvate (**1a.III**) but they only appear in the aqueous NH_3/NH_4Cl solution, we speculate that it could also be an autocondensation adduct of pyruvate with its corresponding imine form.

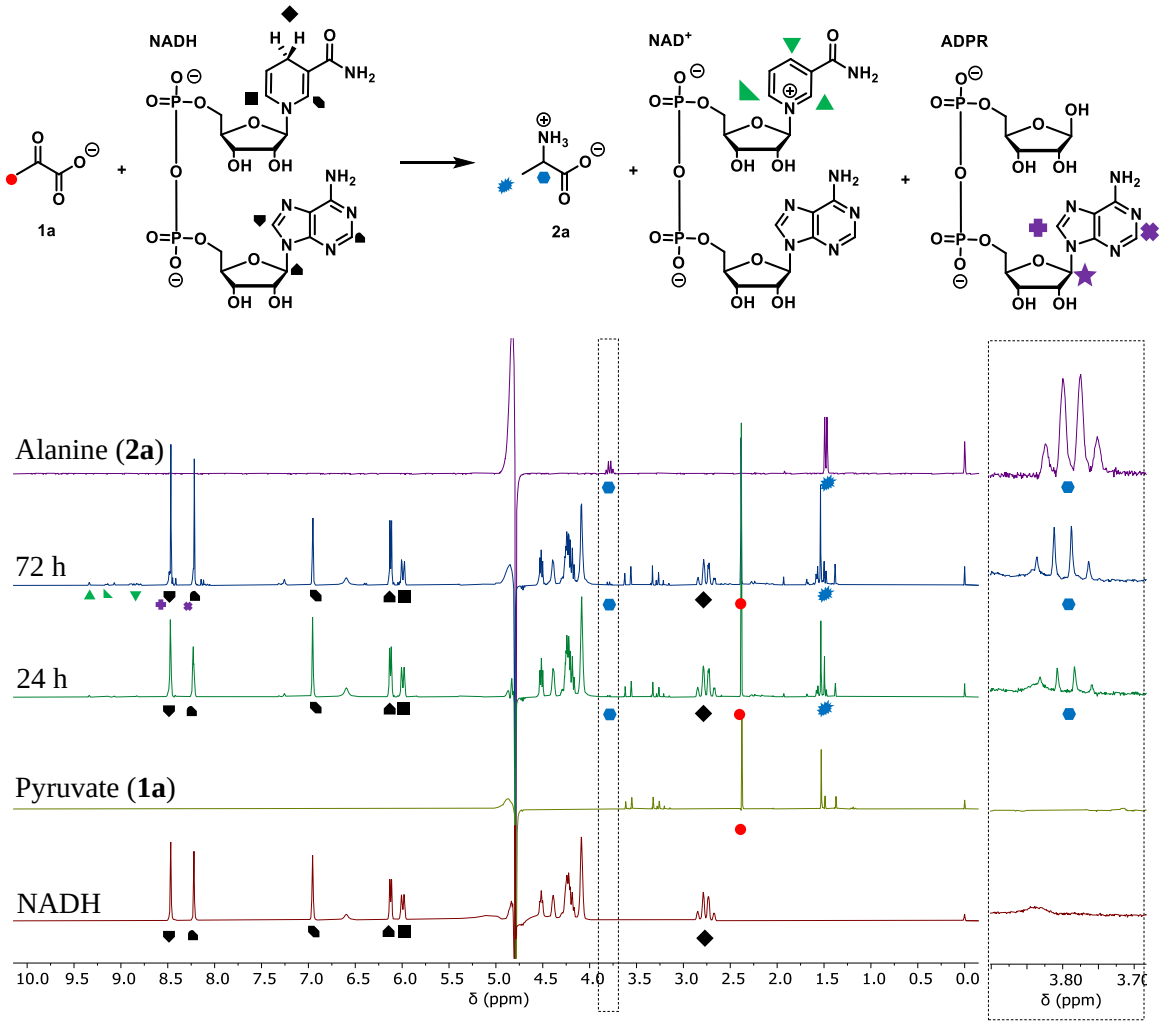

Figure S14. ^{1}H-NMR (300 MHz, H_2O:D_2O 9:1, noesygppr1d) spectra of the reaction between pyruvate (**1a**, 30 mM) and NADH (30 mM) to give alanine (**2a**) in aqueous NH_3/NH_4Cl solution (200 mM) at pH 8, after 24 h and 72 h of reaction. The reaction spectra are compared with those of pure NADH (30 mM), pyruvate (**1a**, 30 mM) and alanine (**2a**, 3 mM) in the same NH_3/NH_4Cl solution.

In these conditions, the signals of alanine (**2a**) are the following ones:

^{1}H NMR (300 MHz, H_2O:D_2O 9:1, noesygppr1d) δ 3.80 (q, J = 7.2 Hz, 1H) , 1.48 (d, J = 7.2 Hz, 3H). Data match those previously reported.[7]

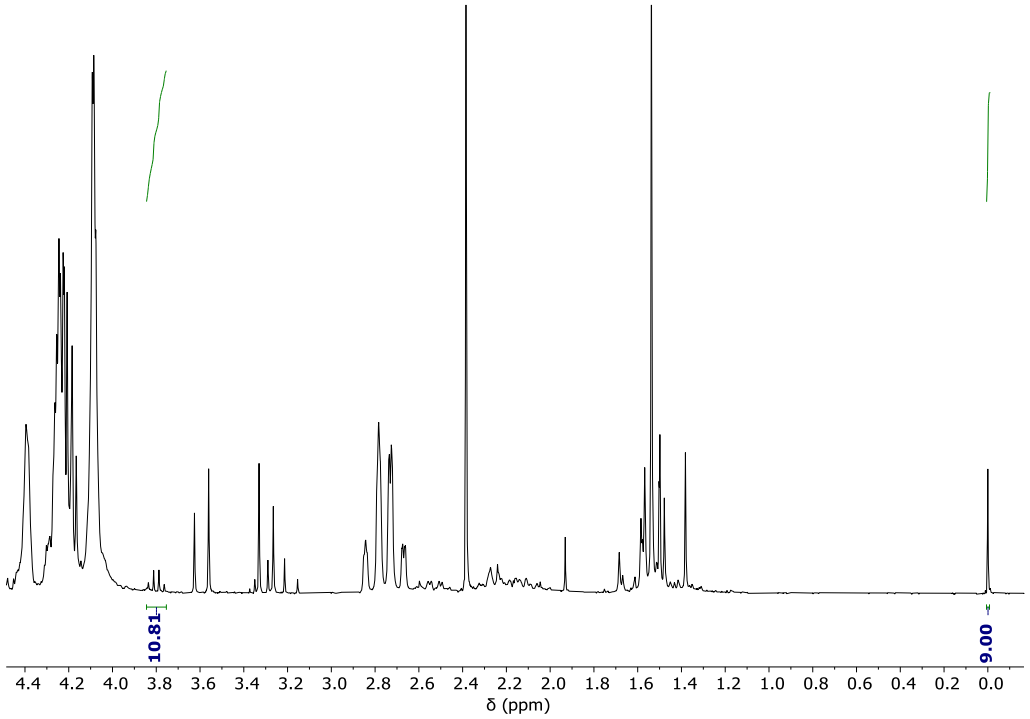

(See section 3.1 for calibration lines and section 3.2 for preparation of samples for NMR analysis)

Initial concentration of pyruvate (**1a**) = 30 mM

Once the integral of TMSP-d_4 [0.00 (s, 9H)] has been set to 9.00, the integral of alanine [3.80 (q, *J* = 7.2 Hz, 1H)] is taken and the concentration of alanine is obtained with the calibration line:

$$y = 3.24231x$$

Reaction time (h)	**Alanine integral**	**Alanine Conc.** (mM)	**Yield (%)**
1	3.60	1.11	**3.7**
24	6.65	2.05	**6.8**
48	9.59	2.96	**9.9**
72	10.81	3.33	**11.1**
168	9.08	2.80	**9.3**

Figure S15. ^{1}H-NMR (300 MHz, H_2O:D_2O 9:1, noesygppr1d) spectrum of the reaction of pyruvate (**1a**, 30 mM) with NADH (30 mM) in NH_3/NH_4Cl solution (200 mM) at pH 8 and 72 h of reaction. The calculations to determine the ^{1}H-NMR yield of alanine (**2a**) using the internal standard TMSP-d_4 are shown below the spectrum. This protocol has been applied to the rest of conditions and reaction times.

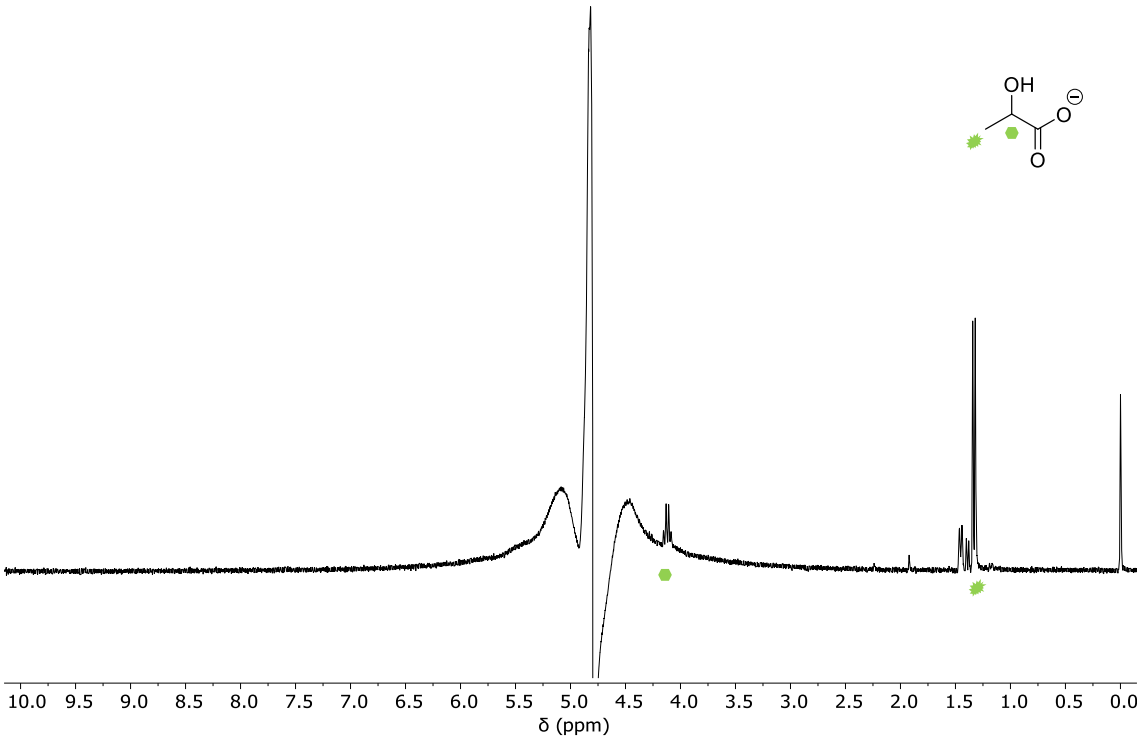

Figure S16. ^{1}H-NMR (300 MHz, H_2O:D_2O 9:1, noesygppr1d) spectrum of lactate (30 mM) in aqueous NH_3/NH_4Cl solution (200 mM) at pH 8.

In these conditions, the signals of lactate are the following ones:

^{1}H NMR (300 MHz, H_2O:D_2O 9:1, noesygppr1d) δ 4.12 (q, J = 6.9 Hz, 1H), 1.33 (d, *J* = 6.9 Hz, 3H).

These signals were not found in the spectra of different reactions of pyruvate (**1a**) with NADH.

5.3 Spectra related to the conversion of α-ketoglutarate (1b) into glutamate (2b)

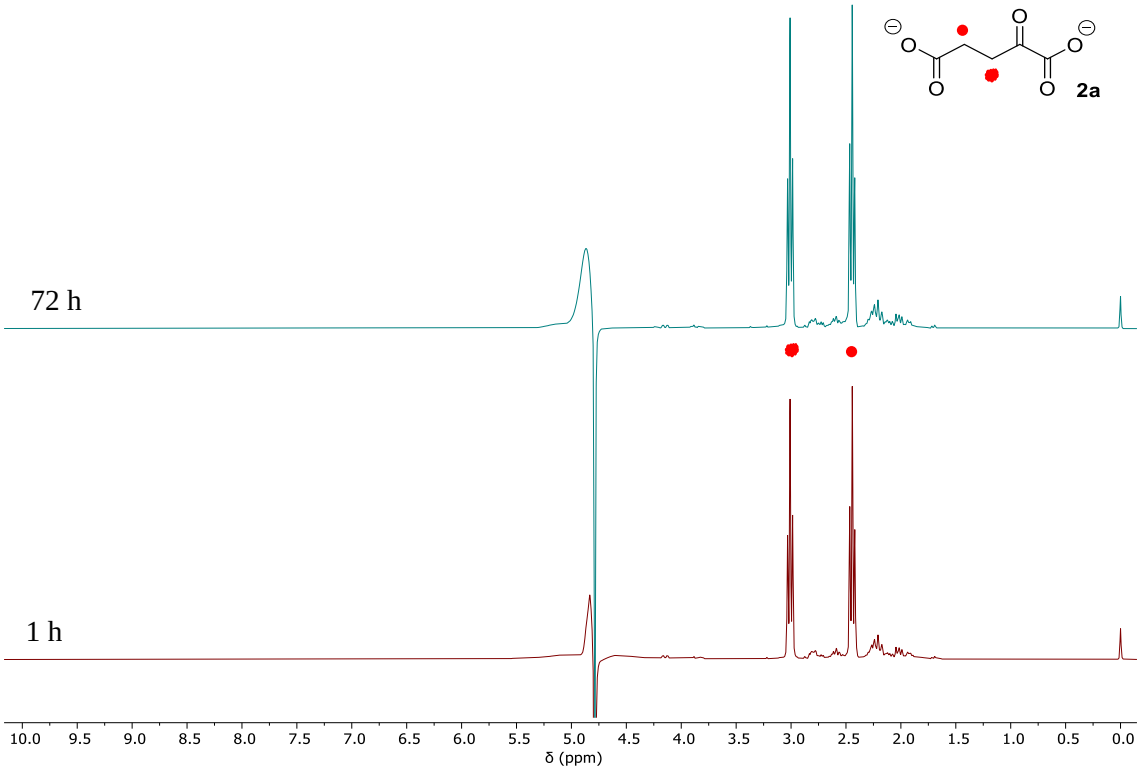

Figure S17. ^{1}H-NMR (300 MHz, H_2O:D_2O 9:1, noesygppr1d) spectra of α-ketoglutarate (**1b**, 30 mM) in aqueous NH_3/NH_4Cl solution (200 mM) at pH 8 and at 1h or 72 h of reaction, showing the stability of this substrate in the reaction medium when it is in absence of NADH. The compound is in equilibrium with several minor forms.

In these conditions, the signals of α-ketoglutarate (**1b**) are the following ones:

^{1}H NMR (300 MHz, H_2O:D_2O 9:1, noesygppr1d) δ 3.01 (t, *J* = 6.9 Hz, 2H), 2.44 (t, *J* = 6.9 Hz, 2H). Data match those previously reported.[4]

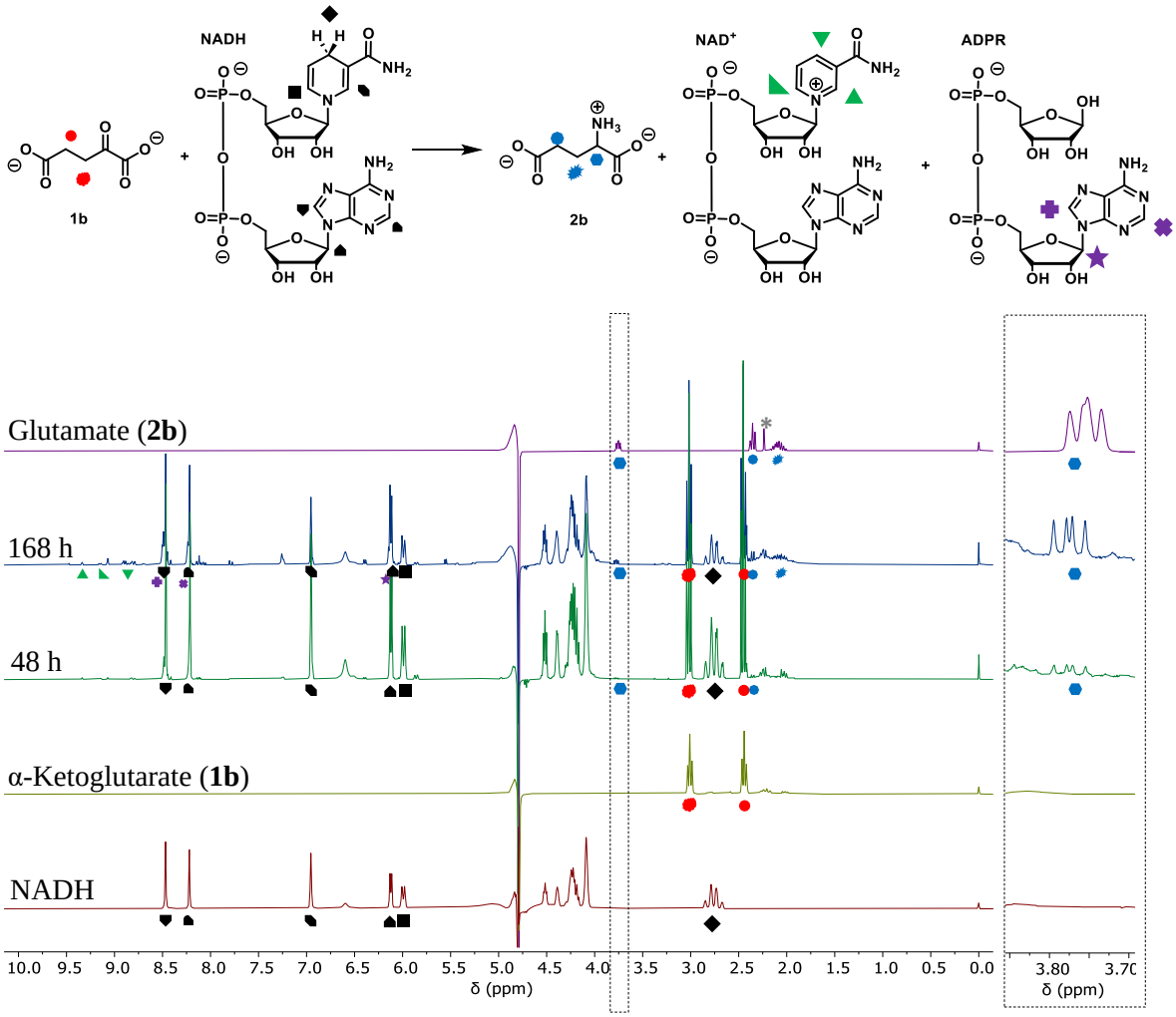

Figure S18. ^{1}H-NMR (300 MHz, H_2O:D_2O 9:1, noesygppr1d) spectra of the reaction between α-ketoglutarate (**1b**, 30 mM) and NADH (30 mM) to give glutamate (**2b**) in aqueous NH_3/NH_4Cl solution (200 mM) at pH 8, after 48 h and 168 h of reaction. The reaction spectra are compared with those of pure NADH (30 mM), α-ketoglutarate (**1b**, 30 mM) and glutamate (**2b**, 10 mM) in the same NH_3/NH_4Cl solution.

(* residual peak of acetone due to washing of the NMR tube)

In these conditions, the signals of glutamate (**2b**) are the following ones:

^{1}H NMR (300 MHz, H_2O:D_2O 9:1, noesygppr1d) δ 3.77 (dd, *J* = 7.1, 4.8 Hz, 1H), 2.35 (t, *J* = 7.5 Hz, 2H), 2.21 – 1.97 (m, 2H). Data match those previously reported.[7]

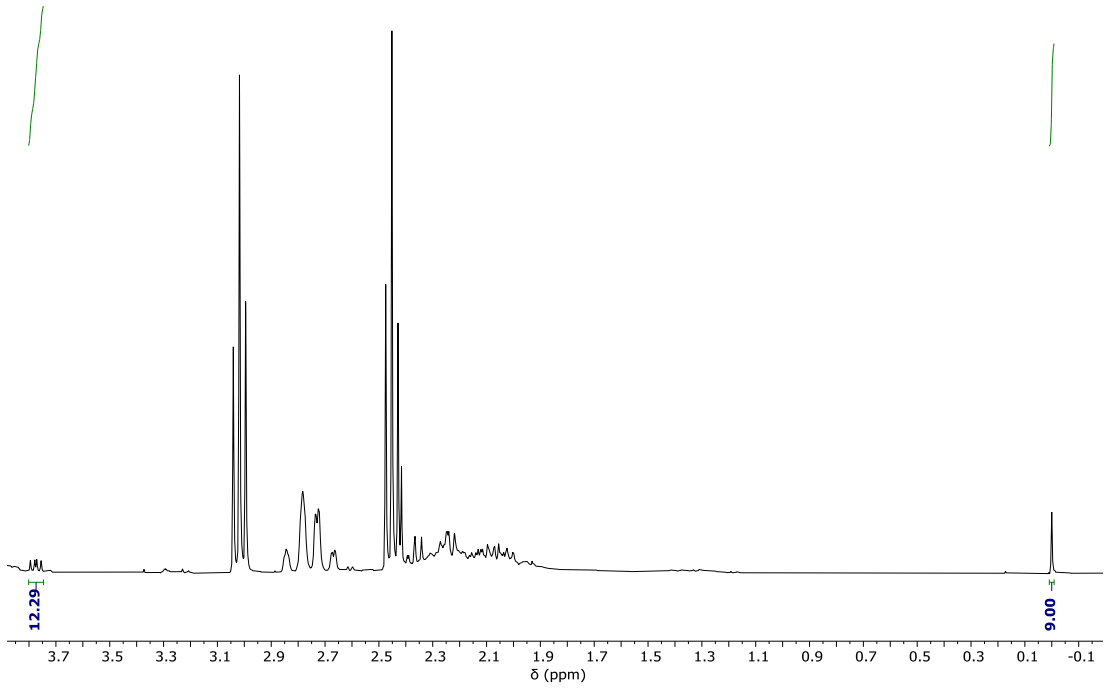

(See section 3.1 for calibration lines and section 3.2 for preparation of samples for NMR analysis)

Initial concentration of α-ketoglutarate (**1b**) = 30 mM

Once the integral of TMSP-d_4 [0.00 (s, 9H)] has been set to 9.00, the integral of glutamate [3.77 (dd, *J* = 7.1, 4.8 Hz, 1H)] is taken and the concentration of glutamate is obtained with the calibration line:

$$y = 3.78785x$$

Reaction time (h)	Glutamate integral	Glutamate Conc. (mM)	Yield (%)
1	0	0.00	**0.0**
24	3.94	1.04	**3.5**
48	5.42	1.43	**4.8**
72	9.01	2.38	**7.9**
168	12.29	3.24	**10.8**

Figure S19. ^{1}H-NMR (300 MHz, H_2O:D_2O 9:1, noesygppr1d) spectrum of the reaction of α-ketoglutarate (**1b**, 30 mM) with NADH (30 mM) in NH_3/NH_4Cl solution (200 mM) at pH 8 and 168 h of reaction. The calculations to determine the ^{1}H-NMR yield of aspartate (**2b**) using the internal standard TMSP-d_4 are shown below the spectrum. This protocol has been applied to the rest of conditions and reaction times.

5.4 Spectra related to the conversion of glyoxylate (1c) into glycine (2c)

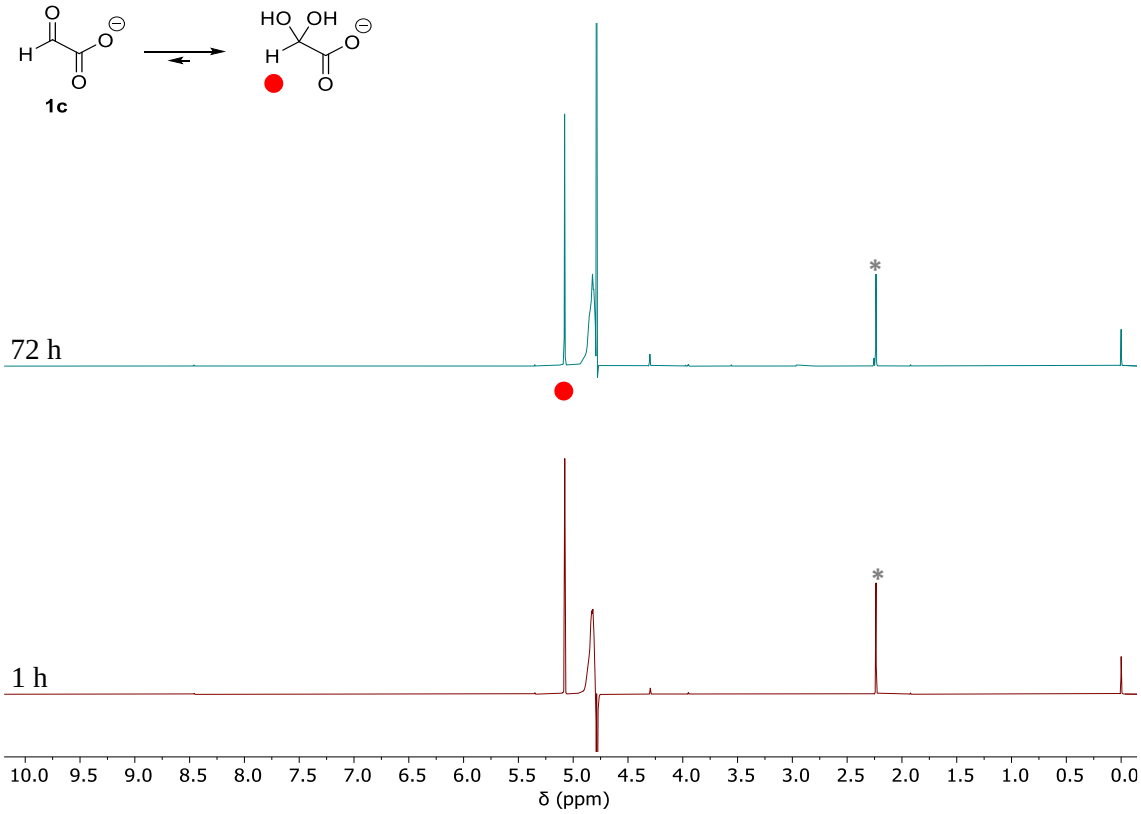

Figure S20. ^{1}H-NMR (300 MHz, H_2O:D_2O 9:1, noesygppr1d) spectra of glyoxylate (**1c**, 27.5 mM) in aqueous NH_3/NH_4Cl solution (200 mM) at pH 8 and after 1h or 72 h of reaction, showing the stability of this substrate in the reaction medium when it is in absence of NADH. The compound is mainly shifted towards the hydrate form.[4]

(* residual peak of acetone due to washing of the NMR tube)

In these conditions, the signals of glyoxylate hydrate are the following ones:

^{1}H NMR (300 MHz, H_2O:D_2O 9:1, noesygppr1d) δ 5.08 (s, 1H). Data match those previously reported.[4]

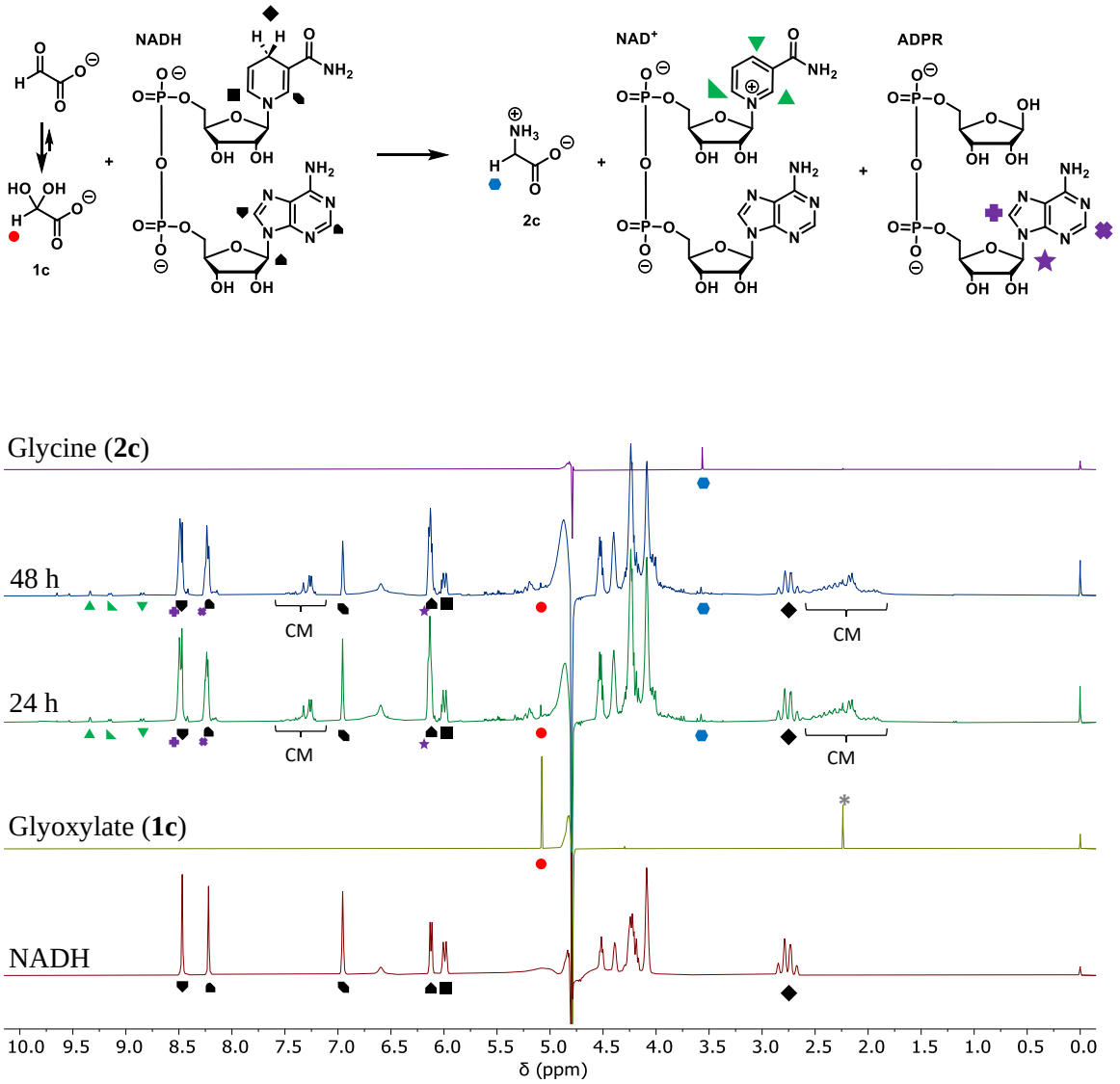

Figure S21. ^{1}H-NMR (300 MHz, H_2O:D_2O 9:1, noesygppr1d) spectra of the reaction between glyoxylate (**1c**, 27.5 mM) and NADH (30 mM) to give glycine (**2c**) in aqueous NH_3/NH_4Cl solution (200 mM) at pH 8, after 24 h and 48 h of reaction. The reaction spectra are compared with those of pure NADH (30 mM), glyoxylate (**1c**, 27.5 mM) and glycine (**2c**, 3 mM) in the same NH_3/NH_4Cl solution.

CM: Complex mixture region.

(* residual peak of acetone due to washing of the NMR tube)

In these conditions, the signals of glycine (**2c**) are the following ones:

^{1}H NMR (300 MHz, H_2O:D_2O 9:1, noesygppr1d) δ 3.58 (s, 2H). Data match those previously reported.[7]

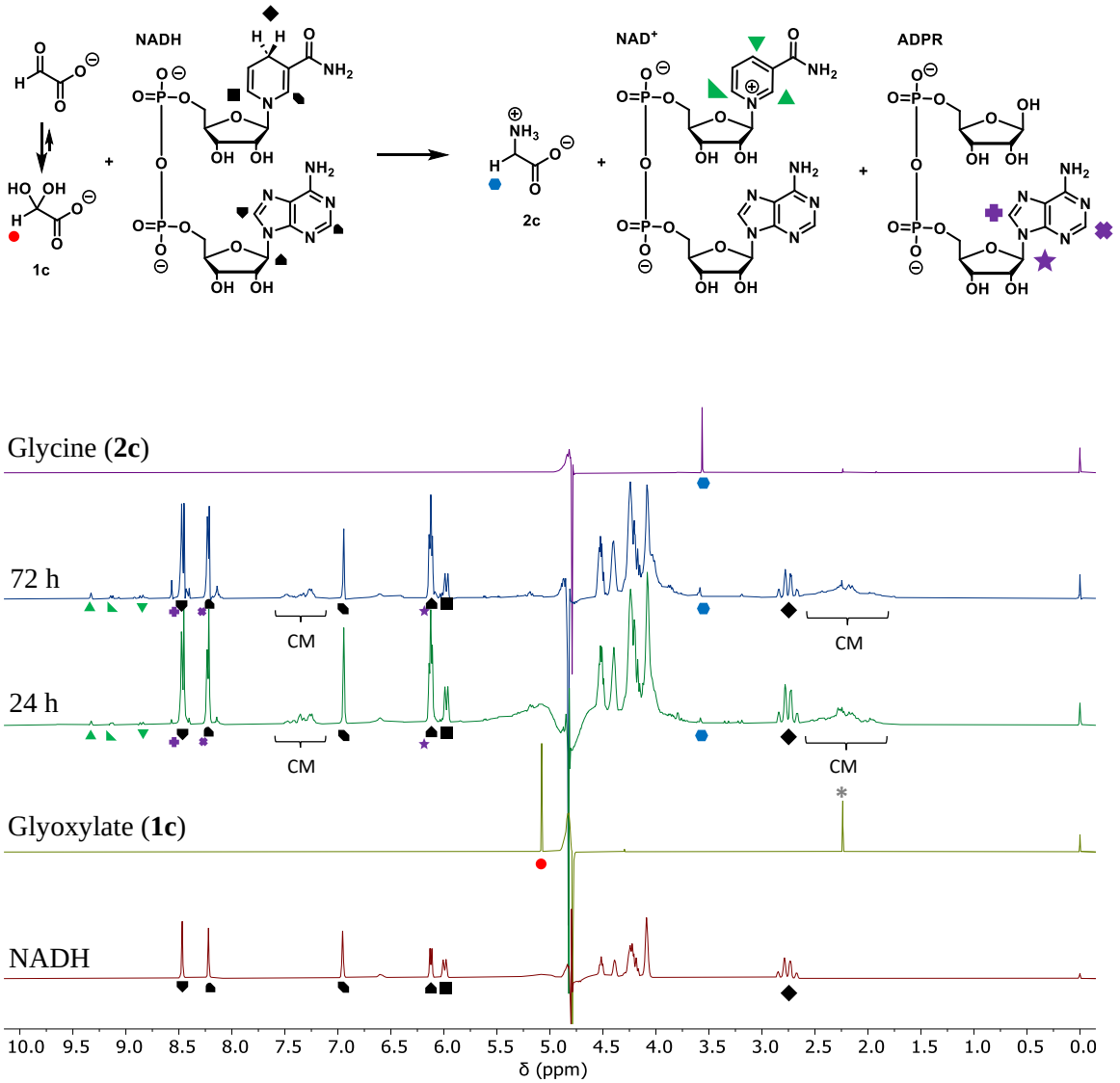

Figure S22. ^{1}H-NMR (300 MHz, H_2O:D_2O 9:1, noesygppr1d) spectra of the reaction between glyoxylate (**1c**, 30 mM) and NADH (30 mM) to give glycine (**2c**) in aqueous NH_3/NH_4Cl solution (1 M) at pH 8, after 24 h and 48 h of reaction. The reaction spectra are compared with those of pure NADH (30 mM), glyoxylate (**1c**, 27.5 mM) and glycine (**2c**, 3 mM) in the same NH_3/NH_4Cl solution.

CM: Complex mixture region.

(* residual peak of acetone due to washing of the NMR tube)

In these conditions, the signals of glycine (**2c**) are the following ones:

^{1}H NMR (300 MHz, H_2O:D_2O 9:1, noesygppr1d) δ 3.58 (s, 2H). Data match those previously reported.[7]

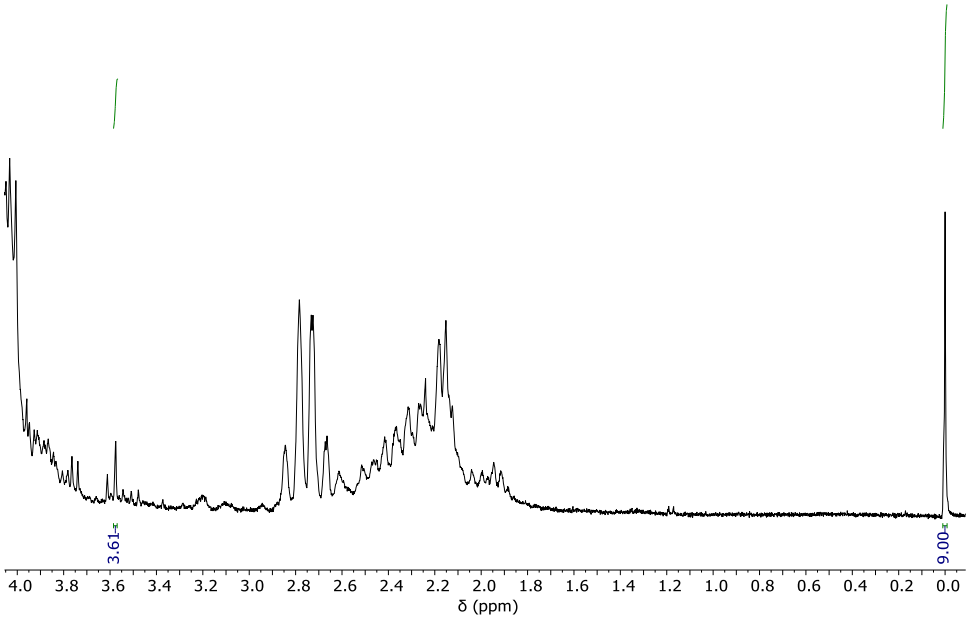

(See section 3.1 for calibration lines and section 3.2 for preparation of samples for NMR analysis)

Initial concentration of glyoxylate (**1c**) = 27.5 mM

Once the integral of TMSP-d_4 [0.00 (s, 9H)] has been set to 9.00, the integral of glycine [3.58 (s, 2H)] is taken and the concentration of glycine is obtained with the calibration line:

$$y = 6.49087x$$

Reaction time (h)	Glycine integral	Glycine Conc. (mM)	Yield (%)
1	0	0.00	**0.0**
24	2.81	0.43	**1.6**
48	3.61	0.56	**2.0**
72	3.41	0.53	**1.9**
168	3.22	0.50	**1.8**

Figure S23. ^{1}H-NMR (300 MHz, H_2O:D_2O 9:1, noesygppr1d) spectrum of the reaction of glyoxylate (**1c**, 27.5 mM) with NADH (30 mM) in NH_3/NH_4Cl solution (200 mM) at pH 8 and 48 h of reaction. The calculations to determine the ^{1}H-NMR yield of glycine (**2c**) using the internal standard TMSP-d_4 are shown below the spectrum. This protocol has been applied to the rest of conditions and reaction times.

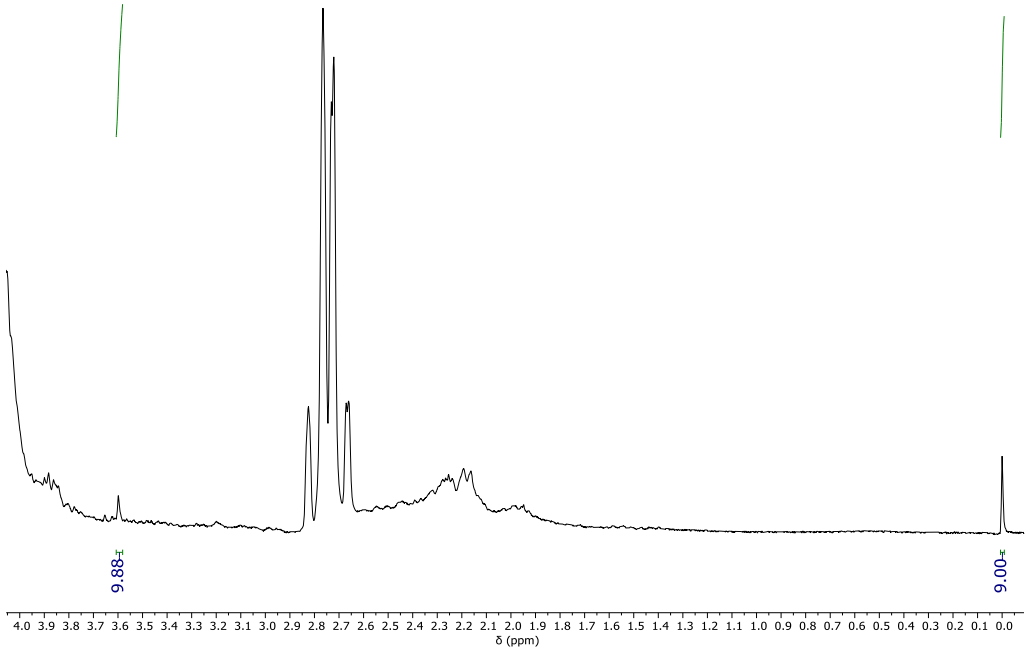

(See section 3.1 for calibration lines and section 3.2 for preparation of samples for NMR analysis)

Initial concentration of glyoxylate (**1c**) = 30.0 mM

Once the integral of TMSP-d_4 [0.00 (s, 9H)] has been set to 9.00, the integral of glycine [3.58 (s, 2H)] is taken and the concentration of glycine is obtained with the calibration line:

$$y = 6.49087x$$

Reaction time (h)	Glycine integral	Glycine Conc. (mM)	Yield (%)
1	5.12	0.79	**2.6**
24	9.54	1.47	**4.9**
48	11.6	1.79	**6.0**
72	9.88	1.52	**5.1**
168	8.27	1.27	**4.2**

Figure S24. ^{1}H-NMR (300 MHz, H_2O:D_2O 9:1, noesygppr1d) spectrum of the reaction of glyoxylate (**1c**, 30 mM) with 3 equivalents of NADH (90 mM) in NH_3/NH_4Cl solution (1 M) at pH 8 and 72 h of reaction (one of the three independent reactions that were carried out in the same conditions). The calculations to determine the ^{1}H-NMR yield of glycine (**2c**) using the internal standard TMSP-d_4 are shown below the spectrum. This protocol has been applied to the rest of conditions and reaction times.

5.5 Spectra of decarboxylation of oxaloacetate (1d) and conversion into alanine (2a)

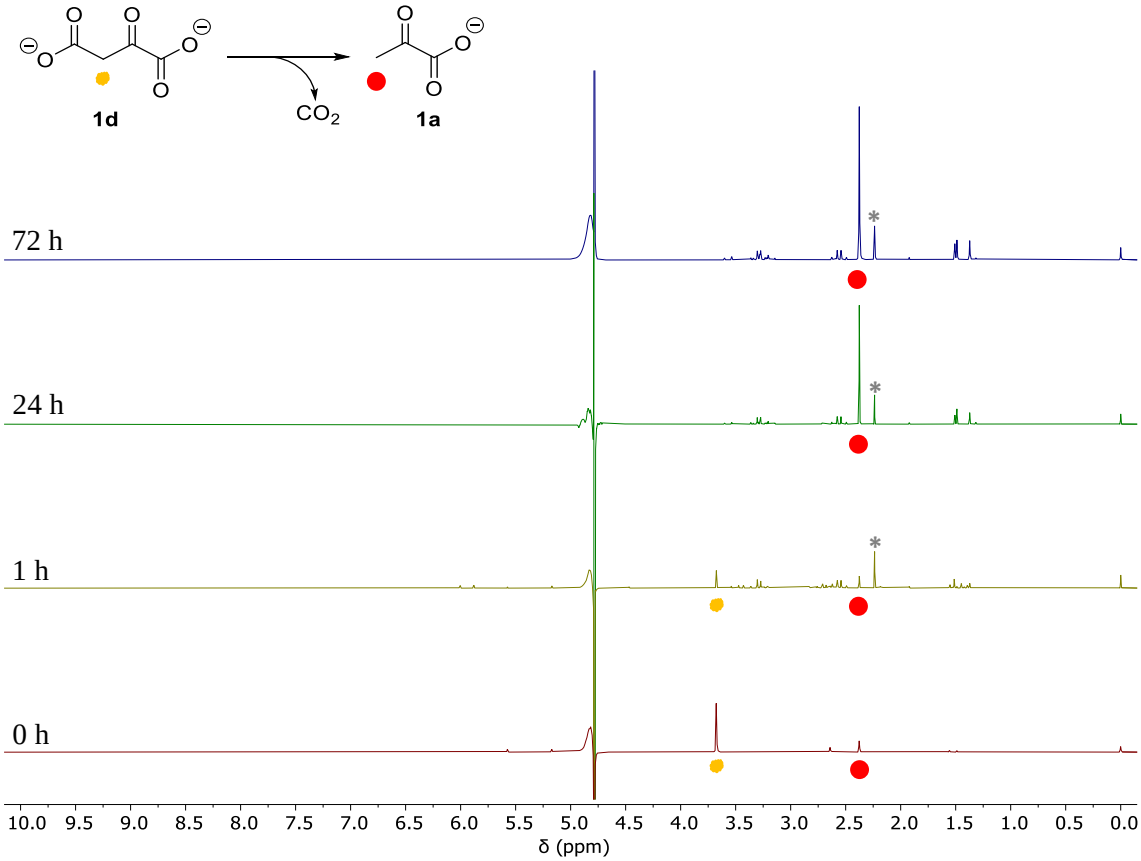

Figure S25. ^{1}H-NMR (300 MHz, H_2O:D_2O 9:1, noesygppr1d) spectra of oxaloacetate (**1d**, 25.6 mM) in aqueous NH_3/NH_4Cl solution (200 mM) at pH 8 after 0 h (before freeze-pump-thaw cycles), 1 h, 24 h and 72 h of reaction, showing the stability of this substrate in the reaction medium when it is in absence of NADH. Oxaloacetate rapidly converts to pyruvate (**1a**).

(* residual peak of acetone due to washing of the NMR tube)

In these conditions, the signals of oxaloacetate (**1d**) are the following ones:

^{1}H NMR (300 MHz, H_2O:D_2O 9:1, noesygppr1d) δ 3.68 (s, 2H). Data match those previously reported.[4]

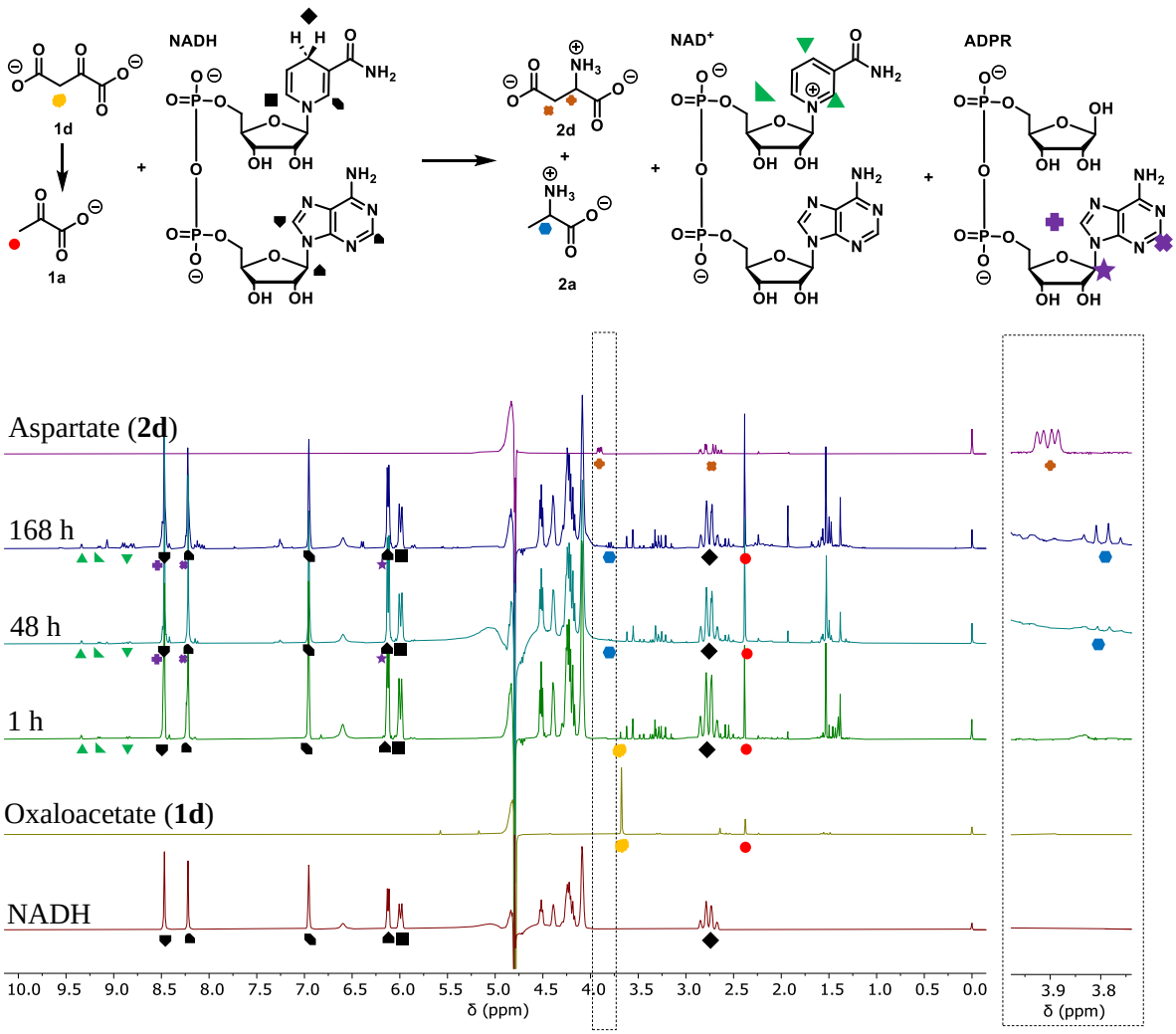

Figure S26. ^{1}H-NMR (300 MHz, H_2O:D_2O 9:1, noesygppr1d) spectra of the reaction between oxaloacetate (**1d**, 25.6 mM) and NADH (30 mM) in aqueous NH_3/NH_4Cl solution (200 mM) at pH 8 and after 1h, 48 h and 168 h of reaction. The reaction spectra are compared with those of pure NADH (30 mM), oxaloacetate (**1d**, 25.6 mM) and aspartate (**2d**, 3 mM) in the same NH_3/NH_4Cl solution. Oxaloacetate-rapidly converts to pyruvate (**1a**), which evolves into alanine (**2a**). No aspartate (**2d**) is observed in the reaction mixture.

In these conditions, the signals of aspartate (**2d**) are the following ones:

^{1}H NMR (300 MHz, H_2O:D_2O 9:1, noesygppr1d) δ 3.91 (dd, *J* = 8.7, 3.9 Hz, 1H), 2.82 (dd, *J* = 17.5, 3.9 Hz, 1H), 2.67 (dd, *J* = 17.4, 8.7 Hz, 1H). These signals were not observed in the reaction mixture. Data match those previously reported.[7]

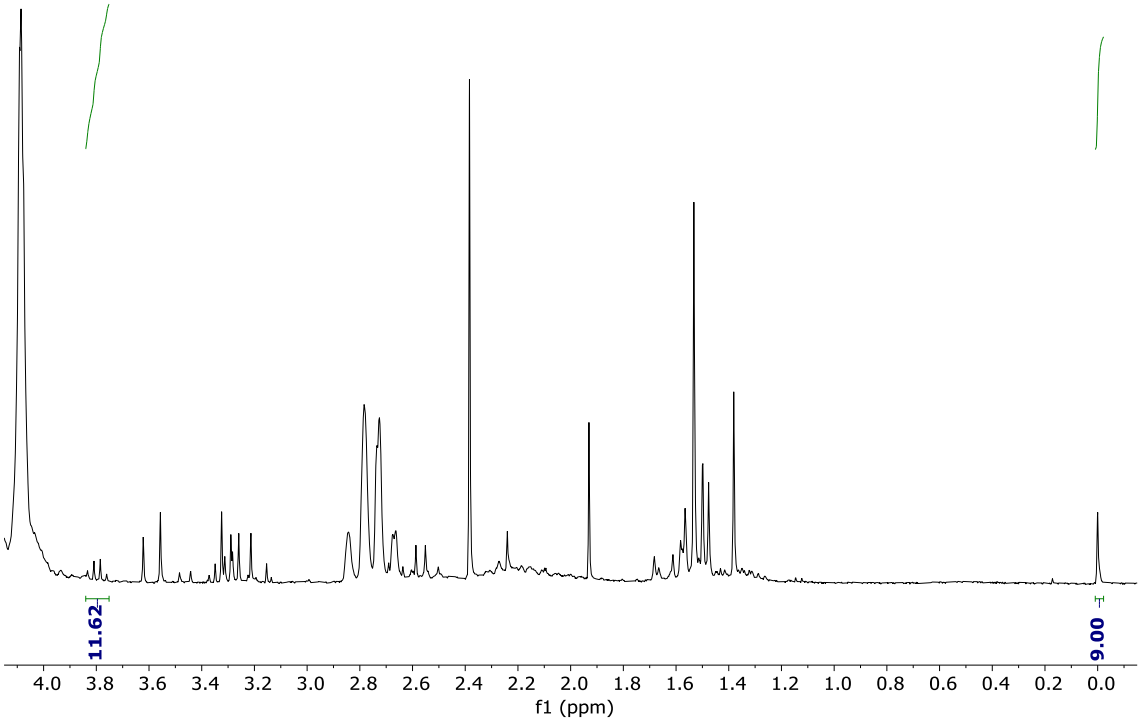

(See section 3.1 for calibration lines and section 3.2 for preparation of samples for NMR analysis)

Initial concentration of oxaloacetate (**1d**) = 25.6 mM

Once the integral of TMSP-d_4 [0.00 (s, 9H)] has been set to 9.00, the integral of alanine [3.80 (q, *J* = 7.2 Hz, 1H)] is taken and the concentration of alanine is obtained with the calibration line:

$$y = 3.24231x$$

Reaction time (h)	Alanine integral	Alanine Conc. (mM)	Yield (%)
1	0	0	**0.0**
24	traces	traces	**traces**
48	traces	traces	**traces**
72	4.13	1.27	**5.0**
168	11.62	3.58	**14.0**

Figure S27. ^{1}H-NMR (300 MHz, H_2O:D_2O 9:1, noesygppr1d) spectrum of the reaction of oxaloacetate (**1d**, 25.6 mM) with NADH (30 mM) in NH_3/NH_4Cl solution (200 mM) at pH 8 and 168 h of reaction. The calculations to determine the ^{1}H-NMR yield of alanine (**2a**) (after decarboxylation of **1d**) using the internal standard TMSP-d_4 are shown below the spectrum. This protocol has been applied to the rest of conditions and reaction times.

5.6 Spectra of control experiments

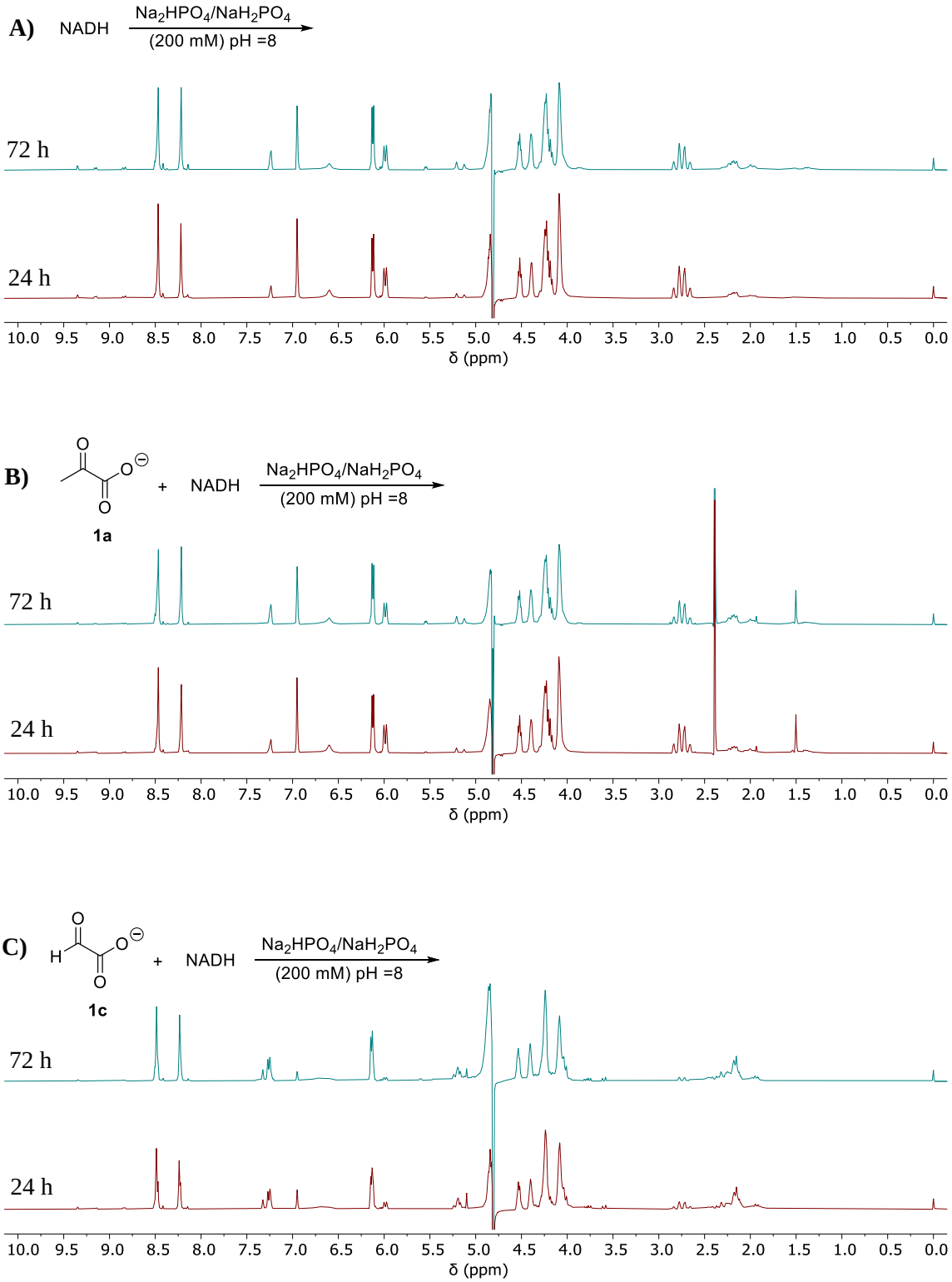

Figure S28. ^{1}H-NMR (300 MHz, H_2O:D_2O 9:1, noesygppr1d) spectra of the reactions carried out in aqueous Na_2HPO_4/ NaH_2PO_4 solution (200 mM) at pH 8 after 24 h and 72 h of reaction. A) Control solution of NADH (30 mM). B) Reaction between pyruvate (**1a**, 30 mM) and NADH (30 mM). C) Reaction between glyoxylate (**1c**, 28.3 mM) and NADH (30 mM). Neither alanine (**2a**) nor glycine (**2c**) were observed in the reaction media.

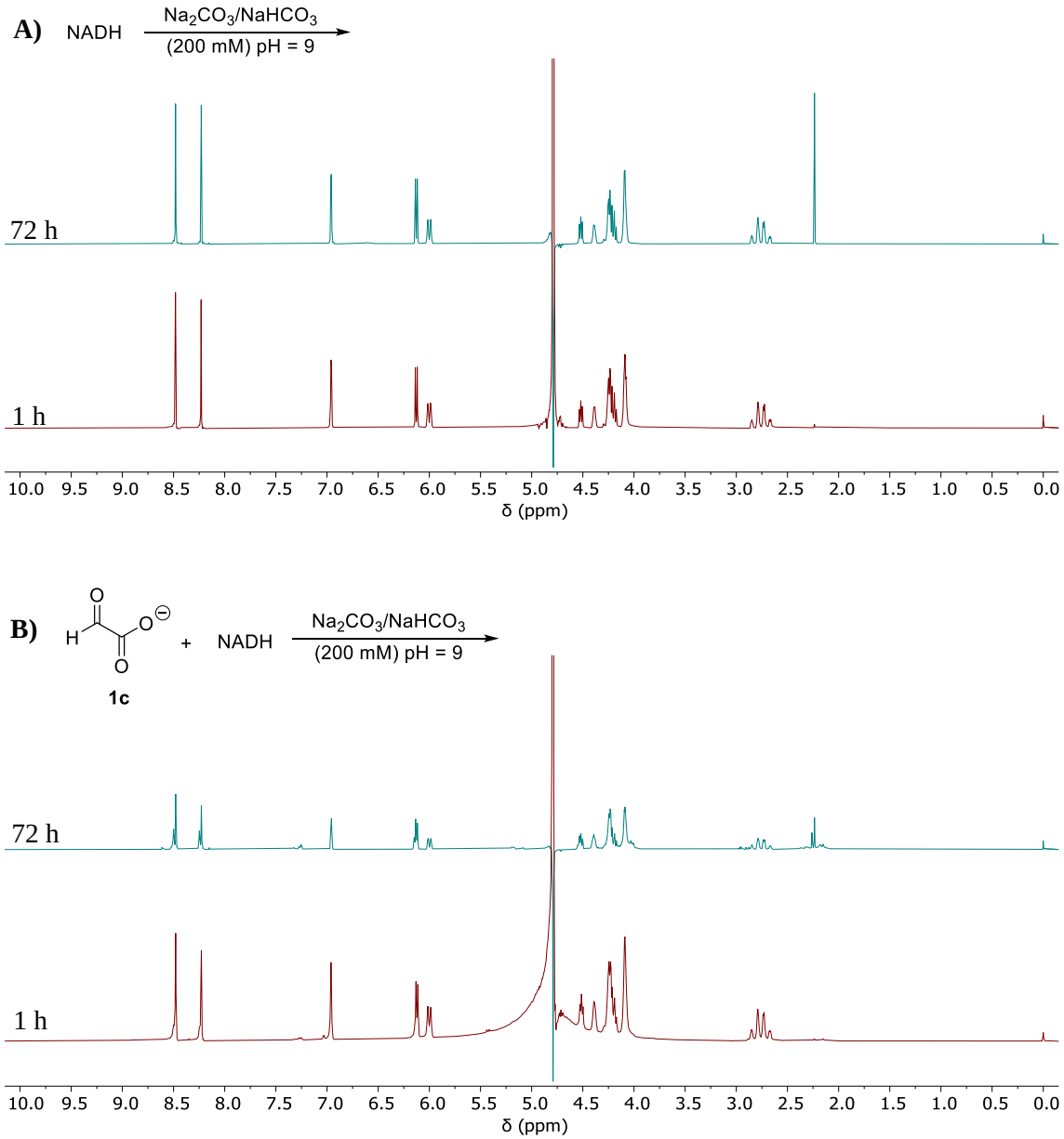

Figure S29. ^{1}H-NMR (300 MHz, H_2O:D_2O 9:1, noesygppr1d) spectra of the reactions carried out in aqueous Na_2CO_3/ $NaHCO_3$ solution (200 mM) at pH 9 after 1 h and 72 h of reaction. A) Control solution of NADH (30 mM). B) Reaction between glyoxylate (**1c**, 28.0 mM) and NADH (30 mM). No glycine (**2c**) was observed in the reaction medium.

6. GC-MS analyses

Pure samples of amino acids and the reaction mixtures were derivatized using ethyl chloroformate, pyridine, ethanol and potassium hydroxide, following the procedure described in the Methods section. Scheme S2 shows the products and their respective ion fragments that are observed in an electron ionization mass spectrum.[1]

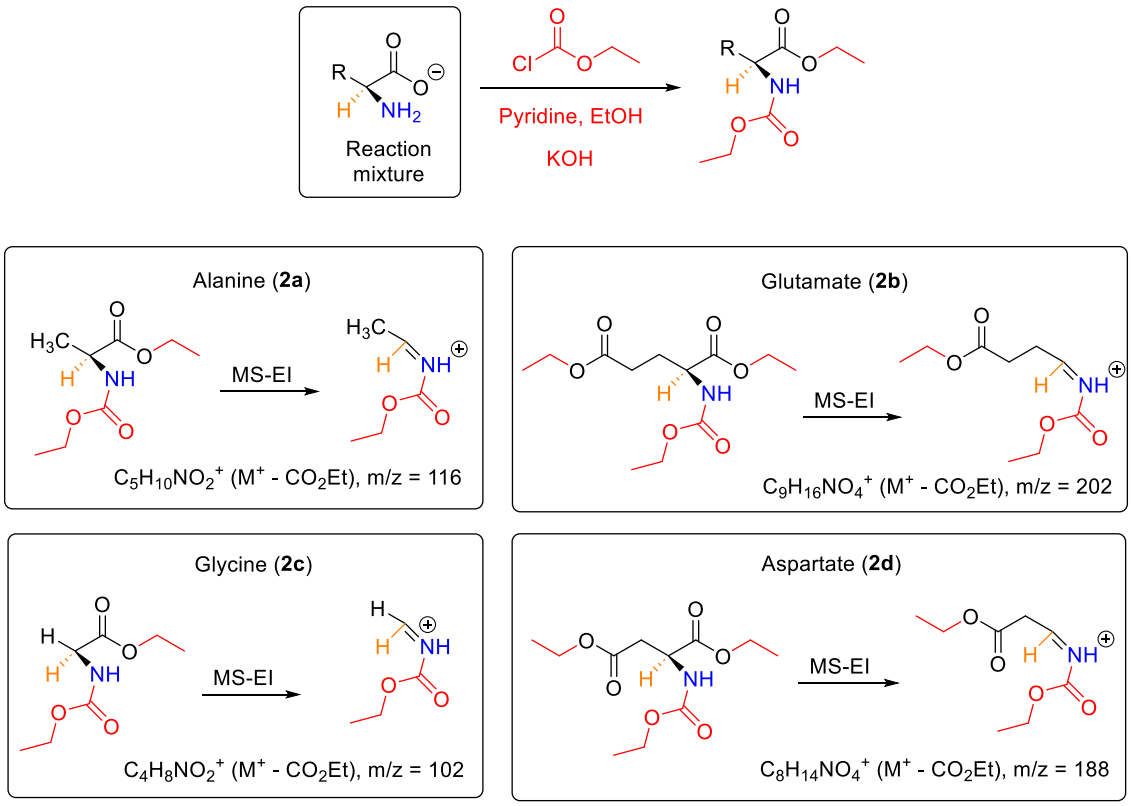

Scheme S2. Derivatized amino acids and their more abundant ion in mass spectrometry.

6.1 NADH

A pure sample of NADH was derivatized with the same protocol and subjected to GC-MS analysis, giving a peak at 6.9 min with a characteristic pattern of mass signals. This peak is indicative of NADH presence, and in the following chromatograms it is marked with a green label (these chromatogram peaks always present the same mass spectrum)

In addition, in most of the chromatograms there is a peak at 6.5 min with the same mass spectrum, which could be a byproduct from the derivatization process. In the following chromatograms, it is marked with a red label (these chromatogram peaks always present the same mass spectrum).

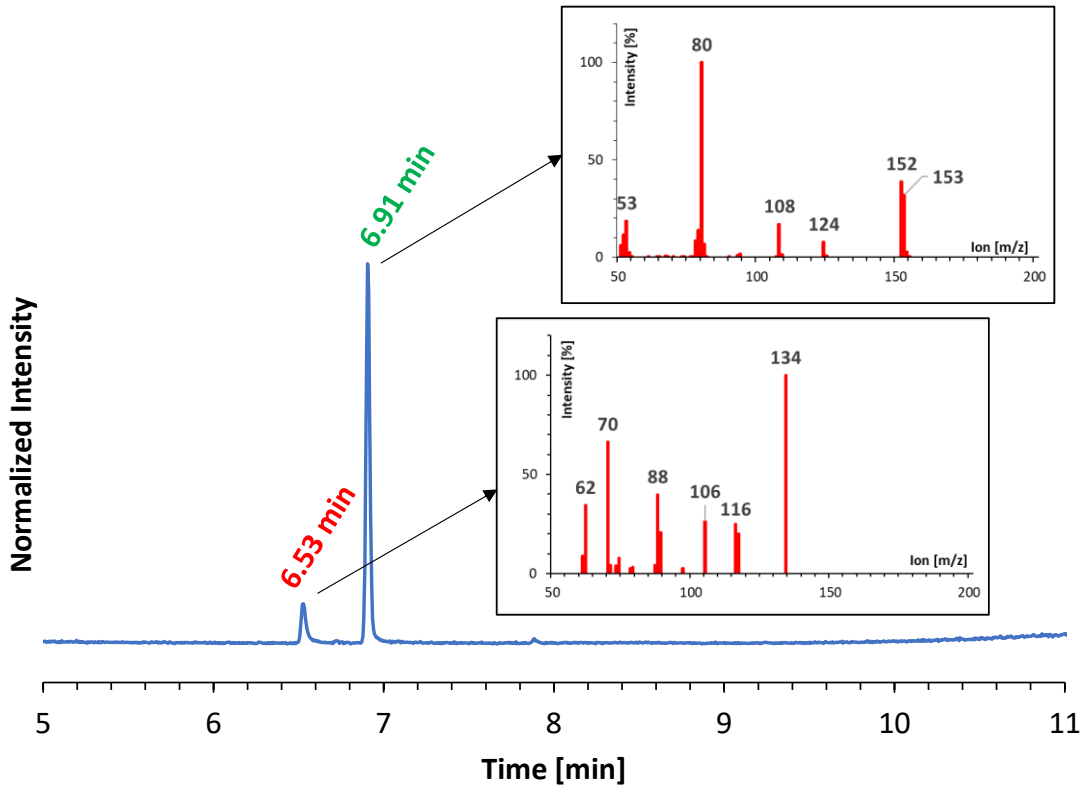

Figure S30. GC-MS analysis of a NADH authentic sample derivatized following the standard protocol with ECF. The MS spectra for the GC peaks with RT of 6.5 min and 6.9 min are shown in the insets.

6.2 Reaction of pyruvate (1a) to alanine (2a)

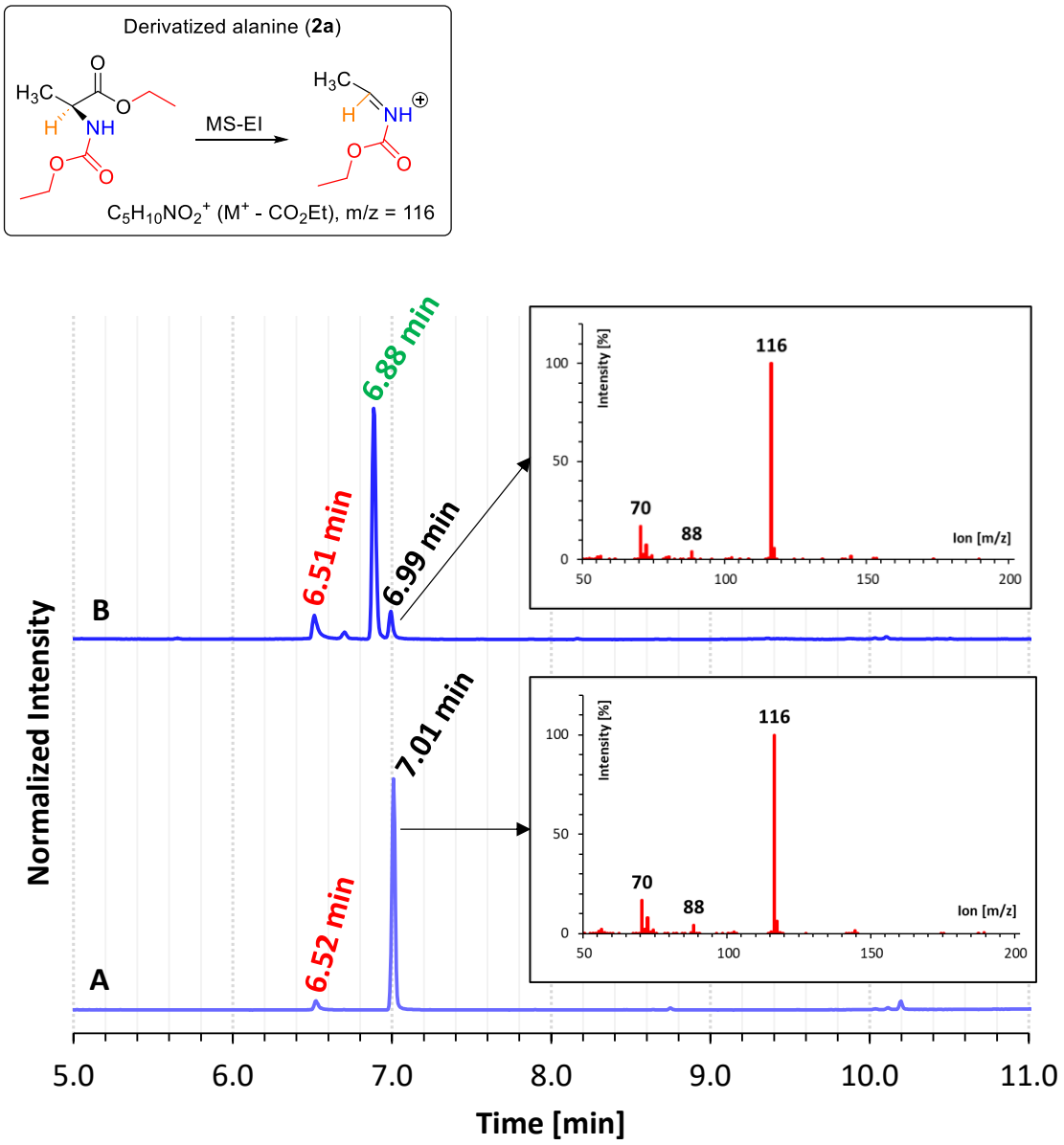

Figure S31. (**A**) GC-MS analysis of an alanine (**2a**) authentic sample derivatized following the standard protocol with ECF. (**B**) GC-MS analysis of the reaction between pyruvate (**1a**, 30 mM) and NADH (30 mM) to give alanine (**2a**), carried out in aqueous NH_3/NH_4Cl solution (200 mM) at pH 8 and derivatized after 168 h following the standard protocol with ECF. In both cases, the MS spectra for the GC peak with RT of 7.0 min, which corresponds to derivatized alanine, are shown in the inset.

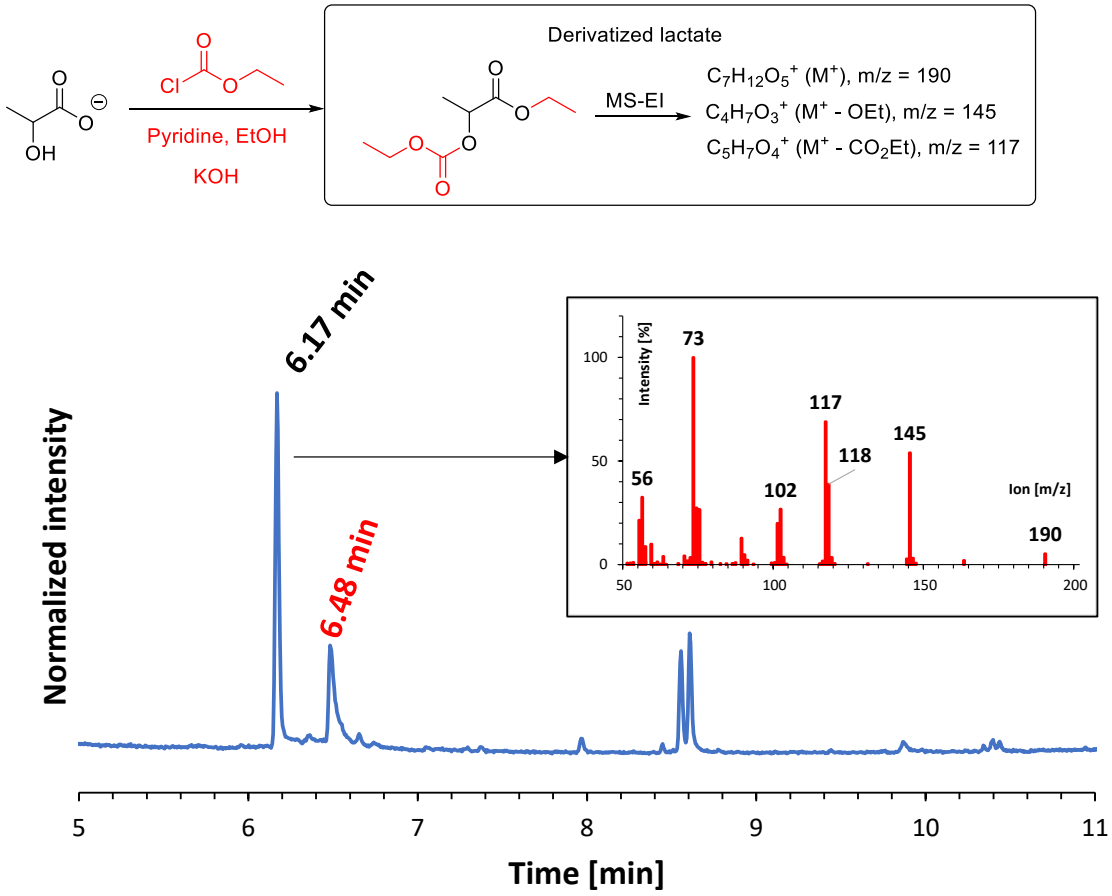

Figure S32. GC-MS analysis of a lactate authentic sample derivatized following the standard protocol with ECF. The peak of 6.17 min and its corresponding mass spectrum is not observed in the chromatogram of the reaction of glyoxylate (**1a**), suggesting that this compound is not formed during the reaction.

6.3 Reaction of α-ketoglutarate (1b) to glutamate (2b)

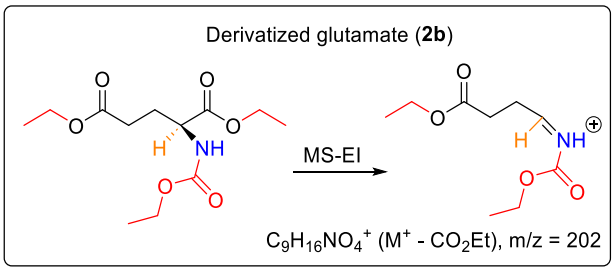

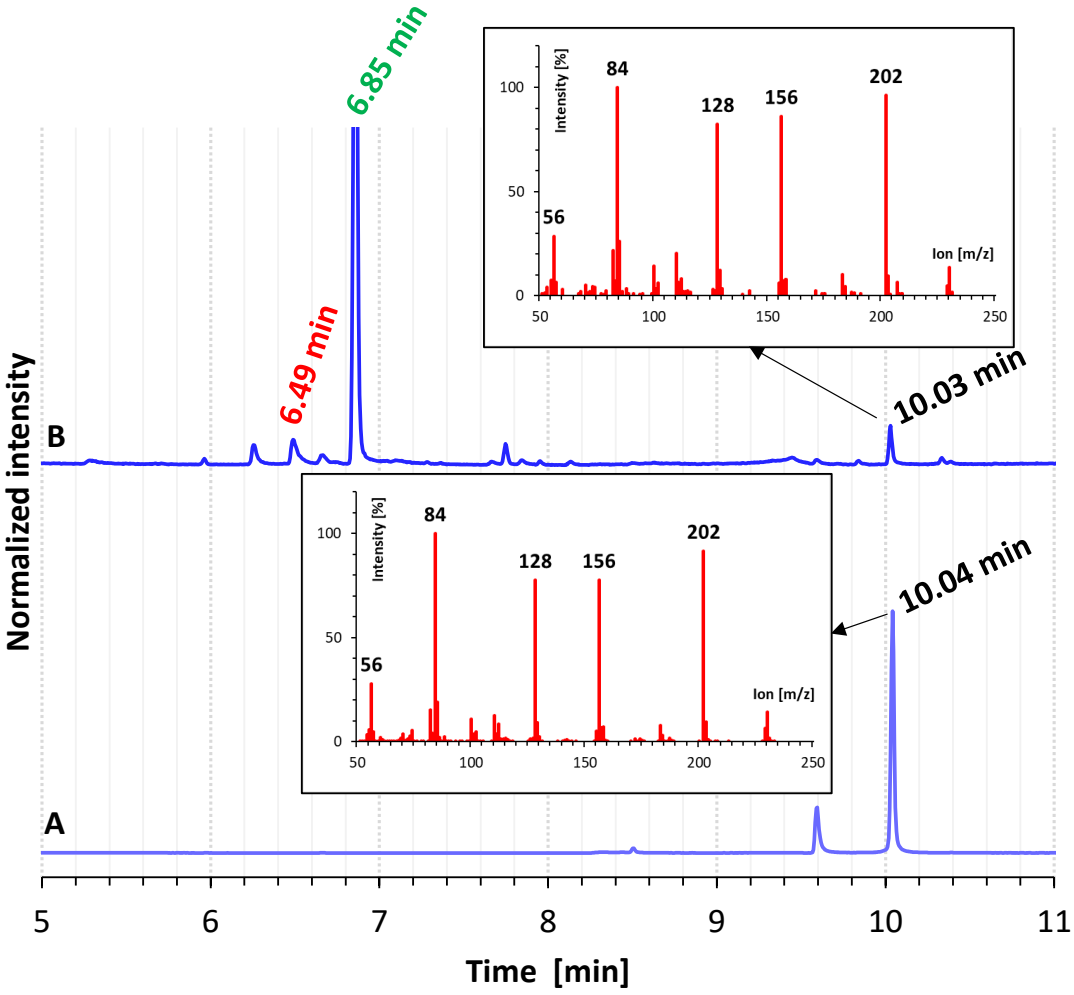

Figure S33. (**A**) GC-MS analysis of a glutamate (**2b**) authentic sample derivatized following the standard protocol with ECF. (**B**) GC-MS analysis of the reaction between α-ketoglutarate (**1b**, 30 mM) and NADH (30 mM) to give glutamate (**2b**), carried out in aqueous NH_3/NH_4Cl solution (200 mM) at pH 8 and derivatized after 168 h following the standard protocol with ECF. In both cases, the MS spectra for the GC peak with RT of 10.0 min, which corresponds to derivatized glutamate, are shown in the insets.

6.4 Reaction of glyoxylate (1c) to glycine (2c)

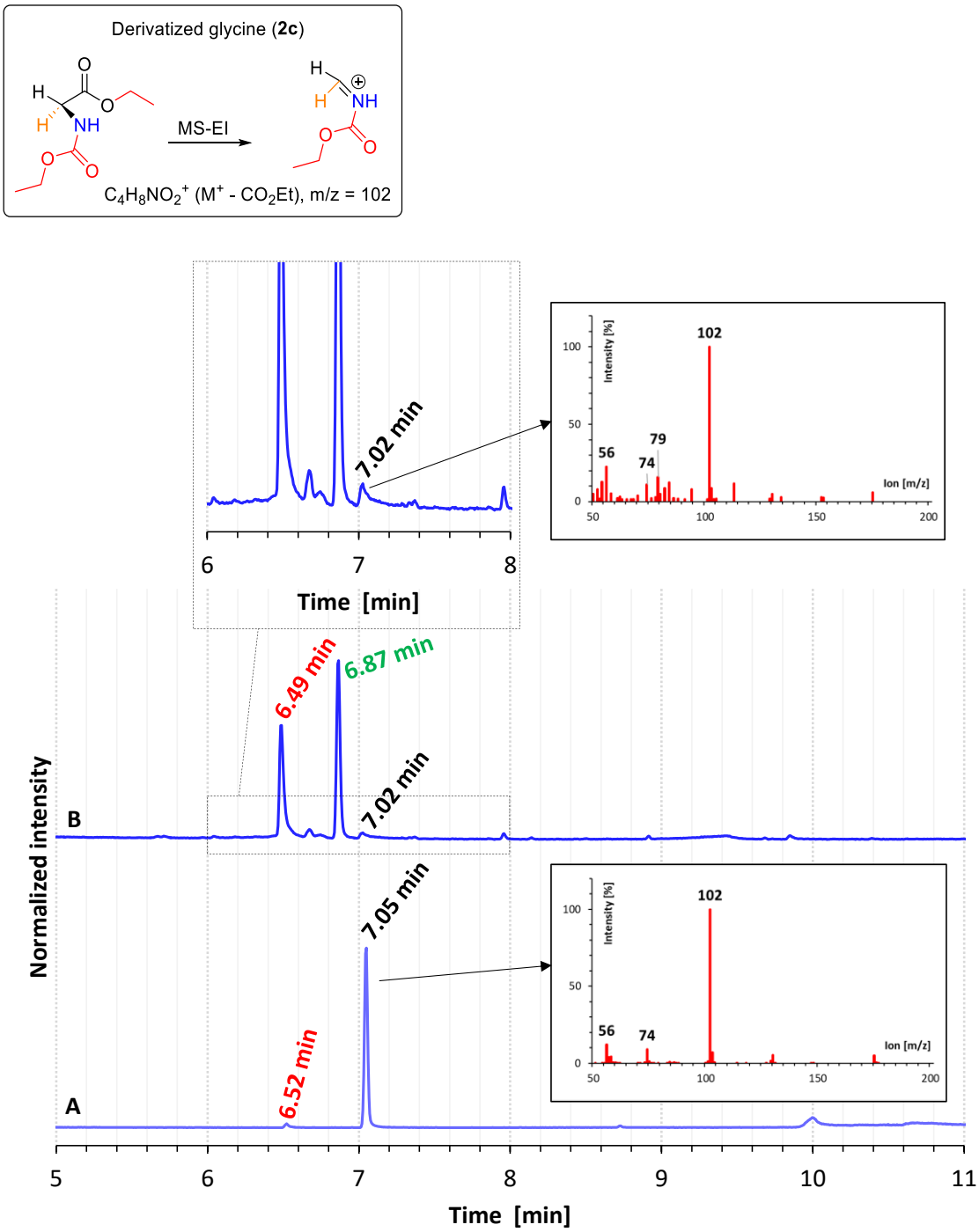

Figure S34. (**A**) GC-MS analysis of a glycine (**2c**) authentic sample derivatized following the standard protocol with ECF. (**B**) GC-MS analysis of the reaction between glyoxylate (**1c**, 27.5 mM) and NADH (30 mM) to give glycine (**2c**), carried out in aqueous NH_3/NH_4Cl solution (200 mM) at pH 8 and derivatized after 96 h following the standard protocol with ECF. In both cases, the MS spectra for the GC peak with RT of 7.0 min, which corresponds to derivatized glycine, are shown in the insets.

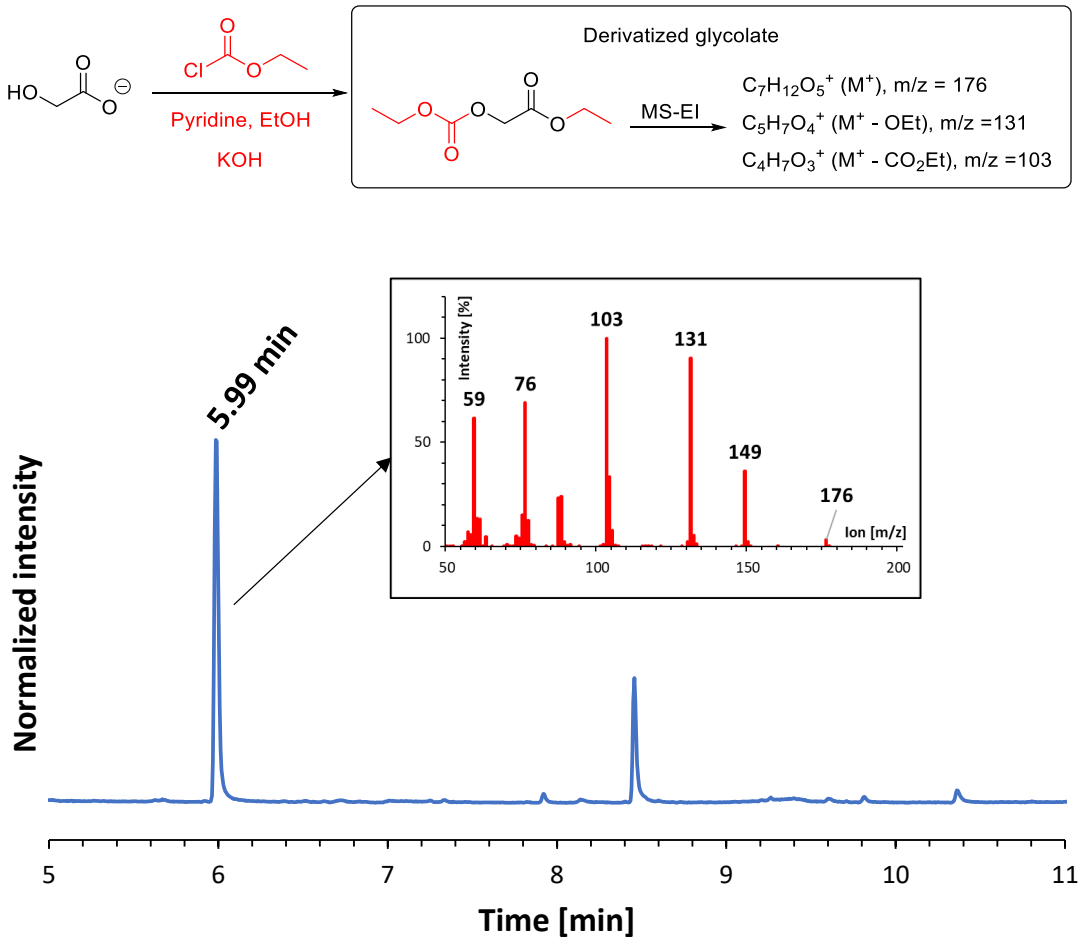

Figure S35. GC-MS analysis of a glycolate authentic sample derivatized following the standard protocol with ECF. The peak of 5.99 min and its corresponding mass spectrum is not observed in the chromatogram of the reaction of glyoxylate (**1c**), suggesting that this compound is not formed during the reaction.

6.5 Reaction of oxaloacetate (1d)

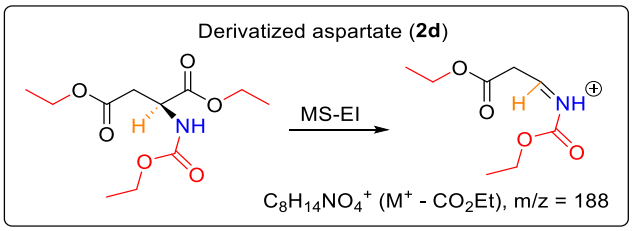

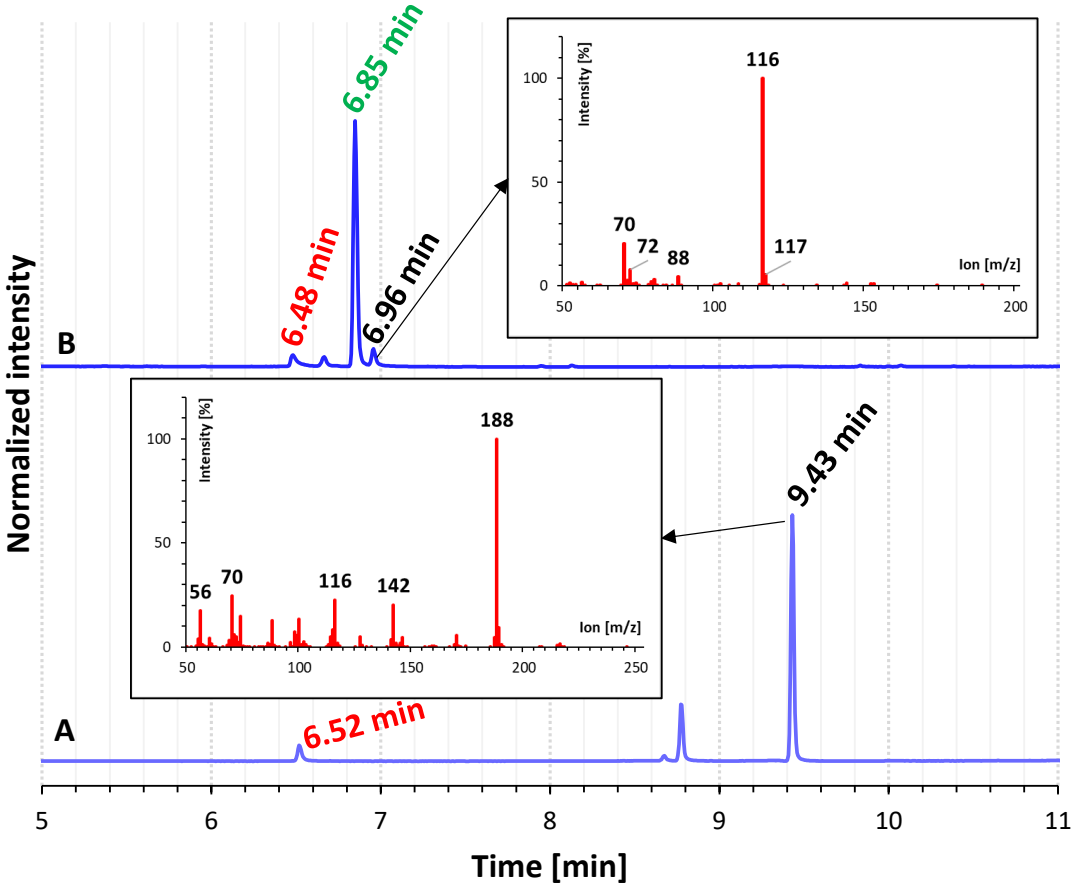

Figure S36. (**A**) GC-MS analysis of an aspartate (**2d**) authentic sample derivatized following the standard protocol with ECF. (**B**) GC-MS analysis of the reaction between oxaloacetate (**1d**, 25.6 mM) and NADH (30 mM), carried out in aqueous NH_3/NH_4Cl solution (200 mM) at pH 8 and derivatized after 168 h following the standard protocol with ECF. As it can be noted, the peak at 9.4 min and its MS spectra corresponding to aspartate are not present in the GC-chromatogram of the reaction mixture. On the other hand, the reaction mixture chromatogram presents a peak at 7.0 min whose retention time and MS spectrum match those from alanine (See **Figure S31**).

7. MALDI-TOF analyses

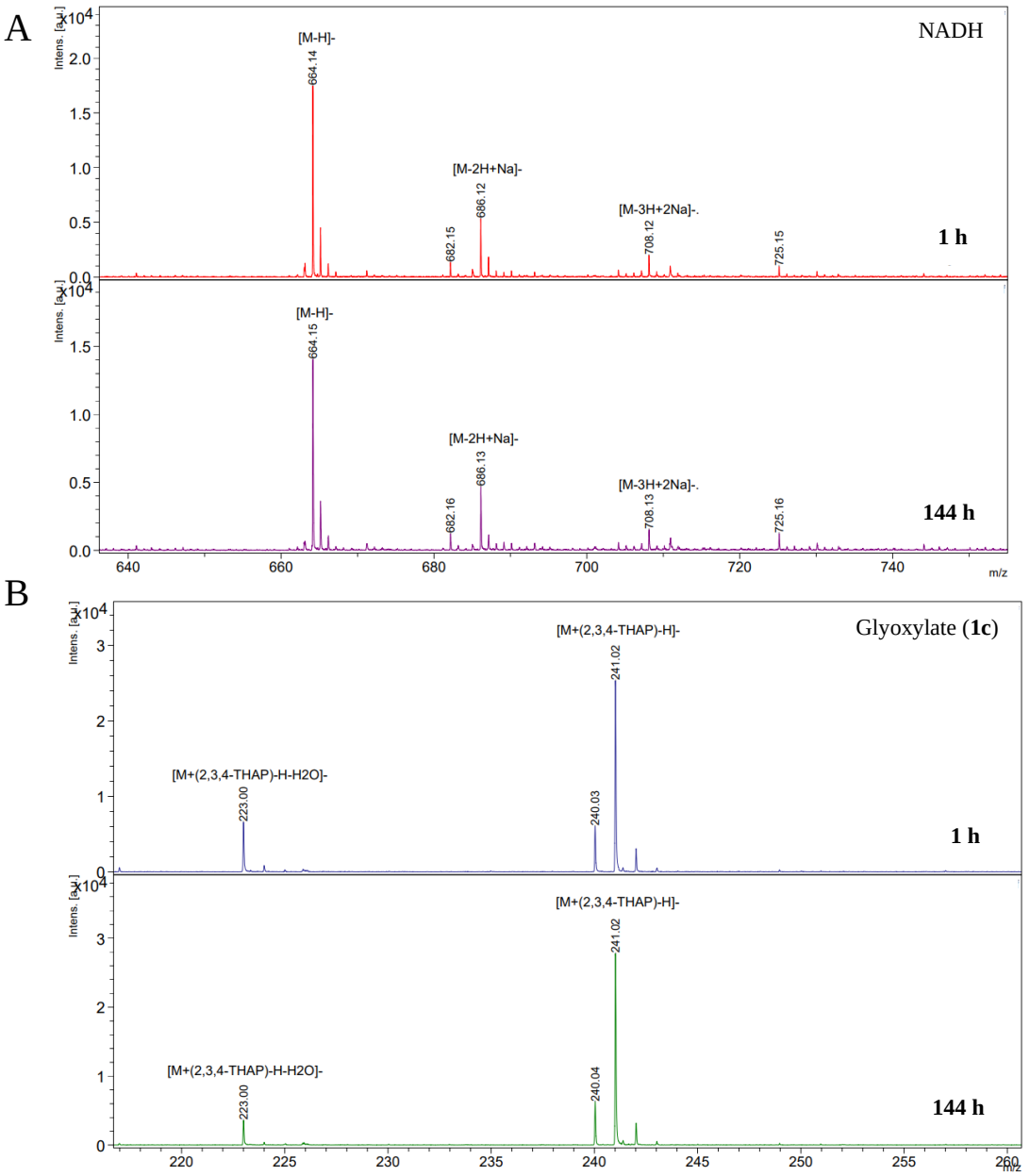

Figure S37. (A) MALDI-TOF spectra of NADH from pH 9 NH_3/NH_4Cl solution (200 mM) with 2,3,4-trihydroxyacetophenone (2,3,4-THAP) + ammonium citrate as matrix, registered in the negative mode at time 1 h **(red)** and 144 h **(purple)**. The spectra show a stable composition, with the molecular ion being with two, one or none sodium counterions. The spectra at pH 8 show the same features. **(B)** MALDI-TOF spectra of glyoxylate (**1c**) from pH 9 NH_3/NH_4Cl (200 mM) with 2,3,4-trihydroxyacetophenone (2,3,4-THAP) + ammonium citrate as matrix, registered in the negative mode at time 1 h **(blue)** and 144 h **(green)**. The spectra show a stable composition, with the molecular ion being associated with 2,3,4-THAP. The spectra at pH 8 show the same features.

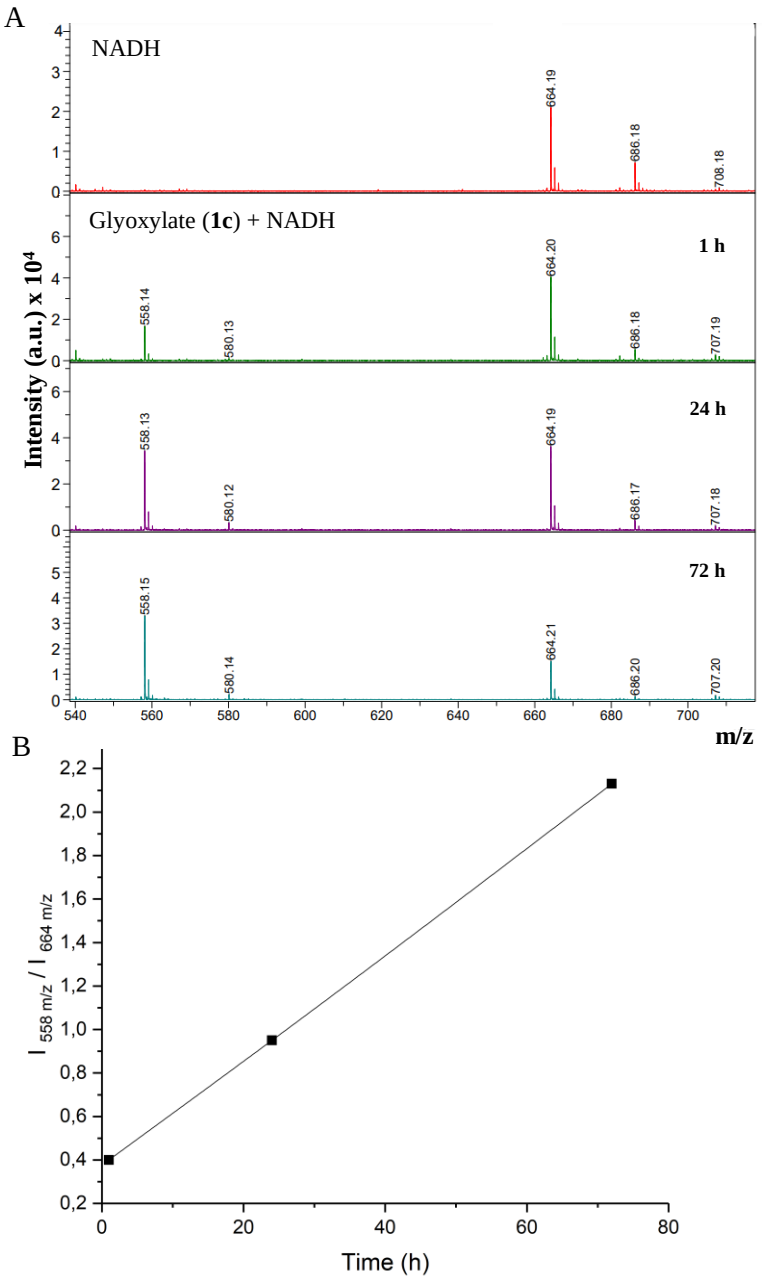

Figure S38. (A) Amplified region (between *m/z* 540 and 710 Da) of the MALDI-TOF spectra of the reaction between glyoxylate (**1c**, 27.5 mM) and NADH (30 mM) in pH 8 NH_3/NH_4Cl (200 mM) with 2,3,4-trihydroxyacetophenone (2,3,4-THAP) + ammonium citrate as matrix, registered in the negative mode at the reaction start **(green)**, and after 24 h **(purple)** or 72 h **(blue)**. A comparison with the spectrum of pure NADH (**red**) is also shown. **(B)** Plot of the ratio of relative intensities of ADPR mass peak (m/z = 558) respect to NADH mass peak (m/z = 664).

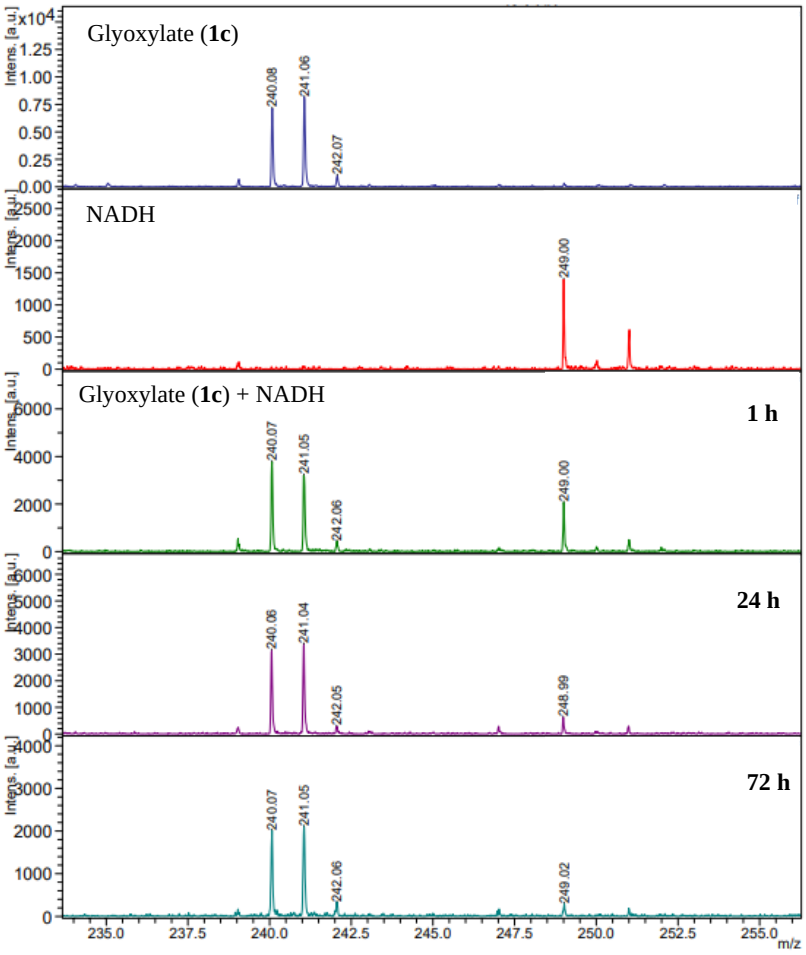

Figure S39. Amplified region (between *m/z* 235 and 255 Da) of the MALDI-TOF spectra of the reaction between glyoxylate (**1c**, 27.5 mM) and NADH (30 mM), registered in the negative mode, at the reaction start **(green)**, and after 24h **(purple)** or 72h **(blue)**, in comparison to **1c (blue)** and NADH **(red)**, all in pH 8 NH_3/NH_4Cl (200 mM), showing a gradual reduction of the relative intensity of the peak for the glyoxylate molecular ion at 241.1 ($[M_{glyo}+(2,3,4\text{-THAP})\text{-H}]^-$).

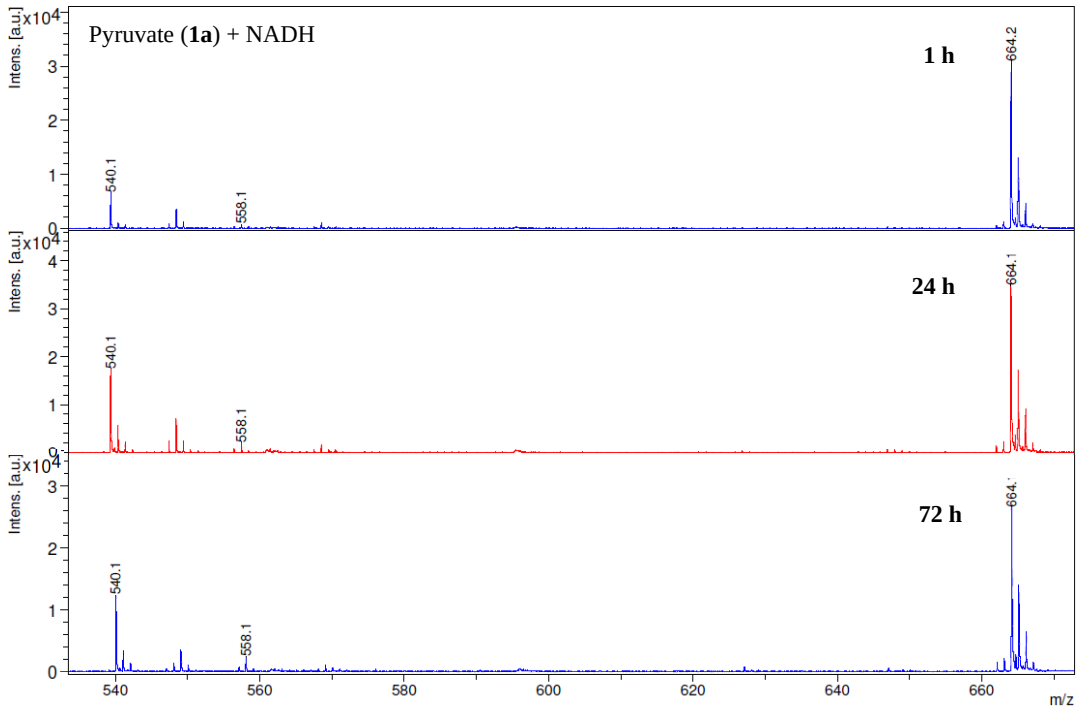

Figure S40. Amplified region (between *m/z* 540 and 670 Da) of the MALDI-TOF spectra of the reaction between pyruvate (**1a**, 30 mM) and NADH (30 mM) in pH 8 NH_3/NH_4Cl solution (200 mM) with 2,4,6-trihydroxyacetophenone (2,4,6-THAP) + ammonium citrate as matrix, registered in the negative mode at the reaction start **(blue)**, and after 24 h **(red)** or 72 h **(blue)**.

The increase of the relative intensity of ADPR mass peak (m/z = 558) respect to NADH mass peak (m/z = 664) is less prominent than in the reaction of glyoxylate (**1c**) with NADH (Figure S38).

8. UV-visible spectra

A) NADH

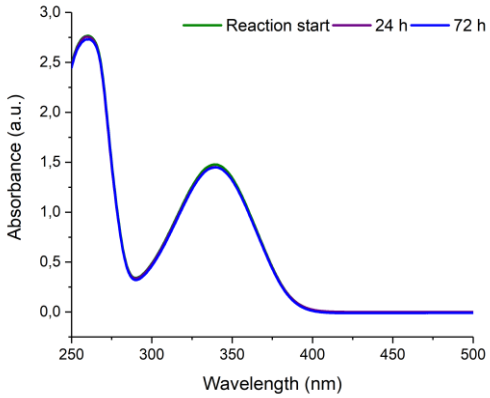

B) NADH + **1a**

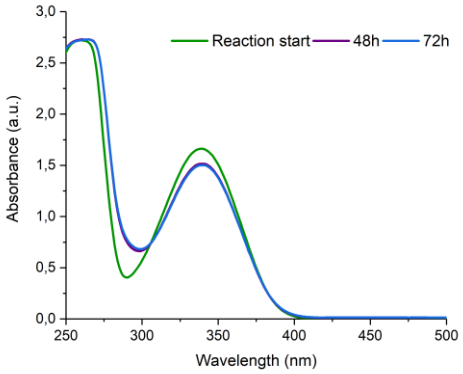

C) NADH + **1c**

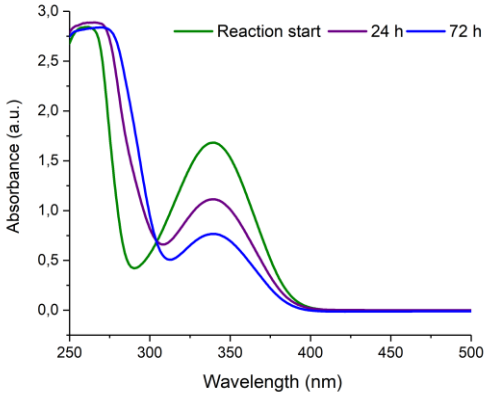

Figure S41. Monitoring of the cofactor UV-Vis absorption decay during the reaction in aqueous NH_3/NH_4Cl solution (200 mM) at pH 8: **A)** Control solution of NADH (30 mM). **B)** Reaction between pyruvate (**1a**, 30 mM) and NADH (30 mM) to give alanine (**2a**). **C)** Reaction between glyoxylate (**1c**, 27.5 mM) and NADH (30 mM) to give glycine (**2c**). As can be observed, there are no appreciable changes in the absence of keto acid and the decay is low in the presence of pyruvate. In contrast, the highest decay is given in the presence of glyoxylate, despite the fact that glycine is obtained in very low yield.

9. Theoretical calculations

Computational details. Geometry optimizations were performed using Gaussian16[8] in the framework of the Density Functional Theory (DFT) with the M06-2X functional,[9] which has been widely used to describe the chemical reactivity of organic molecules,[10] and the cc-pVTZ triple-zeta basis set. Solvent (water) was described using the SMD implicit model.[11] All stationary points were characterized as minima or transition states (TS) through the analysis of the second derivatives. After frequency calculations, thermodynamic corrections (*e.g.*, ZPE, H, and G) were provided by Gaussian, at its default values of pressure = 1 atm and temperature = 298.15 K. Conformational space was sampled with the GFN2-xTB method[12] using the CREST software.[13] The most stable conformers were then optimized at DFT level.

In order to describe in an accurate way the protonation energy, we have considered the energy of the proton as the energy difference between NH_4^+ and NH_3, since ammonium is the main proton source given the experimental conditions. Only the active part of the cofactor (the nicotinamide ring and a simplified ribose unit) was considered explicitly, as shown in Figure S42, in order to reduce the computational effort.

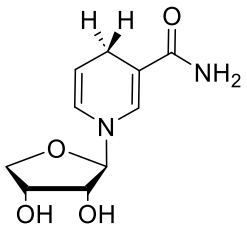

Figure S42. Active part of NADH that has been involved in the DFT calculations: nicotinamide ring with an adjacent simplified ribose unit.

Note: As indicated above, the proton energy is considered as the difference between NH_4^+ and NH_3. Therefore, in the energetic profiles, the difference in free energy between the components of a conjugated acid-base pair must be understood as the reaction energy in which the compound exchanges a proton directly with NH_3/ NH_4^+. For example, in Fig. 4 (of main text), there is a difference of 0.8 kJ/mol between **III** and **II**, which would correspond with the reaction free energy of:

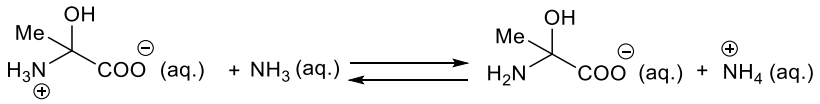

II **III**

In previous studies, the proton energy has been considered as the solvated proton by water, in order to study the acid-base reaction energy directly with water.[4]

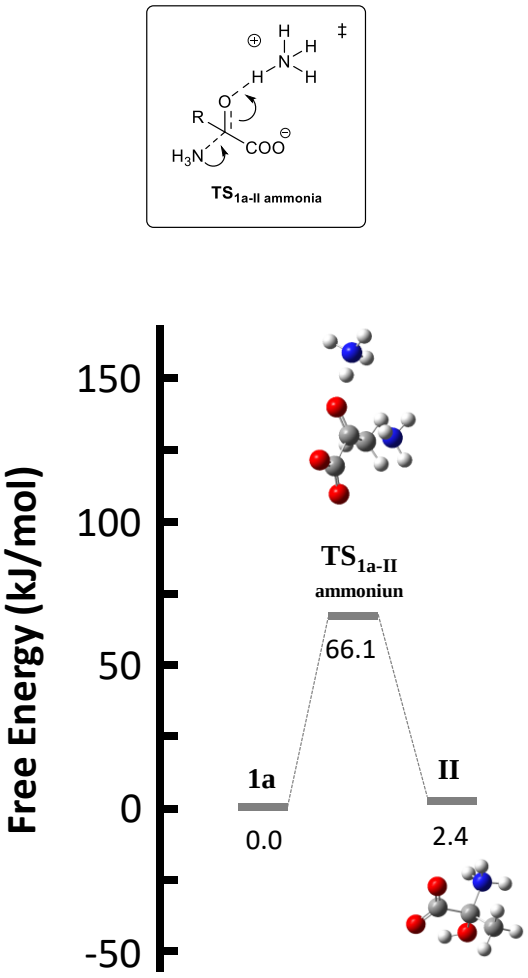

Figure S43. Structure and free energy of the addition of ammonia to pyruvate assisted by an explicit ammonium through hydrogen bond with the carbonyl oxygen. The addition of ammonia and protonation from ammonium resulted an asynchronous one-step process. This process has very similar activation barrier to that in which explicit protonation source was not considered (**$TS_{1a\text{-}I}$** in Fig. 4 of main text).

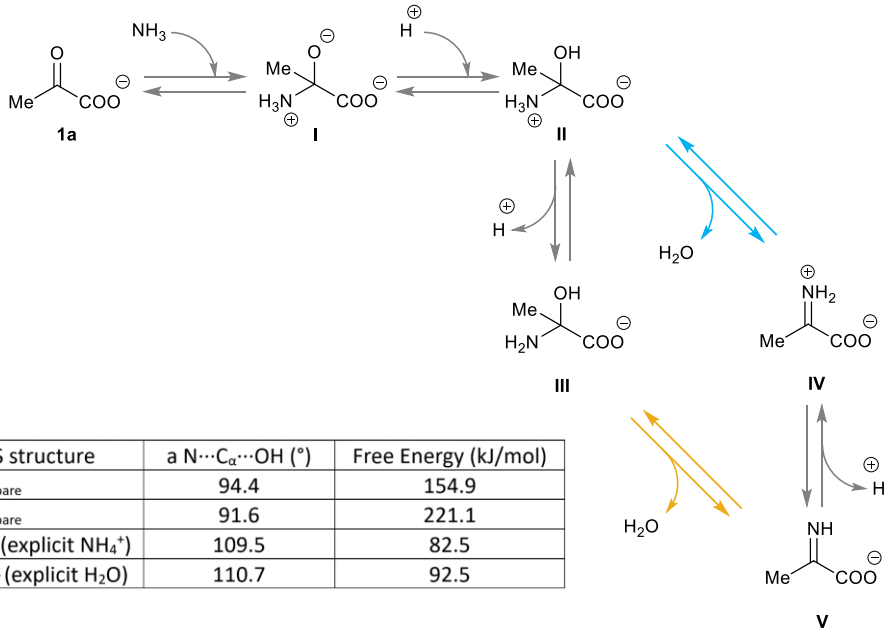

TS structure	a N···C_α···OH (°)	Free Energy (kJ/mol)
$TS_{II-IV\ bare}$	94.4	154.9
$TS_{III-V\ bare}$	91.6	221.1
TS_{III-IV} (explicit NH_4^+)	109.5	82.5
TS_{NII-IV} (explicit H_2O)	110.7	92.5

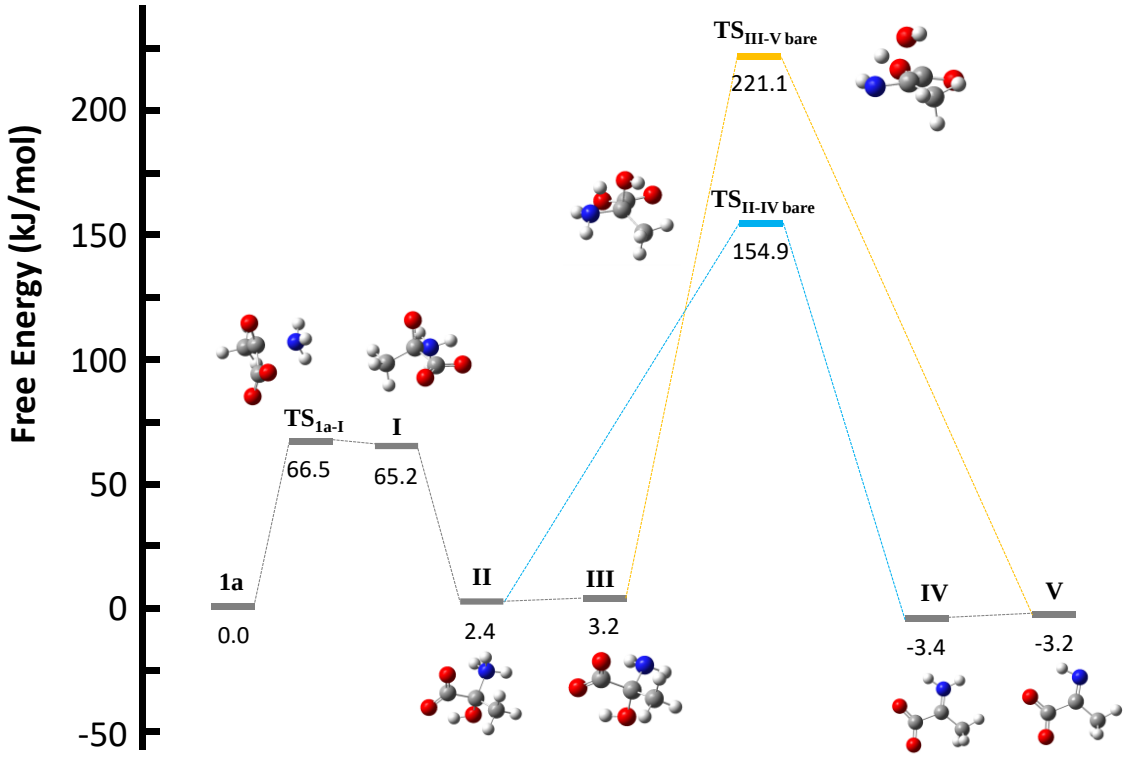

Figure S44. Energetic profile for the formation of the imine/iminium ion in which explicit molecules of water or ammonium have not been considered. In both **TS_{II-IV}** and **TS_{III-V}**, the leaving hydroxyl attracts a proton from the amine group, which leaves the molecule too. This leaving proton provokes distorted transition states, resulting in high-energy. However, explicit molecule of solvent (**TS_{NII-IV}** in Fig. 4 of main text) or protonation source (**TS_{III-IV}** in Fig. 4 of main text), can counteract this effect, decreasing their energy, and favouring this mechanism. The relevant angle N···C_α···OH and free energies of these TS are shown in the table.

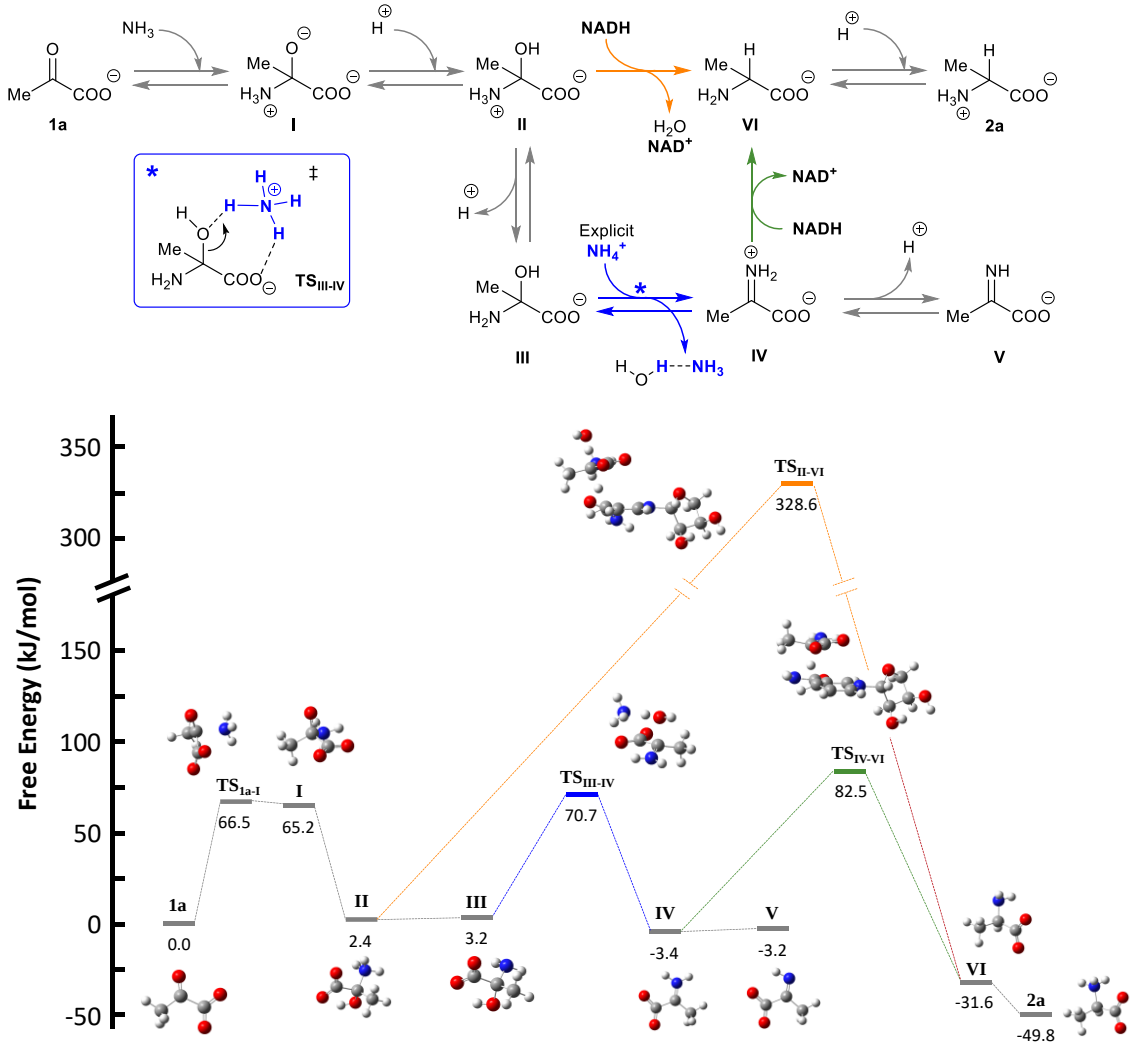

Figure S45. Energy profile for the formation of amino acid **2a** in which two possible modes of action of NADH are shown for comparison: hydride transfer to hemiaminal **II** (unfavorable S_N2 mechanism, orange pathway) or hydride transfer to iminium ion **IV**. For simplicity, only the ammonium-assisted formation of **IV** is shown.

Coordinates (Angstroms)

Electronic energy (a.u.) Gibbs free energy (a.u.)

H_2O

-76.43746766 -76.43448366

O	2.902892000	1.156374000	0.000000000
H	3.863752000	1.202286000	0.000000000
H	2.625415000	2.077463000	0.000000000

NH_3

-56.55494873 -56.53974873

N	1.298032000	-1.353519000	0.025420000
H	1.605178000	-2.318686000	-0.030473000
H	1.605257000	-0.919351000	-0.838400000
H	0.285766000	-1.385679000	-0.030197000

NH_4^+

-57.01768407 -56.98808507

N	1.287220000	-1.368256000	0.000001000
H	1.627957000	-2.330332000	-0.000002000
H	1.628243000	-0.887040000	0.832917000
H	1.628244000	-0.887043000	-0.832916000
H	0.266967000	-1.368376000	-0.000000000

NADH (active part)

-799.88944389 -799.68565689

C	0.411721000	-0.276695000	1.408897000
C	-0.665156000	0.098767000	2.120751000
C	-1.615341000	1.169800000	1.634242000
C	-1.119839000	1.754649000	0.338841000
C	-0.039271000	1.310700000	-0.294815000
N	0.735226000	0.252578000	0.191381000
H	1.075197000	-1.048581000	1.776221000
H	-1.675485000	2.568863000	-0.104420000
H	0.304656000	1.733521000	-1.228277000
C	2.017363000	-0.049468000	-0.406417000
O	2.186826000	-1.450146000	-0.510989000
C	3.231930000	0.458427000	0.382367000
H	2.012384000	0.403542000	-1.400532000
C	3.485623000	-1.826495000	-0.016750000
C	4.305648000	-0.556644000	0.001955000
H	3.032502000	0.383062000	1.452194000
H	3.905387000	-2.578450000	-0.680944000
H	3.388417000	-2.236162000	0.990037000
H	5.122953000	-0.600963000	0.720870000
O	3.535557000	1.806794000	0.112537000
H	3.682186000	1.899828000	-0.837689000
O	4.788877000	-0.304340000	-1.309072000
H	5.374176000	0.461201000	-1.276094000
H	-2.624404000	0.761686000	1.500955000
H	-1.719891000	1.961181000	2.384951000
C	-0.895990000	-0.587189000	3.400975000
O	-0.134764000	-1.455574000	3.857895000
N	-2.000377000	-0.218443000	4.074643000
H	-2.645207000	0.466057000	3.717865000
H	-2.203877000	-0.667393000	4.953509000

NAD$^+$ (active part)

-799.15070371 -798.95455971

C	0.281427000	-0.378362000	1.288150000
C	-0.857631000	-0.002103000	1.967587000
C	-1.530694000	1.143873000	1.561179000
C	-1.049279000	1.877379000	0.488437000
C	0.081241000	1.449068000	-0.164515000
N	0.713112000	0.334628000	0.242233000
H	0.857482000	-1.250020000	1.559703000
H	-1.545483000	2.774290000	0.152449000
H	0.507764000	1.963637000	-1.013162000
C	1.990145000	-0.046747000	-0.434067000
O	2.139163000	-1.429012000	-0.415780000
C	3.202004000	0.554140000	0.299450000
H	1.906800000	0.328385000	-1.453887000
C	3.405844000	-1.773069000	0.197341000
C	4.254409000	-0.531393000	0.066103000
H	2.984989000	0.615755000	1.366489000
H	3.814731000	-2.623235000	-0.340574000
H	3.244737000	-2.029230000	1.244866000
H	5.054694000	-0.495247000	0.803442000
O	3.531658000	1.844537000	-0.139019000
H	3.754208000	1.799845000	-1.078458000
O	4.757999000	-0.455927000	-1.255876000
H	5.417160000	0.246659000	-1.294769000
H	-2.418180000	1.484270000	2.076748000
C	-1.254237000	-0.861178000	3.135238000
O	-0.438632000	-1.639407000	3.621468000
N	-2.497979000	-0.722422000	3.593585000
H	-3.188442000	-0.148044000	3.139223000
H	-2.787775000	-1.295966000	4.371806000

1a

-341.96307226 -341.93459426

C	-0.473718000	0.410138000	0.554101000
O	-0.967254000	-0.323011000	1.383227000
C	0.960751000	0.112902000	0.017940000
O	1.413665000	0.933683000	-0.807360000
O	1.512290000	-0.910649000	0.465087000
C	-1.179648000	1.606349000	0.007831000
H	-0.584479000	2.498923000	0.203895000
H	-1.260466000	1.514415000	-1.076015000
H	-2.165015000	1.700574000	0.455859000

TS_1a-I

-398.51319108 -398.44899608

C	0.545091000	0.243943000	-0.588705000
O	1.031677000	1.372666000	-0.303570000
N	1.397874000	-1.012857000	0.545234000
H	2.385510000	-0.989742000	0.309566000
H	1.060443000	-1.969699000	0.490275000
H	1.268327000	-0.660979000	1.488673000
C	-0.881437000	-0.079697000	-0.058179000
O	-1.606367000	-0.815170000	-0.768490000
O	-1.195769000	0.428869000	1.042676000
C	0.899155000	-0.375461000	-1.924000000
H	0.646370000	-1.431049000	-1.980305000
H	0.340807000	0.153676000	-2.698351000
H	1.963786000	-0.237825000	-2.109636000

I

-398.51835128 -398.44951728

C	-0.572513000	-0.062514000	0.105782000
O	-0.923672000	0.121181000	1.377822000
N	-1.048633000	1.188302000	-0.712588000
H	-2.034392000	1.343973000	-0.508361000
H	-0.914570000	1.087146000	-1.718215000
H	-0.491167000	1.977985000	-0.388197000
C	0.971511000	-0.050165000	-0.052639000
O	1.556978000	-1.151121000	0.072259000
O	1.529159000	1.066169000	-0.209677000
C	-1.223500000	-1.255372000	-0.581771000
H	-2.308393000	-1.159230000	-0.515697000
H	-0.932476000	-1.341254000	-1.630329000
H	-0.920596000	-2.161314000	-0.061609000

II

-399.00366220 -398.92177620

C	-3.609960000	-0.799457000	0.278414000
O	-4.961010000	-1.083952000	0.107650000
N	-2.845235000	-2.071523000	0.012113000
H	-5.238180000	-0.546681000	-0.654964000
H	-1.843433000	-1.863888000	-0.016375000
H	-3.124103000	-2.471733000	-0.886744000
C	-3.116008000	0.232295000	-0.770738000
O	-4.015738000	0.807598000	-1.414099000
O	-1.881354000	0.373273000	-0.853669000
H	-3.027663000	-2.759514000	0.746783000
C	-3.309044000	-0.355279000	1.690558000
H	-3.810655000	0.594258000	1.868277000
H	-3.687362000	-1.096174000	2.394994000
H	-2.237865000	-0.226572000	1.834268000

III

-398.54129952 -398.47311752

C	-3.501672000	-0.811572000	0.236323000
O	-4.922340000	-0.897255000	0.302871000
N	-2.890289000	-2.078418000	-0.133943000
H	-5.223029000	-0.586192000	-0.565623000
H	-3.305158000	-2.391293000	-1.007135000
C	-3.130757000	0.200592000	-0.876657000
O	-4.019336000	0.407130000	-1.742098000
O	-1.989022000	0.705611000	-0.854412000
H	-3.147991000	-2.765982000	0.568571000
C	-3.003159000	-0.385437000	1.599749000
H	-3.421973000	0.583568000	1.867934000
H	-3.318406000	-1.120752000	2.342133000
H	-1.918492000	-0.318781000	1.608198000

TS_{III-IV}

-455.54540802 -455.43548402

C	-0.72217400	-0.40956600	0.28998600
O	0.33130500	-0.88402700	-1.15037800
N	-0.17697800	-0.86809600	1.40765900
H	0.25944200	-1.84703400	-1.21207100
H	0.59134300	-0.34878700	1.80763500
H	2.49150600	0.55377100	0.26782300
C	-0.52097900	1.10800800	0.06322900
O	-1.32759100	1.66097100	-0.70434800
O	0.43522700	1.62285600	0.67923300
H	-0.31938400	-1.82635700	1.68872000
C	-1.99665100	-1.04041500	-0.15896900
H	-2.22457000	-0.76711100	-1.18324300
H	-1.93735200	-2.12423100	-0.06402500
H	-2.79508100	-0.67504100	0.48788300
N	2.69280600	-0.22137200	-0.35805700
H	3.19624900	-0.92575400	0.17058000
H	1.32755000	-0.66718600	-0.85944700
H	3.31669500	0.12050800	-1.08123500

IV

-322.54503048 -322.48947448

C	-0.372843000	0.639848000	-0.821984000
N	-1.370864000	-0.122712000	-0.599680000
H	-2.256817000	-0.008882000	-1.082888000
C	0.906846000	0.337911000	-0.003798000
O	1.876170000	1.065566000	-0.262198000
O	0.801231000	-0.597041000	0.808457000
H	-1.260616000	-0.862649000	0.092204000
C	-0.415566000	1.741023000	-1.789812000
H	-0.166559000	2.665555000	-1.266278000
H	0.372317000	1.580693000	-2.527262000
H	-1.384582000	1.822401000	-2.273477000

V

-322.08429194 -322.04107894

C	-0.365022000	0.589479000	-0.771707000
N	-1.392769000	-0.140127000	-0.597976000
H	-1.151099000	-0.841034000	0.108106000
C	0.934126000	0.327252000	0.015660000
O	1.910268000	1.060097000	-0.257397000
O	0.902248000	-0.595549000	0.860539000
C	-0.366413000	1.725505000	-1.738544000
H	-0.131705000	2.656963000	-1.221625000
H	0.408755000	1.580409000	-2.491732000
H	-1.335696000	1.811332000	-2.223391000

TS_II-VI

-1198.78412884 -1198.48317584

C	-0.421768000	0.881407000	0.120855000
C	0.764690000	1.284488000	0.643600000
C	1.541296000	0.384376000	1.486209000
C	0.802503000	-0.776040000	1.945770000
C	-0.373631000	-1.109412000	1.379550000
N	-0.970206000	-0.315625000	0.433287000
H	2.204523000	0.862209000	2.205302000
H	-0.992911000	1.491740000	-0.566531000
H	1.220010000	-1.414513000	2.708493000
H	-0.925271000	-1.994648000	1.660696000
C	-2.292708000	-0.667645000	-0.092717000
O	-2.333460000	-0.418356000	-1.474476000
C	-3.432392000	0.150776000	0.530810000
H	-2.430407000	-1.730280000	0.112972000
C	-3.504699000	0.361894000	-1.796389000
C	-4.437733000	0.202919000	-0.618443000
H	-3.082318000	1.161289000	0.745386000
H	-3.929549000	-0.025444000	-2.718682000
H	-3.219694000	1.406763000	-1.926654000
H	-5.135116000	1.034346000	-0.527994000
H	2.513681000	-0.083673000	0.782082000
O	-3.903270000	-0.392577000	1.738506000
H	-4.236496000	-1.282439000	1.562036000
O	-5.122179000	-1.033892000	-0.733459000
H	-5.822087000	-1.057691000	-0.070834000
C	3.553980000	-0.589614000	-0.019351000
O	4.819717000	-1.558351000	-1.442726000
N	3.365096000	0.399262000	-1.080249000
H	5.337732000	-2.112117000	-0.852247000
H	3.233209000	1.351945000	-0.694827000
H	2.539343000	0.110886000	-1.619735000
C	2.728382000	-1.857860000	-0.172352000
O	2.950414000	-2.767825000	0.646829000
O	1.839275000	-1.807418000	-1.052701000
H	4.190069000	0.335671000	-1.685236000
C	1.347651000	2.603669000	0.314195000
O	2.582175000	2.743202000	0.296062000
N	0.517141000	3.609829000	0.044746000
H	-0.478044000	3.527841000	0.175487000
H	0.904544000	4.504520000	-0.215358000
C	4.656244000	-0.335715000	0.958890000
H	4.747966000	-1.196815000	1.616012000
H	5.594767000	-0.177380000	0.434493000
H	4.445139000	0.550065000	1.560840000

TS_IV-VI

-1122.42182639 -1122.14242139

C	-3.343606000	0.650737000	-0.774481000
C	0.015595000	-0.826780000	0.204907000
C	-1.237439000	-1.101743000	0.663031000
C	-1.987249000	-0.074047000	1.354933000
C	-1.215577000	1.088696000	1.742446000
C	0.019917000	1.286518000	1.245655000
N	0.627567000	0.348463000	0.446794000
H	-2.758201000	-0.383904000	2.055873000
H	0.578417000	-1.558379000	-0.358568000
H	-1.649662000	1.831076000	2.393776000
H	0.608965000	2.163432000	1.470240000
C	1.998191000	0.565007000	-0.032066000
O	2.087778000	0.203265000	-1.386584000
C	3.043246000	-0.275787000	0.714830000
H	2.202425000	1.629019000	0.095976000
C	3.198844000	-0.698239000	-1.579281000
C	4.089379000	-0.509105000	-0.373889000
H	2.607063000	-1.233407000	1.001400000
H	3.694718000	-0.433601000	-2.509554000
H	2.830165000	-1.723582000	-1.631410000
H	4.710123000	-1.381961000	-0.176773000
H	-2.845914000	0.353955000	0.438379000
O	3.506582000	0.339838000	1.890382000
H	3.900345000	1.189739000	1.652792000
O	4.878983000	0.654331000	-0.559427000
H	5.521094000	0.703495000	0.158497000
O	-1.740848000	2.289502000	-1.376719000
O	-3.379835000	2.877037000	0.033020000
N	-2.753554000	-0.150572000	-1.681898000
H	-1.821441000	0.083636000	-1.990404000
H	-3.096161000	-1.086734000	-1.834550000
C	-2.778765000	2.079913000	-0.715839000
C	-1.787420000	-2.446152000	0.361316000
O	-1.094027000	-3.328687000	-0.152161000
N	-3.072471000	-2.656241000	0.685152000
H	-3.483969000	-3.548533000	0.457548000
H	-3.679015000	-1.919689000	1.006464000
C	-4.809768000	0.439437000	-0.525593000
H	-5.111705000	0.898775000	0.411368000
H	-5.375094000	0.901746000	-1.337211000
H	-5.043162000	-0.624364000	-0.501286000

VI

-323.29650951 -323.23133751

H	0.70692900	0.61147800	-1.42242000
C	0.68420800	0.19523500	-0.41486300
N	1.53278300	-0.99398300	-0.38970500
H	1.09890900	-1.70377700	-0.97182700
H	1.48353900	-1.37543400	0.55127600
C	-0.79178100	-0.04834200	-0.06737900
O	-1.09243500	-1.09084000	0.56420000
O	-1.60314800	0.84875600	-0.41758700
C	1.23331300	1.22956400	0.55919600
H	2.26800000	1.47028900	0.31687000
H	0.64357700	2.14435200	0.53096000
H	1.20248100	0.83081300	1.57625100

2a

-323.76555896 -323.68658396

H	-3.353178000	0.445606000	1.280240000
C	-3.743832000	-0.130202000	0.445052000
N	-3.201100000	-1.513949000	0.583975000
H	-3.567429000	-1.972299000	1.419884000
H	-2.181615000	-1.501106000	0.630207000
C	-3.226350000	0.470409000	-0.868859000
O	-3.475560000	1.682255000	-1.039871000
O	-2.625492000	-0.300520000	-1.649940000
C	-5.258232000	-0.180003000	0.477368000
H	-5.610117000	-0.622440000	1.408720000
H	-5.649924000	0.831167000	0.401037000
H	-5.636313000	-0.767049000	-0.360970000
H	-3.457748000	-2.063104000	-0.239302000

TS_1a-II ammonium

-455.54534308 -455.43724108

C	-0.12418500	0.14408900	-0.68955100
O	-0.21808700	1.35959700	-0.41476700
N	1.50331400	-0.54609200	0.39995300
H	2.32343700	-0.06500400	0.04537000
H	1.67292100	-1.54651100	0.37495100
H	1.34417400	-0.26240600	1.36100300
C	-1.05318200	-0.84111100	0.06917700
O	-1.27304000	-1.94153900	-0.48292300
O	-1.50468500	-0.44296700	1.16389300
C	0.38314600	-0.28316700	-2.03875500
H	0.66242300	-1.33141800	-2.05752100
H	-0.42551900	-0.12791300	-2.75697900
H	1.23131300	0.33338800	-2.33254900
H	0.54190700	2.45435000	-1.28172200
H	1.73377600	3.68296000	-1.22757000
H	1.48688100	2.86493200	-2.64785600
H	0.35213900	3.94532000	-2.10619200
N	1.03071600	3.24203900	-1.81832900

TS_II-IV bare

-398.94072261 -398.86369861

C	-0.472028000	-0.030260000	-0.052000000
O	-0.949691000	-0.189685000	1.355439000
N	-1.041485000	1.300672000	-0.213304000
H	-1.636278000	-0.874817000	1.436080000
H	-1.377386000	0.863359000	1.052840000
H	-0.314487000	1.995074000	-0.366208000
C	1.075532000	-0.028865000	-0.014862000
O	1.591491000	-1.066752000	0.437227000
O	1.634153000	0.993050000	-0.456916000
H	-1.761131000	1.353577000	-0.926665000
C	-1.044488000	-1.082452000	-0.953321000
H	-2.134088000	-1.045646000	-0.928249000
H	-0.703417000	-0.893054000	-1.970371000
H	-0.700348000	-2.064684000	-0.638064000

TS_III-V bare

-398.45106005 -398.39011405

C	-0.490782000	0.103671000	0.622711000
O	-1.390195000	0.867372000	-0.789273000
N	-1.308267000	-0.974918000	0.610061000
H	-1.850585000	1.670041000	-0.508147000
H	-1.840009000	-0.146497000	-0.248542000
H	-0.865036000	-1.667263000	0.007784000
C	0.921520000	-0.001352000	0.003203000
O	1.733461000	0.900361000	0.298410000
O	1.121812000	-0.985134000	-0.740117000
C	-0.689123000	1.121710000	1.694494000
H	-0.163578000	0.765171000	2.583396000
H	-0.278262000	2.088250000	1.418526000
H	-1.747288000	1.211353000	1.934468000

TS_II-NII (explicit water)

-475.43375893 -475.33480093

C	0.52537400	-0.50527800	0.05922500
O	0.01118400	-0.87583400	1.32006000
N	-0.36535500	-1.08416300	-0.97811200
H	0.28284700	-1.78396900	1.50786000
H	-0.09784200	-0.73957600	-1.89852100
H	-1.77130300	0.72811500	0.07829500
C	0.40135000	1.04418400	0.01779100
O	-0.77244700	1.53667200	0.17154100
O	1.41689800	1.71754000	-0.12766000
H	-0.23116200	-2.09375800	-0.98582700
C	1.95030900	-0.97156300	-0.11897600
H	2.58383000	-0.54820600	0.65704300
H	1.97589500	-2.06057900	-0.05070400
H	2.33146400	-0.66918100	-1.09251000
O	-2.50416700	-0.09071300	-0.19496100
H	-1.64495600	-0.70008800	-0.61967400
H	-2.79592700	-0.52207600	0.61886100

NII (explicit water)

-475.44528149 -475.34206049

C	-0.59791500	-0.50515300	0.01478000
O	0.26102800	-0.97617600	-1.02732300
N	-0.20563800	-0.93936600	1.33410700
H	0.11176700	-1.92610300	-1.11993400
H	0.79310500	-0.80642000	1.46187300
H	1.50867300	0.83655300	-0.03419400
C	-0.45206600	1.02284000	-0.00363600
O	-1.40645300	1.76557400	0.01799100
O	0.77544000	1.51533400	-0.00281300
H	-0.40031300	-1.93151900	1.42677300
C	-2.02556400	-0.91787000	-0.26536100
H	-2.33806800	-0.55076700	-1.24045200
H	-2.07669200	-2.00783200	-0.26231600
H	-2.69701100	-0.53040600	0.49637300
O	2.80627100	-0.16349500	-0.12436700
H	3.07256500	-0.43600300	0.76139600
H	2.26069000	-0.88941700	-0.46113500

TS_NII-IV (explicit water)

-475.42343128 -475.32193628

C	-0.63880600	-0.43973600	0.22364100
O	0.34531200	-0.95622800	-1.07121000
N	-0.15381400	-0.89230000	1.40319000
H	0.24354200	-1.91702400	-1.16192700
H	0.70483000	-0.46925500	1.72717100
H	2.17020700	0.57465100	0.10969200
C	-0.43162100	1.08625800	0.04574100
O	-1.37282200	1.72376400	-0.44602900
O	0.67525800	1.53377000	0.43507300
H	-0.27514200	-1.87292000	1.61199300
C	-1.96159100	-1.00228100	-0.18943800
H	-2.20062400	-0.71605400	-1.20888600
H	-1.94899700	-2.08877900	-0.10087100
H	-2.72390500	-0.60275700	0.47718600
O	2.65505100	-0.16533900	-0.31343300
H	2.99370300	-0.70254000	0.41232700
H	1.31870900	-0.76617600	-0.82185200

10. References cited in ESI

[1] K. B. Muchowska, S. J. Varma and J. Moran, Synthesis and breakdown of universal metabolic precursors promoted by iron, *Nature*, 2019, **569**, 104-107.

[2] K. Shabalin, K. Nerinovski, A. Yakimov, V. Kulikova, M. Svetlova, L. Solovjeva, M. Khodorkovskiy, S. Gambaryan, R. Cunningham, M. E. Migaud, M. Ziegler and A. Nikiforov, NAD Metabolome Analysis in Human Cells Using ^{1}H NMR Spectroscopy, *Int. J. Mol. Sci.* 2018, **19**, 3906.

[3] F. Ravalico, I. Messina, M. V. Berberian, S. L. James, M. E. Migaud and J. S. Vyle, Rapid synthesis of nucleotide pyrophosphate linkages in a ball mill, *Org. Biomol. Chem.*, 2011, **9**, 6496-6497.

[4] R. J. Mayer and J. Moran, Quantifying Reductive Amination in Nonenzymatic Amino Acid Synthesis, *Angew. Chem. Int. Ed.*, 2022, **61**, e202212237.

[5] A. Lopalco, J. Douglas, N. Denora and V. J. Stella, Determination of pKa and Hydration Constants for a Series of α-Keto-Carboxylic Acids Using Nuclear Magnetic Resonance Spectrometry, *J. Pharm. Sci.*, 2016, **105**, 664-672.

[6] E. Redina, A. Greish, R. Novikov, A. Strelkova, O. Kirichenko, O. Tkachenko, G. Kapustin, I. Sinev and L. Kustov, Au/Pt/TiO_2 catalysts prepared by redox method for the chemoselective 1,2-propanediol oxidation to lactic acid and an NMR spectroscopy approach for analyzing the product mixture, *Appl. Catal. A: Gen.*, 2015, **491**, 170-183.

[7] a) G. C. K. Roberts and O. Jardetzky, Nuclear Magnetic Resonance Spectroscopy of Amino Acids, Peptides, and Proteins, *Adv. Protein Chem.*, 1970, **24**, 447-545. b) A. Zivkovic, J. J. Bandolik, A. J. Skerhut, C. Coesfeld, N. Zivkovic, M. Raos and H. Stark, Introducing Students to NMR Methods Using Low-Field 1H NMR Spectroscopy to Determine the Structure and the Identity of Natural Amino Acids, *J. Chem. Educ.* 2017, **94**, 115–120.

[8] M. J. Frisch, G. W. Trucks, H. B. Schlegel, G. E. Scuseria, M. A. Robb, J. R. Cheeseman, G. Scalmani, V. Barone, G. A. Petersson, H. Nakatsuji, X. Li, M. Caricato, A. V. Marenich, J. Bloino, B. G. Janesko, R. Gomperts, B. Mennucci, H. P. Hratchian, J. V. Ortiz, A. F. Izmaylov *et al.* Gaussian'16 Revision C.01; Gaussian, Inc.: Wallingford, CT, 2016.

[9] Y. Zhao and D. G. Truhlar, The M06 suite of density functionals for main group thermochemistry, thermochemical kinetics, noncovalent interactions, excited states, and transition elements: two new functionals and systematic testing of four M06-class functionals and 12 other functionals, *Theor. Chem. Account*, 2008, **120**, 215-241.

[10] a) J. Lawrence, M. S. G. Mohammed, D. Rey, F. Aguilar-Galindo, A. Berdonces-Layunta, D. Peña and D. G. de Oteyza, Reassessing Alkyne Coupling Reactions While Studying the Electronic Properties of Diverse Pyrene Linkages at Surfaces, *ACS Nano*, 2021**, 15**, 4937-4964. b) C. Guerra, S. Kumar, F. Aguilar-Galindo, S. Díaz-Tendero, A. I. Lozano, M. Mendes, J. C. Oller, P. Limão-Vieira and G. García, Total Electron Detachment and Induced Cationic Fragmentation Cross Sections for Superoxide Anion (O_2^-) Collisions with Benzene (C_6H_6) Molecules *Int. J. Mol. Sci.*, 2022, **23**, 1266.

[11] A. V. Marenich, C. J. Cramer and D. G. Truhlar, Universal Solvation Model Based on Solute Electron Density and on a Continuum Model of the Solvent Defined by the Bulk Dielectric Constant and Atomic Surface Tensions, *J. Phys. Chem. B.*, 2009, **113,** 6378-6396.

[12] C. Bannwarth, C. Bannwarth, GFN2-xTB—An Accurate and Broadly Parametrized Self-Consistent Tight-Binding Quantum Chemical Method with Multipole Electrostatics and Density-Dependent Dispersion ContributionsChem. *Theory Comput.*, 2019, **15**, 1652–1671.

[13] P. Pracht, F. Bohle, S. Grimme, Automated exploration of the low-energy chemical space with fast quantum chemical methods, *PhysChemChemPhys*, 2020, **22**, 7169–7192.